Oxygen monitoring in a microfluidic culture device for stem cell bioprocess development

Alexandre Stéphane Marie Super

Department of Biochemical Engineering

University College London

A thesis submitted for the degree of *Philosophiæ Doctor* (PhD)

2014

I, Alexandre Stéphane Marie Super confirm that the work presented in this thesis is my own. Where information has been derived from other sources, I confirm that this has been indicated in the thesis.

Abstract

In this thesis, an online oxygen monitoring system has been presented to quantify the dissolved oxygen concentration levels in a microfluidic device for the adherent culture of pluripotent stem cells. Oxygen is a critical environmental cue regulating stem cell fate. Therefore an online monitoring system, combined with the greater control over the soluble microenvironment provided by microfluidic systems, is of interest to assist the development of robust bioprocessing approaches for regenerative medicine therapies.

An oxygen monitoring system consisting of optical sensors have been designed and integrated with the microfabricated modular culture device technology previously established by the Szita Group. The monitoring system enables non-invasive measurements of bulk and peri-cellular oxygen concentration levels in an adherent culture device.

A platform for the operation of the device and monitoring system has been established to meet the requirements for adherent stem cell culture. It supports the adherent culture of mouse embryonic stem cells for up to one week under continuous perfusion and integrates automated monitoring systems for dissolved oxygen and culture confluency. Standard operating procedures for the microfluidic culture have been defined to ensure the robustness and repeatability of the process.

The seamless integration of online oxygen monitoring with confluency monitoring has enabled for the first time to quantify non-invasively oxygen uptake rates of adherent stem cell cultures.

To my grandmother Françoise

Acknowledgments

First, I would like to thank Dr. Nicolas Szita for his indefectible support and guidance since I started my PhD project under his supervision. I would also like to thank my advisor Dr. Farlan Singh Veraitch for his insights on stem cell bioprocessing. I would like to express my gratitude to the Department of Biochemical Engineering for giving the opportunity to pursue challenging research in a stimulating environment. I would like to acknowledge the invaluable support and advice given by the members of the academic, research and administrative staff I had the pleasure to interact with.

I would like to give a big thanks to my friends and colleagues in the microfluidic group: first, to Nicolas Jaccard and Rhys Macown, who shared with me daily the unique joys and pains of working with stem cells and microfluidics; to Brian O'Sullivan for his support and training; to Matthew Davies, for being himself; to Marcel Reichen, for laying the framework for microfluidic stem cell bioprocessing; and to all the past and present members of the group, for the stimulating discussions and good time in and out of the lab.

I would like to acknowledge the support of the regenerative medicine lab, and in particular Ludmila Ruban, for the embryonic stem cell cultures.

I would like to thank all my friends in London and abroad, for always being there at the right time.

And last but not least, I'm immensely grateful to my family, to my parents and Gianna in particular, for their unwavering and invaluable support and encouragements.

Contents

List of figures

List of tables

1 Introduction

1.1 Stem cells

1.1.1 Characteristics and applications

Metazoan organisms originate from a single-cell zygote that develops through highly regulated processes to give rise to a complex assembly of functional organs composed of different types of specialised cells (Alberts et al., 2002). During embryogenesis, the cell mass increases and organises itself into three germ layers of tissue (ectoderm, mesoderm and endoderm) that will later become specialized organs through organogenesis. These processes are only possible because of two unique properties of the embryonic stem cells (ESCs): self-renewal and potency. ESCs are able to divide and proliferate in a virtually unlimited fashion due to their high telomerase activity. They are also able to undergo several phenotypic changes, organised in a process called differentiation, to gain specialised functions. During the differentiation process they will ultimately lose their self-renewal property in order to prevent malignant proliferation and maintain homeostasis in the organism.

Potency is also gradually lost during embryogenesis. The first generation of ESCs has the ability to differentiate into any kind of cells necessary for the development of a whole organism (totipotency). After blastulation, ESCs found in the inner cell mass of the blastocyst (embryoblast) are only able to differentiate into any kind of cells that forms the three germ layers (pluripotency). At the end of embryogenesis, specific cell lineages retain a potency to specialize in a limited number of cells (multipotency, unipotency) in order to sustain self-healing and regenerative processes in the adult organism.

During differentiation, environmental factors trigger gene regulatory networks that will affect cellular fate. These factors defining the cellular microenvironment can be categorized in four classes: extracellular matrix interactions, soluble factors, physico-chemical parameters, and physical forces.

Differentiation is an irreversible process *in-vivo*, but recent *in-vitro* studies have shown that it is possible to re-activate the genetic machinery responsible for pluripotency and therefore create potent stem cell lines from differentiated adult cells. These "de-differentiated" cells are called induced pluripotent stem cells (iPS cells) (Takahashi et al., 2007).

The specific properties of stem cells open up new perspectives for cell-based therapies. By controlling their microenvironment it is theoretically possible to generate a broad array of specialised cells that could potentially be used to recreate functional tissues or organs. This would then make it possible to use these tissues to repair or replace damaged ones in a patient. If the use of live cells and tissues as a therapeutic technique is not a new concept *per se* (e.g. blood transfusions, organ transplantations, skin grafts), it is often limited by the availability of suitable donors. In a maybe not so distant future, the systematic use of stem cells to produce tailored cell-based products such as blood (Dias et al., 2011) or organs (Takebe et al., 2014) could overcome these problems. For these applications, iPS cells may be particularly suitable as they can be derived from the patient's own tissues and therefore are completely immune-compatible. Alternatively, stem cells could be use to produce tissues and organs for drug discovery and clinical experiments, reducing the need for animal experimentation as they would allow to test directly new therapies on artificial human tissues(Liu et al., 2013).

In order to deliver stem cell-based therapies, there is a need to understand and control proliferation and differentiation. The key to unlock this knowledge is to understand how stem cells interact *in vivo* with their environment and what combinations of specific factors are needed to commit them to a specific fate (Becerra et al., 2011). For that task, current cell bioprocessing strategies may not be suitable as they have primarily been designed to optimise the production of specific molecules such as recombinant proteins from engineered cell lines. In the case of stem cells, the cells are the product, a product that will be ultimately transplanted in a patient or used as an analogue of *in-vivo* tissue to screen for drugs. Therefore, there is a need for novel tools tailored to tackle the new challenges associated with the development of stem cell bioprocesses. These processes should be able to mimic and modulate the stem cell microenvironment in order to deliver cells that possess the correct phenotype for the intended application.

1.2 Stem cell microenvironment

The combination of the biochemical, physical and physicochemical factors of the cell microenvironment determines directly survival, self-renewal and differentiation for stem cells. The following sections briefly introduce the relevant factors to stem cell bioprocessing.

1.2.1.1 Extracellular matrix

In a multicellular organism, most of the cells rely on the extracellular matrix (ECM) for their survival. The extracellular matrix is a complex mesh of proteins such as collagen and fibronectin, and polysaccharides that provides anchorage and support for cells. Its porous structure acts as depot for growth factors and enables diffusion gradients of soluble factors to the cells (Li et al., 2003). Cells anchor to the ECM with cell-surface receptors (such as integrins) that are able to trigger different cellular responses such as apoptosis (Gilmore et al., 2009), migration (Schmidt and Friedl, 2009), proliferation or differentiation (Chen et al., 2007) depending on the physicochemical properties of the matrix where the cells bind.

1.2.1.2 Soluble factors

A stem cell's fate is affected by cytokines, growth factors, hormones and other molecules present as soluble factors in the microenvironment. The combination of these factors forms complex signalling pathways that depends on the concentrations, half-life and and affinity between the receptor and the ligand (Hazeltine et al., 2013; Metallo et al., 2007). In tissues, autocrine and paracrine signalling is regulated by diffusional gradients through the ECM (Matsuo and Kimura-Yoshida, 2013).

1.2.1.3 Physico-chemical parameters

Osmotic pressure and pH are two critical parameters for any kind of cell culture. Osmotic pressure defines the flow of water across the cell membrane and contributes to maintain the membrane selectivity towards specific dissolved species that the cell requires. Extreme variation in the osmotic pressure can lead to physical damage to the cells by collapsing (hypertonicity) or bursting (hypotonicity) their membranes.

pH and osmotic pressure have been shown to have an effect on proliferation and differentiation of mouse embryonic stem cells (Chaudhry et al., 2009), but cells are able to recover their capacities when re-exposed to optimum levels. Effects of low pH has been as well highlighted in human mesenchymal stem cells (MSCs) (Wuertz et al., 2009), being responsible for decreased viability and pluripotency of these cells in degenerating intervertebral discs.

1.2.1.4 Physical forces

Physical parameters, such as temperature and hydrodynamic shear stress, can directly impact stem cell viability and pluripotency (Heng et al., 2006; Veraitch et al., 2008).Temperature is a critical parameter that sustains the cell biochemical processes such as enzymatic reactions. It also affects the fluidity and permeability of the phospholipid bilayer of the membrane and thus contributes to the maintenance of the cell integrity and uptake of external molecules.

1.2.2 Oxygen effects on stem cells

Of all the factors defining the cellular microenvironment, oxygen tension is one of the most important for stem cell fate determination (Mohyeldin et al., 2010). Embryonic stem cells are exposed *in vivo* to oxygen tensions (pO_2) considerably lower (0-4% air saturation) than at the atmospheric level (20% air saturation). The pO_2 values are particularly low during the first stages of the development due to the lack of a complete vascular network (Y. M. Lee et al., 2001). Additionally, the gestational sac acts as protective barrier that limits oxygen transfer to the embryo to protect it from free oxygen radicals. These compounds, resulting from oxidative cell metabolism, can easily damage proteins, lipids and nucleic acids leading to senescence, cell death or teratologic effects that could compromise the outcome of embryogenesis (Jauniaux et al., 2003).

The following sections give an overview of the reported effects of oxygen on stem cell proliferation and differentiation in different pluripotent stem cell lines.

1.2.2.1 Proliferation of mouse embryonic stem cells

Gibbons et al. (2006) reported an increased proliferation of mouse embryonic stem cells (mESCs) and alkaline phosphatase expression at 5% oxygen compared to 20%

oxygen. An extensive study from Powers et al. (2008) noticed no significant differences in pluripotency and proliferation rates between 5% and 20%. However they reported a reduction in the expression of the pluripotency markers Oct4, Nanog and Sox2 at very low (0-1%) and high (40%) pO_2 values as well as decreasing growth rates over time. Similar results are obtained at 1% oxygen by Jeong et al. (2007). He proposed that the high concentration of HIF-1α (hypoxia inducible factor) promotes the suppression of LIF (leukemia inhibitory factor), commonly used in mESC culture to maintain a pluripotent state. The suppression of LIF has as a consequence decreased proliferation rates. In summary, very low oxygen levels (under 5%) seem to weaken the ability of mESCs to proliferate and maintain a pluripotent phenotype. Between 5% and 20% oxygen, results reported are often conflicting.

1.2.2.2 Proliferation of human embryonic stem cells

Low oxygen levels (or hypoxia) do not appear to have the same impact for human embryonic stem cells (hESCs). Two studies on the transcriptome of populations exposed to low (2-4%) and atmospheric pO_2 values (Forsyth et al., 2008; Westfall et al., 2008) reported no change in the expression of Oct4, Nanog and Sox2 . They also noticed an increasing heterogeneity of the transcriptomes among the cell lines studied under atmospheric conditions that could be linked to the appearance of subpopulations that begin to differentiate. Lefty2, one of the downstream targets of Oct4, Nanog and Sox2, is upregulated at 4% oxygen when compared to culture at 20% (Forsyth et al., 2008). Lefty2 belongs to the TGFb (transforming growth factor beta) family that is thought to prevent differentiation. Another factor involved in the maintenance of pluripotency, Notch, is upregulated at low oxygen levels (Prasad et al., 2009). Gustafsson et al. (2005) highlighted that there could a beneficial interaction between Notch and HIF-1a that stabilizes the Notch intracellular domain and strengthen the undifferentiated phenotype. In conclusion, low oxygen levels (<4%) seem to promote the maintenance of pluripotency in hESCs.

1.2.2.3 Differentiation

There seems to be a consensus that stem cell differentiation greatly benefits from hypoxia. Significant increase of the conversion of neural stem cells (NSCs) into neurons have been reported with mouse lines at 3.5% (Kim et al., 2008) and at 2%

oxygen (Mondragon-Teran et al., 2009). Kim *et al.* highlighted the role of HIF-1a in the neuronal differentiation by knocking-down its expression and observing a decrease of the differentiated cells number. The same strategy applied to cardiomyocyte differentiation has shown a suppression of the spontaneously beating phenotype (Ateghang et al., 2006). Another study (Powers et al., 2010) established that 5% oxygen is the optimum for cardiomyocyte differentiation with respect to MF-20-positive (a cardiomyocyte marker) cell number and beating area. The cells have been cultured and differentiated on silicone membranes to improve oxygen transfer; therefore the results cannot be solely attributed to hypoxia: mechanical properties of the substrate certainly had an impact on the final outcome of the differentiaton. HIF-1a is not the only factor affected by low pO_2 values, VEGF (vascular endothelial growth factor) expression is also increased. VEGF is responsible for the differentiation to endothelial cells and hematopoietic progenitor. At low oxygen levels, VEGF will be bind to Flk-1 to promote endothelial differentiation (Purpura et al., 2008). As a consequence, in the embryo, the vascular network will develop in the tissue deprived of oxygen. In culture at 20% oxygen, Flk-1 is inactivated, and stem cells are committed to become hematopoietic progenitors. In conclusion, hypoxia is widely reported to promote the differentiation in neural, cardiac and endothelial lineage through the active of key molecules such as HIF-1a and VEGF.

1.3 Oxygen transfer in adherent culture systems

Current lab-scale techniques for adherent cells and tissue culture rely on the use of polystyrene vessels placed into atmosphere-controlled incubator. It is commonly assumed that the passive oxygen transfer from the incubator's atmosphere to the growth medium is sufficient to meet cells requirements. However plastics are poorly permeable to oxygen and therefore cells are only supplied in oxygen through one-dimensional diffusion from the culture headspace to the bottom. In that case, medium height is the limiting factor to oxygen diffusion.

It has been stated by McLimans et al. (1968) that hepatic epithelial cell cultures cultured in a standard CO_2 incubator are under hypoxic conditions as soon as medium height becomes superior to 0.2 centimetres. Metzen et al. (1995) showed that oxygen requirements of confluent cultures from different cell types (endothelial, mesangial and epithelial) could not be met in 24-wells dishes (0.52 cm medium height).

Powers et al. (2010) created a model of peri-cellular oxygen level evolution in 24-wells polystyrene plates taking in consideration cell density, medium height and gas-phase oxygen tension (equation 1). He showed that with normoxic conditions in the incubator (142 mm Hg or 20% O_2) and a medium height of 5 mm, a culture that has the same oxygen uptake rate than mammalian fibroblasts would be under hypoxic conditions (pO_2 < 5 mm Hg) as soon as it reaches a density of 3.10^5 cells/cm^2.

$$\frac{D\alpha}{L}\left[pO_{2\,gas} - pO_{2\,cell}\right] = \rho\left[\frac{V_{max}pO_{2\,cell}}{K_m + pO_{2\,cell}}\right]$$

Equation 1: Steady-state model of oxygen transfer rate and oxygen uptake rate in static adherent cell culture vessels (Powers et al., 2008); D is the diffusivity of oxygen in cell culture medium, α the solubility, V_{max} the maximum oxygen uptake rate, L the medium height, ρ the cell density, K_m the Michaelis-Menten constant for oxygen consumption, $pO_{2\,gas}$ the oxygen partial pressure in the gas phase and $pO_{2\,cell}$ the oxygen partial pressure at the peri-cellular level.

The Dahmkohler number (equation 2) is a useful parameter to assess oxygen transfer in static systems. It measures the ratio between reaction and diffusion time scales.

$$Da = \frac{\tau_d}{\tau_r} = \frac{V_{max} h \sigma}{D C_{in}}$$

Equation 2: Dahmkohler number; τ_d is the diffusion time constant, τ_r the reaction time constant, $V_{max}$the maximum oxygen uptake rate, h the medium height, σ the cell density, D the diffusion coefficient and C_{in} the initial concentration.

Using Dahmkohler number, Young and Beebe (2010) introduced the concept of critical perfusion time (CPR) for adherent cells cultured under continuous perfusion. They proposed a new dimensionless number, κ (equation 3), to determine which of diffusive or convective transport is dominant in a perfusion system.

$$\kappa = \frac{L V_{max} \sigma}{U_m C_{in} h}$$

Equation 3: L is the length, V_{max} the maximum oxygen uptake rate, σ the cell density, U_m the flow velocity, C_{in} the concentration at the beginning of the channel and h the channel height.

If κ is <1, oxygen will be entirely consumed by the cells before the end of the microchannel. If κ = 1, the concentration will reach zero exactly at the outlet. Finally if κ > 1 convective transport is dominant and oxygen will pass through the microchannel without being totally depleted. For κ =1, it can be calculated the corresponding critical flow rate for which oxygen will entirely consumed at the end of the microchannel.

1.4 Microfluidics

Microfluidics is the science of systems handling very small volume of fluids (10^{-6} to 10^{-18} litres). Microfluidic devices offer various advantages for analytical applications: small quantities of samples and reagents, high resolution and sensitivity, fast response times, compact-sized devices, control of spatial and temporal gradients and patterns (Whitesides, 2006).

Microfluidics has its foundation in the development of microfabrication methods, such as photolithography in 1959 for the semiconductor industry. Progresses made in the microelectromechanical systems (MEMS) and the development of high-resolution analytical methods like capillary electrophoresis gave birth to the field at the beginning of the 1980s. At first applied to sensors and analytical systems, it started to be applied to biological process in the 1990s with the launch of several biodefense programs by the US agency DARPA (Defence Advanced Research Projects Agency).

1.4.1 Fabrication methods

Current fabrication techniques in microfluidics originated in the microelectronics and polymers industries. Photolithographic methods have been used for decades to produce microprocessors. Photolithography is the process of producing structures on a substrate, like glass or silicon, using an energy source (commonly an UV light). A layer of photosensitive photoresist is spin coated on a wafer of substrate and exposed to the energy source through a photo-mask that replicates the features wanted. Exposed photoresist can be dissolved in a developer solution, (exposing the substrate). Features are then created on the substrate by dry (plasma) or wet (chemical) etching. Very small features can be obtained with photolithography, as the minimum feature size is theoretically of the size of wavelength of the energy source employed. The most advanced techniques in development like extreme UV or soft X-ray could achieve resolutions inferior to 100 nm (Xia and Whitesides, 1998).

Fast prototyping methods based on replica molding form the basis for fabrication of microfluidic devices. A negative master of the features is created by photolithography or direct machining, and then an elastomer is casted against the

master to replicate the relief structures on its surface. The advantage of this method is that a single master can be used to create quantities of microfluidic chips, reducing fabrication times. If the master is made by photolithography, expensive chrome masks can be replaced by transparencies on which the patterns have been transferred by high-resolution printer, allowing resolution greater or equal to 20 µm (Duffy et al., 1998).

Traditional photolithographic methods reach the needs for the modern electronics, but present a series of hurdles for chemists, biochemists or biologists interested to use microfluidics devices. It requires specific equipment and facilities, materials used are expensive and complex structures are often long to produce, as they require several photolithographic steps.

1.4.2 Cell culture in microfluidics

Microfluidic systems are particularly suitable for cell culture applications. Because they use small volumes of reagents, they provide a cost-effective solution for screening and characterisation of cell populations. In addition the use of predictable flow and mass transfer patterns permits to test the effect of the microenvironment on cells.

1.4.2.1 Materials

Cell-based microsystems make extensive use of poly(dimethylsiloxane) (PDMS), a optically transparent elastomer known as non-toxic and biocompatible. Being a soft polymer, it allows integration of pneumatic valves and pumps (Unger, 2000). Optical sensors monitoring essential parameters like OD, pO_2, pH can be easily implemented as well as cell imaging, making PDMS a material of choice for cell culture chamber. In addition, it is gas-permeable allowing the exchange of oxygen and carbon dioxide between the media and the atmosphere, which are essentials for cell growth and pH control in mammalian cultures. On the fabrication aspect, PDMS chip are easily produced by replica molding from masters obtained by photolithography or micromachining techniques. Sealing of PDMS device can be achieved irreversibly by plasma treatment or reversibly by clamping. PDMS is cheap and therefore is the perfect material for disposable devices, avoiding the issues of long-term matrix degradation and re-sterilization. However, the

microfluidic community has highlighted some characteristics of the PDMS that may limit its use as universal material for microscale cell culture. Water vapour, as well as organic solvents, is able to permeate PDMS, leading to evaporation of culture medium, which can cause important changes in osmolarity, especially at the scale of microfluidic reactors (Kim et al., 2007). Small molecules like hormones can also be trapped in the polymer matrix and modify the metabolism of cells that are exposed at long-term to PDMS surface (Regehr et al., 2009).

Polystyrene, which is the most common material for cell cultureware, could be an interesting alternative to PDMS. Fabrication techniques for thermoplastic devices are well known and cell culture on polystyrene is well characterized as it has been used for decades in research facilities (Berthier et al., 2012). However the poor permeability to gas of this polymer makes unrealistic that it could totally replace PDMS for microfluidic cell culture. Future microfluidic bioreactors will probably combine the advantages of different materials to obtain the most suitable environment for cells.

1.4.2.2 Microenvironment control

Microfluidics provides several ways to control the environment of the cells. Delivery and removal of soluble factors, as well as shear stress, can be modulated by fluid flow. Cells can be confined on specific area by creating 3D microstructures (Jung et al., 2001; T. H. Park and Shuler, 2003), modifying the chemical composition of the surface (Jiang et al., 2005; Nakanishi et al., 2008) or using electric fields (Mittal et al., 2007; Suzuki et al., 2008). Laminar flow regimes allow easily predicting mass transfer to design systems able to reach cells requirements and to create concentration gradients to study the effects of soluble factors on cells (Dertinger et al., 2001).

Because the different components of the microenvironment act often synergistically to determine cell fate, it is important to examine the combinatorial effects of soluble factors, matrix interactions and physicochemical parameters and for that take advantages of the features of the microscale to design systems able to control independently multiple variables.

1.4.2.3 Oxygen control

Microfluidic reactors use two strategies to delivery oxygen to the cells: perfusion and membrane aeration. In perfusion, oxygen is delivered with the medium flow in the culture, the main limitation being oxygen solubility and flow rate. In membrane-aerated system, oxygen is transferred through a gas-permeable layer like PDMS in the culture chamber: delivery is independent of perfusion flow rate and thus that strategy is particularly suitable for batch culture. In static membrane-aerated systems, the limiting factors are oxygen solubility and medium thickness (McLimans et al., 1968; Metzen et al., 1995).

Mehta and Korin established in their respective studies (Korin et al., 2007; Mehta et al., 2007) the existence of axial oxygen gradients along the channels of perfusion systems, using mass transport models. The combination of the cellular oxygen uptake rate, diffusion rate through the medium layer and convective mass transport by the flow creates such concentration differences. It is possible to reduce these gradients by increasing flow rates but then it has to be balanced with the increase of shear stress generated. Such results demonstrate that the supply of oxygen solely by perfusion may be not the best method, as changing the flow rate has many other consequences on the microenvironment (increased shear stress, wash-out of cells and soluble factors).

Membrane-aerated systems have been used with success to grow cells. Microfluidic reactor stacking culture chambers and oxygen chambers separated by 300µm-thin PDMS walls have been realized for hepatocytes (Leclerc et al., 2004) .Whereas oxygen was not monitored in that system, a 2.5 fold increase in final cell density, compared to culture dish, has been obtained. Mehta proposed a simple design combining perfusion and membrane aeration to infer oxygen uptake rate from cell densities, combining mathematical models for spatial distribution of nutrient and growth factors and oxygen measurements by fluorescent dye in four different points of the microchannel (Mehta et al., 2009). Vollmer designed a micro-oxygenator device composed of two layers of PDMS separated by a 20µm PDMS membrane (Vollmer et al., 2005). Upper-layer channels carry gas above the fluidic network and two oxygen optodes are placed upstream and downstream of the fluidic channels to measure initial and final oxygen levels in the liquids. Experimental

results matched with the prediction of a simple convective mass transfer model. Although no cells have been cultured in that device, it constitutes an interesting proof-of-concept for active aeration through a membrane.

1.4.2.4 Oxygen monitoring

Traditionally oxygen monitoring in bioreactor is carried using polarographic sensors such as Clark-type electrodes. Measurement is accomplished through the reduction of the cathode by oxygen molecules, generating an electrical current. Oxygen being depleted during the process, such sensors usually requires stirring in order to maintain equilibrium with the environment. For microfluidic applications, polarographic sensors are usually poorly adapted due to difficulty in miniaturization, clogging of the oxygen-permeable membrane by proteins, signal variations in non-stirred environment and oxygen depletion.

Optical detection methods constitute an alternative to electrochemical sensors. They are based on the quenching of fluorophores like ruthenium by oxygen molecules. Fluorophores can be immobilized in polymer matrix to create sensor spots (optodes) that can easily be integrated in a microfluidic chip. Based on the Stern-Vollmer relationship, fluorescence is not linear with oxygen concentration but provides high-sensitivity at low oxygen concentrations. In addition, oxygen is not consumed by the sensor, which makes optodes particularly desirable for small volumes or non-stirred systems (Nock et al., 2008).

1.4.2.5 Stem cell culture devices

Microfabricated devices have been already used to culture stem cells. These devices fall into two main categories: those that take advantages of the microscale features and microfabrication techniques to investigate parameters that are unreachable by conventional culture methods and those that rely on multiplexing and complex fluidic automations to enable high-throughput screening of culture variables. At the microscale, the predominance of laminar flow and diffusive mass transfer has been used to design soluble gradient generators and maintain a “steady-state” soluble environment. Gradient generators allowed to study human neural stem cell differentiation in response to a gradient of two different growth factors (Chung et al., 2005). Similar studies have been realised with cytokines gradients (J. Y. Park et al.,

2009) or embryoid bodies exposed to two different factors (Fung et al., 2009). Gradient generators have been as well used to perform specific operations (staining, enzymatical treatment) on localized sections of the culture chamber (Villa-Diaz et al., 2009). Perfusion microfluidic devices have been as well used to investigate the effect of flow rate (as a vector of shear stress and/or nutrients) on stem cell cultures (L. Kim et al., 2006; Korin et al., 2009). Others culture devices rely on microfabrication techniques such as micro-printing and micro-patterning to study the effect of the ECM on stem cells expansion and differentiation (Lanfer et al., 2009), the influence of mechanical forces on the formation and maintenance of embryoid bodies (Karp et al., 2007; Khoury et al., 2010). Multiplexed microfluidic devices can create and maintain independent medium conditions in each of the culture chambers, thus enabling high-throughput screening of relevant soluble factors for stem cells proliferation and differentiation (Gomez-Sjoberg et al., 2007).

The current variety of microfluidic devices developed for stem cell culture offers accurate control on the soluble, physical and mechanical microenvironment, however it still suffers the same limitations than traditional culture methods in term of analytics: there is no online monitoring of the culture variables, environment control is based on modeling/cell-free experiments and the results generated are mostly endpoint staining of relevant pluripotency and differentiation markers.

1.5 Research objectives

It is hypothesised that a microfabricated culture device for adherent stem cell culture will provide a better control over the cellular microenvironment than conventional static culture vessels. Thus such a device may constitute a better tool to understand and control the interactions between cells and their microenvironment and to develop robust bioprocesses for the production of stem cell-derived products such as cell therapies or *in vitro* models for diseases studies and drug discovery. However, to unlock fully the potential of such a device for the development of stem cell bioprocesses, it is needed to couple it with monitoring systems to quantify the changes in critical culture variables during the process. Among the culture variables, oxygen is one of the most critical as it drives not only aerobic cell metabolism but also stem cell fate, and its transport in liquid cultures is limited by its low solubility.

The research in this thesis aims to develop an online oxygen-monitoring platform around an existing prototype cell culture device to provide non-invasive measurements of dissolved oxygen concentrations in adherent stem cell cultures. The monitoring platform should be capable of measuring bulk oxygen levels, to quantify the cellular oxygen uptake rate, and peri-cellular oxygen levels to assess at what oxygen levels the cells are effectively exposed in their microenvironment and how it may modulate cell response. It is therefore necessary to select the location of the oxygen sensors in the system accordingly. The monitoring platform should also integrate seamlessly with the existing cell culture device to enable robust operation and consistent experimental outcome in long-term cultures. Seamless integration requires particular considerations in terms of design, fabrication and integration of the components but also in terms of operation of the culture system. Preparation and operation of the system should satisfy the requirements for aseptic cell culture. Finally, the oxygen-monitoring platform should not restrict the use of other monitoring techniques such as cell imaging by phase-contrast microscopy. The coupling of oxygen and cell growth monitoring would enable to study non-invasively cellular oxygen kinetics in adherent cell cultures and therefore it is valuable that the integration of oxygen monitoring to the cell culture device enables such coupling.

2 Materials and methods

2.1 Fabrication

2.1.1 Design

Moulds and devices' parts were designed with a 3-D CAD software (SolidWorks, Dassault Systems, France). The corresponding CNC-machine code was generated using a CAM software (Mastercam X4, Mastercam, USA).

2.1.2 Micromilling

All parts and moulds were fabricated with a micro-milling machine (M3400E, Folken Industries, USA) using standard length, 2 flute end mills (Kyocera Micro Tools, USA) at 7000 RPM, and 104 $mm.min^{-1}$. Device's parts were milled out of 3 and 5 mm thick polycarbonate sheets (RS, UK) using 2 mm and 1 mm end mills. Moulds were milled out of 5 mm thick PMMA sheets (RS, UK). The aluminium parts presented (bottom frame and brackets) were fabricated by firstcut® CNC Machining Service (Proto Labs, UK).

2.1.3 PDMS chip casting and bonding

PDMS (Sylgard 184, Dow Corning, USA) base with mixed with its curing agent at 10:1 w/w ratio. The mixture was degassed in a vacuum desiccator until no bubble was visible and poured into the mould. The mould with the PDMS was then degassed again to remove any air bubble introduced during the casting. The mould was closed with a 1 mm thick polycarbonate sheet and clamped between two 10 mm thick aluminium plates secured with 4 screws tightened at 250 Ncm. The assembly was placed in an oven to cure the PDMS at 85˚C during at least an hour. The chip was later released from the mould using tweezers.

To fabricate the support layer for the cell culture chip, PDMS was spin-coated on a silicon wafer. To prevent sticking of the PDMS, a 4 inches silicon wafer (Prolog Semicro, Ukraine) was treated with 200 µL of trichloro(1H,1H,2H,2H-perfluorooctyl)silane (448931, Sigma-Aldrich, UK) in a vacuum desiccator for one hour. 5 mL of degassed PDMS were dispensed in a spiral pattern on silanised wafer placed in a spin coater (P6708D, Specialty Coating Systems, USA). The wafer was then spun down at 500 rpm for 50 seconds and placed in an oven at 85˚C for at least one hour to cure.

To bond the support layer with the culture chip, the spin-coated wafer and the cured chip were placed in a plasma asher (PDC-002, Harrick Plasma, USA) and exposed to air plasma at 500 mTorr and 30 W for 90 seconds. The chip and the layer were then brought in contact and placed in an oven 85˚C for at least 2 hours. The bond chip was then released from the wafer by cutting along the edges and the borders of the culture chamber with scalpel.

2.1.4 Ruthenium/PDMS optode casting

The oxygen-sensitive Tris(4,7-diphenyl-1,10-phenanthroline)ruthenium(II) dichloride(Ru(dpp)) complex (76886, Fluka, UK) was weighted and dissolved in ethanol at a concentration of 1 mg/mL. The resulting solution was mixed with the PDMS base and curing agent (Sylgard 184, Dow Corning, USA) at a 1:10:1 v/w/w ratio. The mixture was then degassed, casted and cured following the procedure described in 2.1.3.

2.2 Oxygen monitoring

2.2.1 Intensity measurement setup for ruthenium/PDMS optodes

The sensor material was mounted on a glass slide and placed on the top of an inverted fluorescence microscope (Eclipse TE2000-U, Nikon, Japan) equipped with a camera (Scout scA1400, Basler Vision Technologies, Germany). A cardboard cover was fitted on the top of the stage to decrease the fluctuations in light intensity due to the environment. Two holes created on the top of the cover allowed introducing different gas mixtures (2-4-8-21% O_2/5% CO_2, BOC, UK) above the sensor.

The sensor was excited at 540 nm using an epifluorescence illumination system (IntensiLight C-HGFI, Nikon, Japan) and filters (MBE 45600 C-FL Epi-Fl FilterBlock TRITC, Gentaur, Belgium) and images of the emission at 590 nm were manually captured using an image acquisition software (NIS Elements F, Nikon, Japan).

For the acquisition of the signals emitted by multiple sensors in the chamber of the microfabricated culture device, a motorised stage (MLS203-E, Thorlabs, UK) was added to the microscope. The stage was controlled by a LabVIEW routine (National

Instruments, USA) allowing to zero the coordinates to a user-set position, record that current position, store it in a spreadsheet and recall stored positions in sequence. The routine allowed automated and repeated alignment of the microscope optics with the sensors to acquire timelapse sequences.

To quantify the mean intensity of the sensor, images were processed using the open-source image analysis package ImageJ (NIH Research Services Branch, USA). The sensor area was manually selected using the oval selection tool. Grey pixel values in the selected field were averaged using the function *histogram* and exported in a spreadsheet. Average pixel values were diving by 255 (grey pixel values are coded between 0 and 255) to obtain a normalised value between 0 and 1.

2.2.2 Commercially available optodes

Flow-through cell optodes (FTC-PSt3, PreSens Precision Sensing GmbH, Germany)

A 2 mm diameter, 125 µm deep recess was milled by CNC-machining centred into a TC-PS slide (Nunc Polystrene microslide 160004, Thermo Fischer Scientific, USA). A planar oxygen sensing spot (PSt3, PreSens Precision Sensing GmbH, Germany) was cut down to 1 mm diameter using a hole-puncher, and inserted in the recess of the slide. PDMS was cast to fill the void in the recess around the sensor. The slide was then placed in an oven at 85˚C for at least an hour to allow the PDMS to cure. In addition, bespoke glass slides with 1 mm diameter patterned sensor flush with the surface level were designed in-house and manufactured by PreSens Precision Sensing GmbH.

2.2.3 Measurement setup for commercially available optodes

Flow-through cell optodes were connected to a transmitter (Oxy-4 mini, PreSens Precision Sensing GmbH, Germany) using 2 mm internal diameter optical fibres with SMA connectors (POF-L2.5, PreSens Precision Sensing GmbH, Germany).

Planar sensors integrated in the microfabricated culture device (see 2.3.1) were interrogated using using optical fibre brought in close proximity of the culture slide underneath the microfabricated device. To align the fibre tip with the sensor a SMA

flat Adapter (PreSens Precision Sensing GmbH, Germany) and a bespoke SMA adapter for microscope objective (UCL, UK) were used

2.3 Microfluidic culture platform

2.3.1 Microfabricated culture device

The microfabricated culture device was derived from a previously established design (Reichen et al., 2012). It consisted of disposable PDMS parts (culture chip and sealing gasket), a reusable packaging in polycarbonate (frames, interconnects, lid) and a microscope format slide in TC-PS or glass (figure 1).

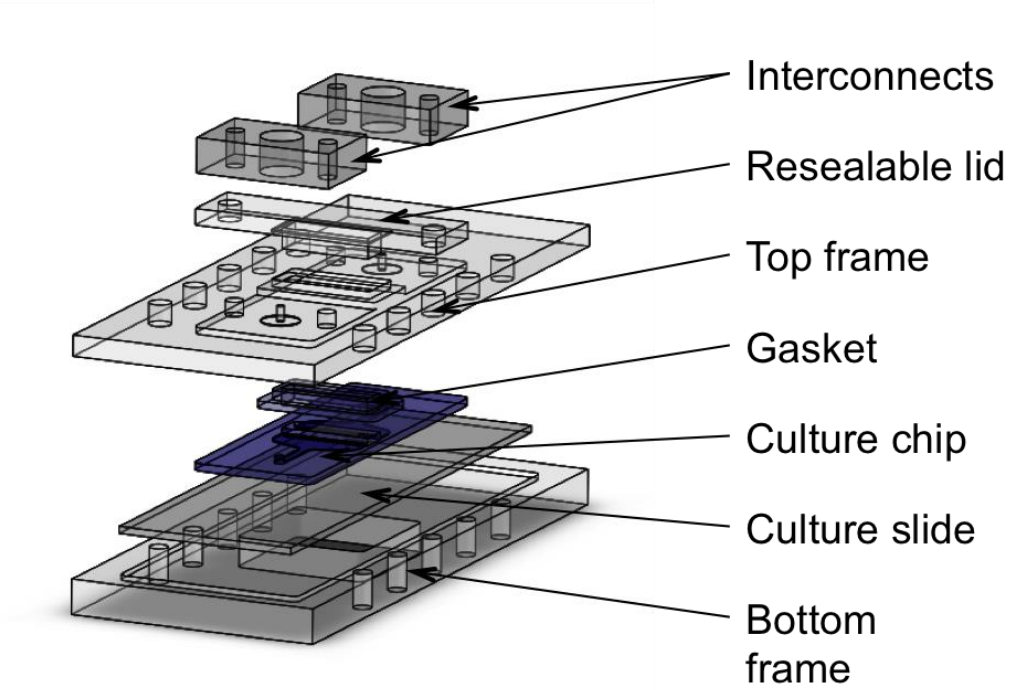

Figure 1: Exploded view of the microfabricated culture device.

The top frame (87 mm x 36.5 mm x 3 mm) was milled out of PC (see section 2.1.2) and included an opening matching the position and footprint of the culture chamber. The bottom face of the frame had two recesses: one of the dimensions (50 mm x 20 mm x 0.8 mm) of the PDMS culture chip in order to align it with the fluidic connections and the chamber opening, and another 1 mm deeper to hold the sealing gasket between the culture chip and the lid. The top frame also had 10 bores (2.80 mm diameter) near its edges that served to align and clamp with the bottom frame. Two additional set of bores (2.50 mm diameter) on each side of the fluidic ports

(0.80 mm diameter) enabled attaching the fluidic interconnects. Around the fluidic ports, on the bottom face, a boss (5.50 mm diameter, 0.125 mm height) enabled sealing by pressing against the PDMS culture chip.

The parallelepipedic interconnects (20 mm x 12 mm x 5 mm) had a threaded bore (1/4-28 UNF) in their center to accomodate a male thread to male Luer adapter (P-683, UpChurch Scientific, USA), allowing connection with external fluidic systems (figure 2a). Complete sealing between the fittings and the top frame was enabled by the addition of a flat bottom nanoport gasket (N-132-02, Anachem Instruments, UK) in the threaded bore (figure 2b).

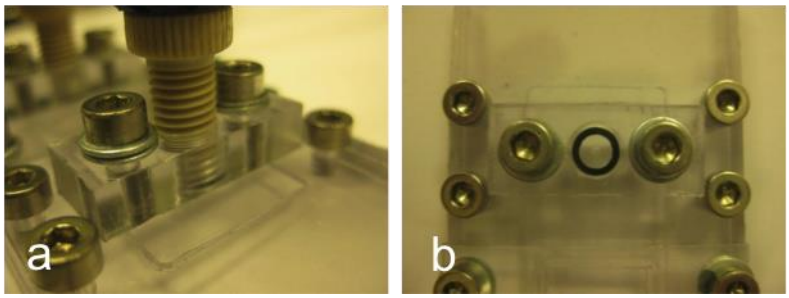

Figure 2: Interconnects on the microfabricated culture device. (a) thread to male Luer adapter screwed in the interconnect bore. (b) top-down view of the interconnecting bore. showing the position of the nanoport gasket providing sealing between the fitting and the top frame

The culture chip was made out of a two PDMS layers: the main fluidic layer (50 mm x 20 mm x 0.9 mm) and a support layer (50 mm x 20 mm x 0.120 mm) placed underneath. The main fluidic layer featured flow equalization barriers placed on each side of the central culture chamber (4 mm x 13 mm). The chip sat on a microscope format (75 mm x 25 mm x 1 mm) culture slide acting as the substrate for adherent cell culture.

The bottom frame had the same footprint than the top frame and a matching set of threaded (M3) bores. Its recess matched the dimensions of the microscope slide. An opening in the centre was designed to bring into proximity of the slide optical fibre ends for DO monitoring or inverted microscope objectives for cell imaging.

The T-shaped lid was composed of an upper bar acting as a bed stop against the top frame and a lower bar pressing against the gasket to seal the culture chamber. This defined a chamber height of 450 µm and a chamber volume of 23.4 µL perfusion system.

The pump consisted of a gas pressure regulator (ITV0011-2BL-Q, SMC, UK) and a liquid reservoir (250 ml amber pressure-resistant DURAN bottle, Schott, Germany).

A cylinder of cell culture gas mixture (21% O_2/5% CO_2/N_2, BOC, UK), fitted with a two-stage regulator, was connected to the inlet of the pressure regulator using pneumatic tubing (SMC, UK).

A 3-ports screw cap (GL-45, Schott, Germany) sealed the liquid reservoir. Connections were created on the three ports using autoclavable tubing (R1230, Upchurch Scientific, USA), flangeless M6 nuts (P-207, Upchurch Scientific, USA) and female M6 to male Luer lock adapters (P-660, Upchurch Scientific, USA). One of the connections was fitted with a sterile air particle filter (Minisart 16556HY, Sartorius AG, Germany) that was connected to the outlet of the pressure regulator. The second port was used to connect the reservoir to the microfabricated culture device using autoclavable tubing and Luer-lock fittings. The last port was closed with a Luer-lock female cap and could be used as an exhaust port to release pressure from the headspace if needed.

The pressure regulator was connected to a DAQ card (NI USB 6008, National Instruments, USA), connected by USB to a computer, to the control voltage using a LABView routine (National Instruments, USA). The pressure regulator was powered by a 12.5V DC source (EP-920, Eagle Technologies, South Africa).

2.3.2 Setup for pressure and flow-rate measurements

To measure the pressure generated in the fluidic system in function of the control voltage of the pressure regulator, a pressure sensor (40PC100G, Honeywell Inc., USA) was glued to a flangeless nut (P-207, Upchurch Scientific, USA) with an epoxy resin and inserted (see figure 1) between the reservoir outlet connection and the inlet of the microfabricated device using a three-way stopcock with Luer lock (92845x, Polymed, Italy). A LABView routine was used to record and convert in pressure values the voltage readings acquired from the sensor with a data acquisition card (NI USB 6008, National Instruments, USA).

To measure the flow rates, the setup was placed in an incubator at 37˚C. The water was collected at the outlet of the system in micro-centrifuge tubes (0030120094, Eppendorf Ltd, UK) previously individually weighed and labeled. The water was

collected in triplicates for 10 minutes for each control voltage tested. The filled tubes were weighed and the empty tube weight subtracted to calculate the mass of water collected. Flow rates were calculated by dividing the mass of water by the time spent to collect it.

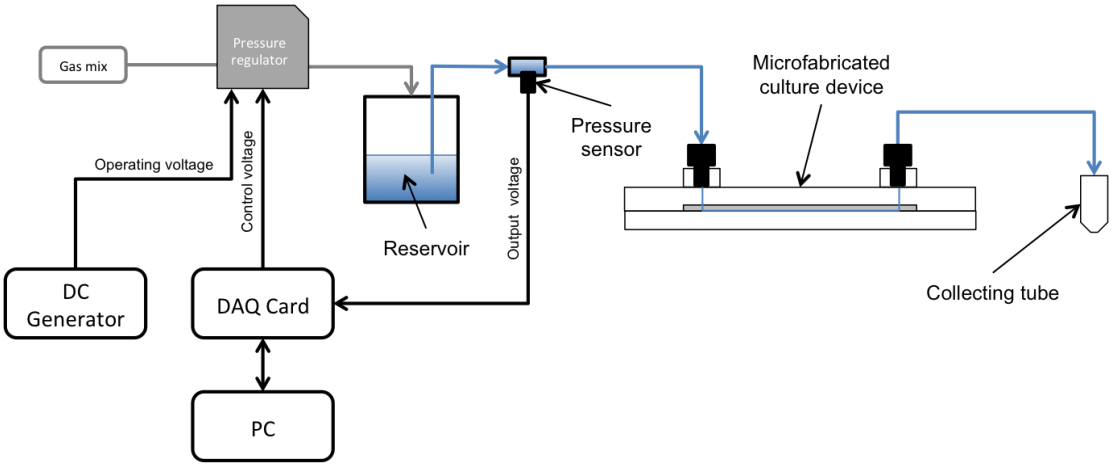

Figure 3: Schematic representation of the setup for flow rate and pressure measurements.

2.4 Cell culture

2.4.1 Mouse embryonic stem cell maintenance and passaging

The E14tg2A mESC line (< passage 50) was used for all the experiments. Cells were cultivated in Knock-Out Dulbecco's Modified Eagle Medium (DMEM) (10829, Gibco, USA) supplemented with 15% (v/v) Fetal Bovine Serum (FBS)(26140, Gibco, USA), 1% (v/v) Modified Eagle Medium Non-Essential Amino Acids (11140, Gibco, USA), 10% (v/v) Glutamax (35050, Gibco, USA) and 0.1 mM ß-mercaptoethanol (31350, Gibco, USA). 10-6 U.L-1 Leukemia Inhibition Factor (LIF)(ESG1106, Millipore, UK) were added after sterile filtration (Vacuum Filtration System PES 0.2µm, TPP, Switzerland). For passaging, cells were washed with Dulbecco's Phosphate Buffer Solution (DPBS) (D1408, Sigma-Aldrich, UK), and incubated 3 minutes with 2 mL Trypsin-EDTA (T4049, Sigma-Aldrich UK). 5 mL of fresh medium was then added to quench the trypsin and the total was collected and spun down at 300G for 3 minutes (Heraeus MultiFuge X3R, ThermoScientific, USA). The supernatant was then carefully discarded and the pellet resuspended in medium and seeded at a 1:10 ratio in T-25 flasks (Nunc EasYFlask 156367, Thermo Fischer Scientific, USA) pre-coated with 0.1% DPBS Gelatin (G1890, Sigma-Aldrich, UK) for 10 minutes at room temperatures.

2.4.2 Immunocytochemistry

Cells were fixed in 4% paraformaldehyde (43368, Alfa Aesar, UK) for 15 min at room temperature and then permeabilised with 0.25% Triton X-100 (BP151, Fisher Scientific, UK) for 10 min. Anti-Nanog and Anti-SSEA-1 (ab107156, abcam, UK) were used as the primary antibodies, diluted (1:200) in 5% FBS and incubated with cells one hour at room temperature. Primary antibodies were detected using the corresponding secondary antibodies (Alexa Fluor® 488 Goat Anti-rabbit IgG, Alexa Fluor® 555 Goat Anti-rabbit IgG, Santa Cruz, USA). Samples were imaged using phase-contrast and epifluorescence microscopy (Inverted Microscope System Ti-E, Nikon Ltd, UK with CoolLED).

2.4.3 Cell counting

To prepare the inoculum for experiments in the microfabricated device, the cells harvested from maintenance cultures (see 2.4.1) were manually counted in a haemocytometer (Improved Neubauer AC1000, Hawksley, UK). The counts of four big squared areas were averaged and multiplied by 10^4 to obtain the cell density of the sample.

2.4.4 Confluency determination by image analysis

Phase contrast microscopy (PCM) images of the culture area were acquired manually and automatically with an inverted microscope at a 10x magnification (Inverted Microscope System Ti-E, Nikon Ltd, UK). During manual acquisition, 10 field-of-views were randomly imaged at each time point. The pictures were then processed with PHANTAST (Jaccard et al., 2013) to determine confluency values (http://www.code.google.com/p/phantast). The 10 values were averaged to obtain the mean confluency of the culture at a given time point.

During automated acquisition, 60 field-of-views covering the whole device chamber with a 10% overlap were imaged using the automated microscope stage to recall the recorded positions at each time point. The images were then automatically stitched together and processed to determine confluency with a MatLab routine (MathWorks, USA)(Jaccard et al., 2014).

To approximate cell densities from confluency values, a training set of 120 PCM images was processed with PHANTAST to calculate confluency and corresponding packing-correcting confluency (PCC) values. An exponential function was fitted to establish the correlation between the two. This function was used to convert all confluency value sets in PCC sets. The PCC values were then converted to cell densities by applying a correction factor established experimentally before cell seeding based on the cell counts of the inoculum.

3 Integration of online oxygen monitoring to an adherent cell culture microfluidic device

3.1 Design considerations

Particular considerations must be made when designing an online oxygen-sensing setup for the monitoring of 2-D adherent cell cultures in a microfluidic culture device. Such a setup must be suitable for oxygen measurements in small volumes, compatible with cell culture protocols, and able to extract meaningful information from a non well-mixed environment with minimal effort. It should also be possible to integrate additional sensors to monitor other important analytes of interest, such as pH. Finally, a significant advantage of microfluidic systems lies in the ability of time-lapse imaging of the cell culture by placing the microfluidic system directly on the stage of an inverted microscope (Jaccard et al., 2014). It is therefore also necessary to consider the spatial constraints of the sensors and the ancillary equipment for data acquisition (e.g. connections for read-outs) integrated with the culture device. A particular attention is required to the positioning and dimensions of the sensors in locations such as the culture chamber whose form factor is primarily defined by culture requirements.

3.1.1 Sensor type

Two types of oxygen sensing methods are commonly available: polarographic methods (e.g. the Clark-type electrode) and optical methods (optodes). In a Clark-type electrode, oxygen diffuses through a permeable membrane and is reduced at the cathode, to create an electric current that can be correlated with the oxygen concentration in the environment (Clark et al., 1953). This type of sensor is routinely used for oxygen monitoring in suspension cell cultures. However, it presents several disadvantages for its use in a microfluidic adherent cell culture system that relates to two of its characteristics: the invasiveness of the measurement method and the form-factor of the device. As the oxygen is reduced during the measurement, a continuous transfer of oxygen molecules through the membrane is required to accurately determine oxygen concentration levels in the culture (Barnbot et al., 1995). Therefore the measurement is dependent on the flow at the sensor tip. Thus, a Clark-type electrode operates optimally in well-mixed system such as suspension culture with active mixing, where flow movement ensure the replenishment of oxygen molecules at the sensor tip. In a non-well mixed environment, the oxygen will be depleted at the membrane surface and resulting

measurements will drift towards artificially low values. In addition, the oxygen consumption of these sensors, whilst negligible at larger scales, constitutes a limiting step for measurements of low oxygen tensions (Y. H. Lee and Tsao, 1979) and induces a significant bias in small volume systems. Clark-type electrodes are also typically bulky and therefore difficult to integrate seamlessly in a microfluidic device. The membrane of the sensor is prone to fouling and requires regular cleaning to maintain its transfer efficiency. Therefore the integration must be reversible to allow for the cleaning and maintenance of the electrode and compromises the sterility of the culture and the sealing of the device.

Optical electrodes, or optodes (Lübbers and Opitz, 1976), are based on the dynamic quenching of an oxygen-sensitive dye photoluminescence by oxygen molecules. The higher the oxygen concentration levels, the lower the photoluminescence of the sensor will be. As the quenching is a reversible process, no oxygen is actually consumed during measurement and no stirring is required for optimal results. Therefore, optodes are particularly well suited for adherent cell culture monitoring (Randers Eichhorn et al., 1996) and measurements in small volume (Nock, 2009). There is also no report on flow dependency, thus the sensors are also suitable in perfused microfluidic devices where different flow rates might be used to manipulate the growth conditions of the cells.

3.1.2 Sensor design and location

Optodes come in two different physical implementations: as soluble dyes or as solid layers coated onto a surface. Soluble dyes are injected in an aqueous phase and the emitted fluorescence is quantified by intensity or phase-shift measurements that can be correlated to oxygen concentrations in the aqueous phase by calibration. This approach has been previously used to quantify the oxygen concentration levels in adherent cell culture in microfluidic devices (Mehta et al., 2007; Sud et al., 2006). However it presents several technical and economical disadvantages. As the dye is carried by the culture medium, it is continuously washed out, if used in a perfusion culture. Therefore, in the long term, this approach is not economical, as the dye would be continuously discarded as waste. In principle, recycling the dyes could be considered, however, this adds a layer of complexity to both the design and the

operation of the system. If the monitoring is carried out in batch culture, removal of the dye will still be necessary. Introducing a fluorescent compound in the culture medium may interfere with subsequent luminescence-based analytical methods (such as immunocytochemistry assays for the detection of protein markers), which share overlapping excitation and emissions wavelengths. In addition, it is not trivial to achieve an even distribution of the dye in the culture chamber or the sub-volume of interest to perform accurate intensity measurements. A more elaborate fluidic design may be required to improve mixing and dispersion of the dye. However, improved mixing may increase of the hydrodynamic shear stress and damage the cells grown in the culture device. Phase-shift measurements are largely insensitive to the dye concentration and are therefore more accurate in conditions with the fluorophores might not be homogeneously distributed. However, the cost of fluorescence lifetime imaging modules suited to perform phase-shift measurements on solutions prevent the widespread use of this technique for monitoring purposes. Finally, there are no reports on the potential biological effects of these dyes on cells, and therefore they cannot yet be considered as safe for routine monitoring of bioprocesses.

Oxygen-sensitive dyes can be immobilised in polymer matrices to create patches, which spatially confine the location of the dye. These patches can then be integrated in the culture devices to measure the oxygen levels. As two-dimensional adherent cell cultures are heterogeneous environments with regard to the temporal and spatial distribution of soluble factors (including dissolved oxygen) it is critical to design the spatial arrangement of the sensors accordingly with the type of information one requires. For stem cells, oxygen acts both as a nutrient sustaining cell metabolism and as a signaling molecule, determining the cell fate and potential differentiation in different lineages. Therefore, an oxygen-sensing system must be able to provide the data to enable the investigation of these two aspects.

In order to quantify the oxygen consumption of the culture, the concentrations levels of the dissolved oxygen in the culture medium entering and exiting the culture vessel have to be known. This means that, for a perfusion system, oxygen must be monitored upstream and downstream of the culture chamber. To achieve this, sensors can be integrated in the fluidic system as flow-through cells at the device's inlet and outlet. The balance of the two readouts gives the bulk oxygen

consumption of the culture for a given time point. When measurements are repeated over time, temporal profiles of the oxygen consumption in the culture can be established. If cell densities are known, then specific oxygen uptake rates can be determined. Therefore, integration of online oxygen monitoring in parallel with cell density monitoring would enable to study the effect of the culture conditions (such as medium composition, medium renewal rate, dissolved oxygen tensions, pH, temperature) on the cell growth kinetics.

To understand the effect of oxygen on cell fate during proliferation and differentiation, the level of oxygen to which the cells are exposed (i.e. peri-cellular level) must be known. In adherent cell culture, distribution of oxygen is heterogeneous due to mass transfer dominated by diffusion and dynamic cellular oxygen uptake rates. Therefore, measurement of the bulk oxygen concentrations is not sufficient to investigate the effects of oxygen on cells. Sensors must be as well integrated directly *in situ*: in the culture chamber, in close vicinity of the cells, to obtain an accurate understanding of the peri-cellular oxygen concentration levels.

3.1.3 Sensor integration

The integration of sensors in a cell culture device has to comply with several layers of requirements.

In order to carry out successfully cell studies, the integration has first to comply with the principle of asepsis: sensors must be free of microbial contaminants while in contact with the cells or the culture medium. To achieve that, they should withstand accepted sterilisation methods. Compatibility with a sterilization method is given by the materials constituting the sensors and device as well as by practical considerations such as availability and costs. The materials are limited by other factors: compatibility with 2-D cell culture (promotion of cell adhesion), with imaging (optical transparency), and availability and costs of the fabrication methods. Ultimately, each of these requirements has to be analysed in order to determine the optimal choice of materials for the integration of the sensors in the culture device.

3.1.4 Measurement methods

Using optical sensing methods, oxygen concentrations can be correlated with the light intensity emitted by the excited sensor or with the fluorescence decay time of the dye. The relation between the oxygen concentration and the intensity or phase-shift measured can be expressed by a Stern-Volmer relationship. Intensity measurements can be performed, in a non-invasive way, using fluorescence imaging techniques such as epi-fluorescence microscopy, thus allowing monitoring of oxygen tensions in parallel with other imaging-based analysis. In addition, it can be used to map oxygen distribution on the horizontal plane by acquiring simultaneously multiple sensors in the same field of view. Intensity measurements are therefore a rather simple and inexpensive way to interrogate optical oxygen sensors.

Fluorescence decay time can be detected by a phase-shift measurement. This method has the advantage of being independent of the dye concentration in the optode, making it more reproducible and less dependent on the optode quality and the reliability of the read-out instruments. However it necessitates hardware that enables the creation and detection of an amplitude-modulated signal.

3.2 Results and discussion

3.2.1 Development and integration of optodes

To implement online oxygen monitoring successfully in the existing microfluidic device for stem cell culture, it is necessary to address each of the design considerations described previously in function of the requirements of the existing microfluidic bioreactor design (Reichen et al., 2012) and the objectives set for the monitoring system.

Optodes offer the ability to perform non-invasive oxygen measurements in adherent cell culture in microfluidic devices. However, the heterogeneity of oxygen distribution in the system requires the integration of multiple sensors in the device in order to characterize oxygen consumption rates and peri-cellular concentrations. Oxygen can be measured at the inlet and outlet of the device using commercially available solutions that use standard connections for tubing and fittings and can withstand a range of sterilization methods including autoclaving. For peri-cellular measurements, the optodes have to be placed inside the culture chamber, on the microscope slide where the cells are growing, in a way that doesn't conflict with the existing features of the device such as the possibility to track cell growth and morphology by online imaging. Taking advantage of the modular design of the device, the microscope slide can be independently modified, using rapid prototyping methods such as micromilling and casting/moulding, to integrate planar sensors positioned as desired on the growth surface area inside the culture chamber. These fabrication methods allow the rapid generation of prototypes to test different strategies of peri-cellular oxygen sensors integration.

3.2.1.1 Development of ruthenium-based optodes

The first approach to integrate optodes in the microscope slide was based on the encapsulation of a ruthenium dye in a PDMS matrix as previously described in the literature (Lin et al., 2008; Thomas et al., 2009). Ruthenium salts were dissolved in ethanol and mixed with PDMS to obtain a uniform mixture that would form the sensor once cured.

To characterise the sensitivity of the sensors generated, a test chip was fabricated (figure 4). The chip was composed of a 1 mm-thick PDMS layer, bearing 200 µm deep recesses on the top with diameters of 0.4, 1, 1.5 and 2 mm. it was fabricated by moulding against a PMMA negative replica, The ruthenium/PDMS mixture was poured in the recesses of the support chip and cured. The chip was placed on a glass slide supported by a polycarbonate frame providing rigidity to the ensemble. The format of the frame was designed to fit the sample holder of the microscope used for measurements. Gas mixtures at known oxygen concentrations were blown above the chip. The epifluorescence system of the microscope was used to excite the sensors and acquire the read-outs. Using image analysis software packages, the pixel values of the sensor area were quantified and averaged in order to establish calibration curves.

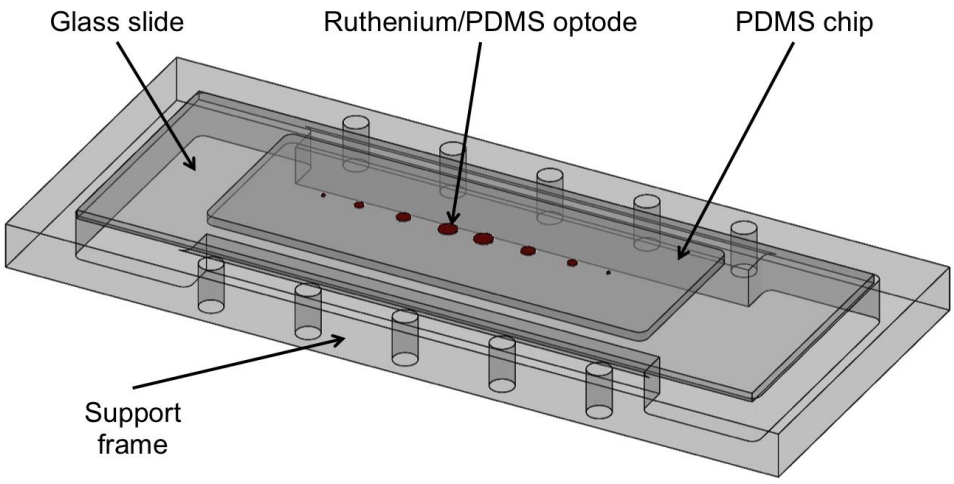

Figure 4: CAD rendering of the testing chip for ruthenium/PDMS optodes characterization.

To test the optodes in conditions closely resembling cell culture conditions, TC-PS slide was machined to create three recesses (200 µm deep, 1 mm diameter) aligned perpendicularly to the direction of flow. Ruthenium/PDMS was cast in the recesses and cured together with the slide to create three sensing spots. The resulting

assembly was used with the microfabricated perfusion culture device to test the optodes under continuous flow (figure 5).

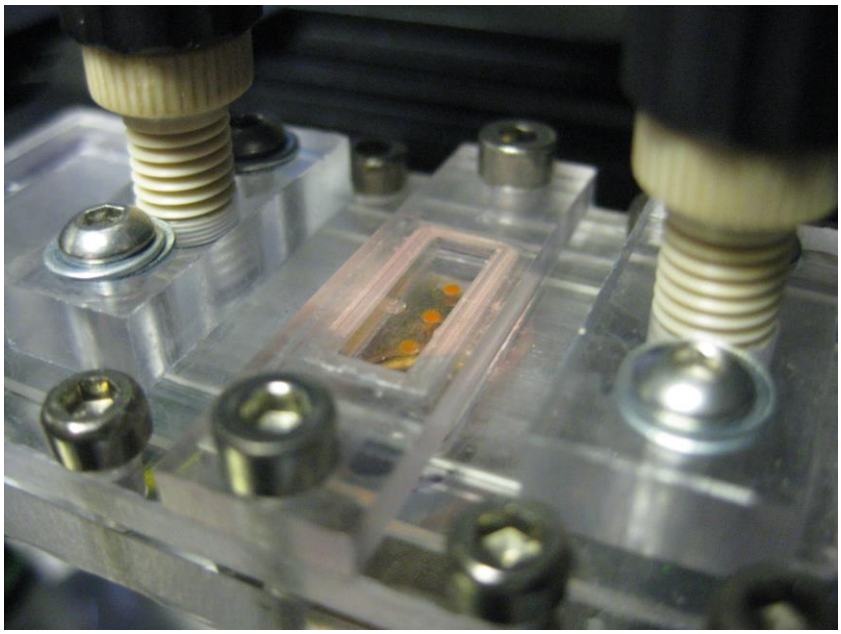

Figure 5: Close-up picture of the culture area in the microfabricated culture device with three ruthenium/PDMS optodes patterned on the substrate slide.

3.2.1.2 Design & fabrication

Optodes for the detection of oxygen were designed and developed, based on the encapsulation of an oxygen-sensitive ruthenium dye in a PDMS matrix. PDMS presented several advantages for this application. PDMS has been widely used for cell culture applications, due to its low cytoxicity and therefore the optodes shouldn't impact the outcome of the culture they are placed in. Cured PDMS can be sterilised by autoclave. Its high permeability to oxygen (Merkel et al., 2000) allowed creating single layer sensors, where the dye is uniformly dispersed in the matrix, simplifying the fabrication process to a single step of casting and curing. The simplicity of the fabrication process allowed the rapid generation of prototypes for testing different design and configuration of sensors.

A testing chip was developed in order to determine the optimum sensor diameter and characterize the sensitivity of the oxygen measurements. Given the footprint of

the culture chamber (4 by 13 mm), the maximal possible diameter for a sensor was set at 2 mm. Recesses with diameters of 0.4, 1, 1.5 and 2 mm were created in duplicate in a PDMS chip by moulding against a negative master. A mixture of Ruthenium/PDMS (0.1mL of Ruthenium solution per gram of PDMS base) was cast in the recesses and cured to create the test sensors. The completed chip was placed on a glass slide supported by a rigid frame and exposed to a 2% O_2 gas mix in order to visualise the distribution of the dye in the matrix. The images of the sensor acquired by epifluorescence imaging were then processed to determine pixel values. Epifluorescence images of the sensors are visible in figure 6. The average normalised intensities (average gray scale pixel value divided by 255 to obtain a value between 0 and 1) of each sensor are summarized in figure 7. The average intensity measured for the 8 sensors was 0.28 with a standard deviation of 0.04. This represented a 14% variation across sensors fabricated from the same batch of oxygen sensitive material. In addition to the intensity variability between sensors, differences in the distribution of the dye inside each spot could be quantified. The larger the diameter, the larger was the variation in intensity inside the same sensor as the error bars in figure 7 represent. The variations were due to a pronounced meniscus effect in the larger sensors (1.5 and 2 mm diameter) as visible in the panels 2 to 4 of figure 6 pushing the dye to the edges of the sensor. Smaller sensors (panel 1 and 6, figure 6) displayed a more homogeneous distribution, however the fabrication process for the smallest sensor spot (0.4 mm diameter) was more challenging due to the difficulty to dispense accurately small volumes of a viscous solution in a confined area. In conclusion a sensor size of 1 mm diameter provided the best results in terms of ease of fabrication, homogeneity of the dye distribution and area occupied relatively to the culture chamber footprint.

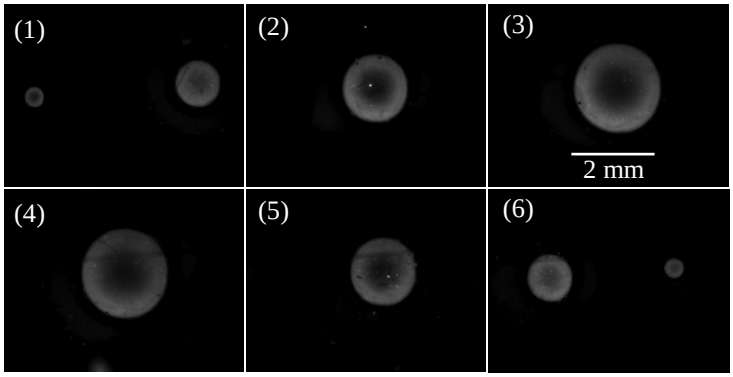

Figure 6: Fabricated ruthenium/PDMS optodes under fluorescence microscopy. (1) and (6) 0.4 and 1 mm diameter, (2) and (5) 1.5 mm diameter, (3) and (4) 2 mm diameter.

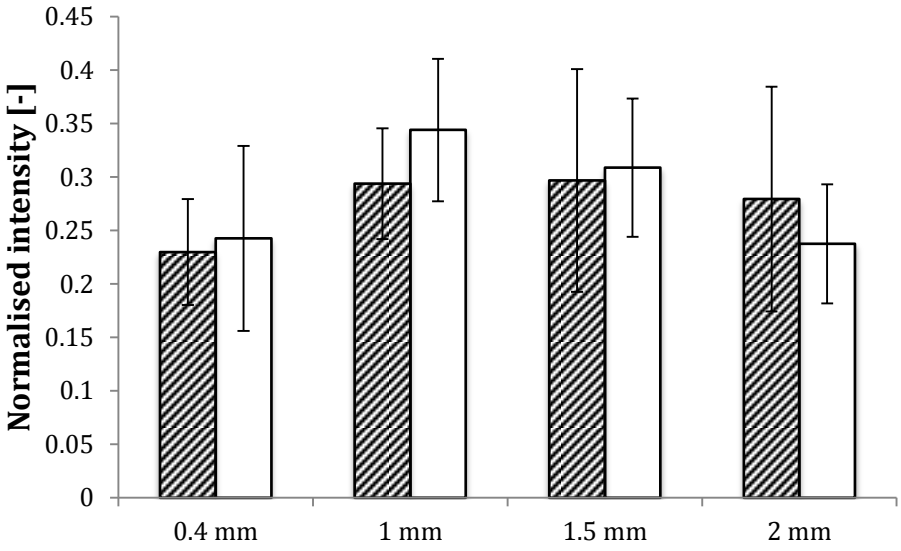

Figure 7: Normalised intensities of the ruthenium/PDMS optodes at 475EX/590EM exposed to 2% oxygen gas phase. Errors bars represent the standard variation of the intensity inside the sensor area.

3.2.1.3 Calibration

The test chip was exposed to gas phases with known oxygen concentrations in order to establish the correlation between intensity emitted and oxygen partial pressure and to assess the sensitivity and repeatability of the sensing method. The test chip was placed on the microscope stage under a box cover, in order to diminish background light from the outside environment and create a stable gas phase above the sensors. The sensors were exposed to 0% (100% nitrogen), 2%, 4% and 21% oxygen gas mixture consecutively and the calibration experiment was repeated 5

times with the same sensor set. Epifluorescence images of the 1 mm sensor were taken and processed to determine the pixel values corresponding to each oxygen pressure tested. Normalised intensities for each experiment are displayed in figure 8. For each of the experiments, the sensor intensity decreased with the increase of the oxygen up to 4% and there were no significant differences in intensity between 4% and 21% oxygen. However, the repeatability between experiments was poor: a variation in intensities measured for a same oxygen pressure up to 4-fold was observed between the experiments with no dependence to the order of the experiments.

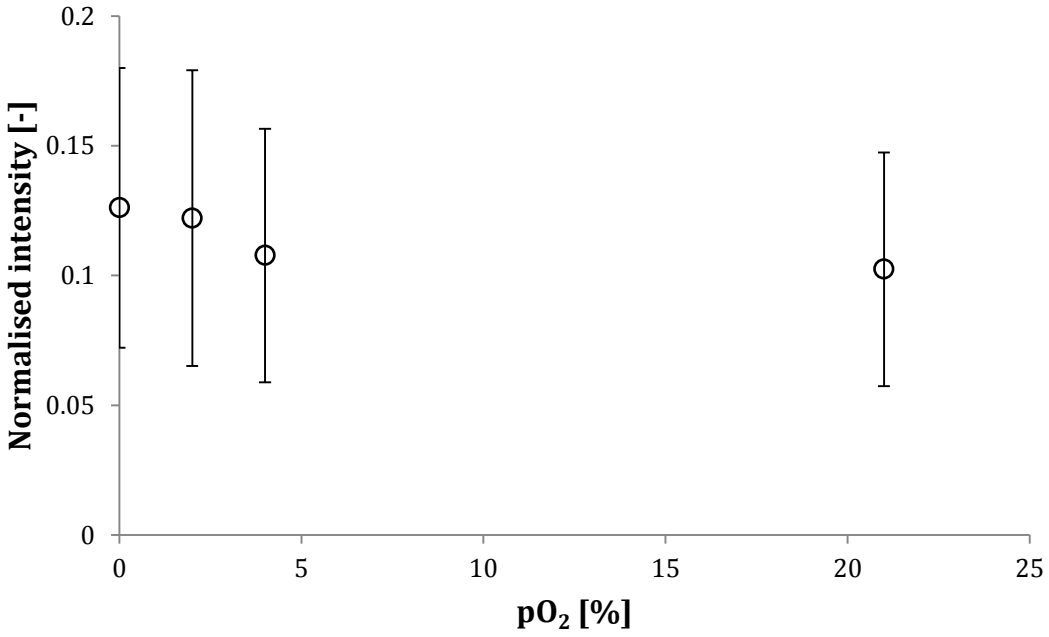

Figure 8: Calibration of a 1mm diameter ruthenium/PDMS optode at 0, 2, 4 and 21% oxygen in the gas phase. Error bars represent the standard variation of the mean normalised intensity (n=5).

A Stern-Volmer plot (figure 9), describing the relation between the chemical species (ruthenium diimine chloride) and its quencher (oxygen), was established with the data of the calibrations experiments. A linear relation was found between 0 and 4% oxygen, with a Stern-Volmer slope (K_{sv}) of 0.061, which was consistent with the values provided by the manufacturer of the dye. If this linear correlation held for the entire oxygen range, the intensity at 21% should have been 4.5 times higher than what was effectively measured. This loss in sensitivity could be attributed to several factors: the loss of sensitivity of the optical sensor of the

camera with decreasing light intensities and the loss of linearity in the response due to the encapsulation in a polymer matrix.

As the calibrations were done in a gaseous environment, it is necessary to convert the results from a volume percentage or partial pressure to a molar concentration in order to predict the performance in liquid culture. Ideal conditions were assumed to apply the ideal gas law:

$$pV = nRT$$

To obtain the molar concentration of oxygen in the atmosphere in function of the partial pressure of oxygen, the equation is transformed:

$$c = n/V = p/RT$$

R, the ideal gas constant being 0.08206 $L.atm.mol^{-1}.K^{-1}$, and the temperature assumed to be 20˚C or 293.15K:

$$c = p/24.06$$

Using this relation, 4% of oxygen in the atmosphere corresponded to a concentration of 1.66 mM. Assuming that the culture medium used for culture is pure water at 37˚C at atmospheric pressure, the solubility of oxygen would be 210 µM. Thus, the sensor tested offered a linear response on a range of an order of magnitude higher than the theoretical limit of solubility of oxygen in similar conditions.

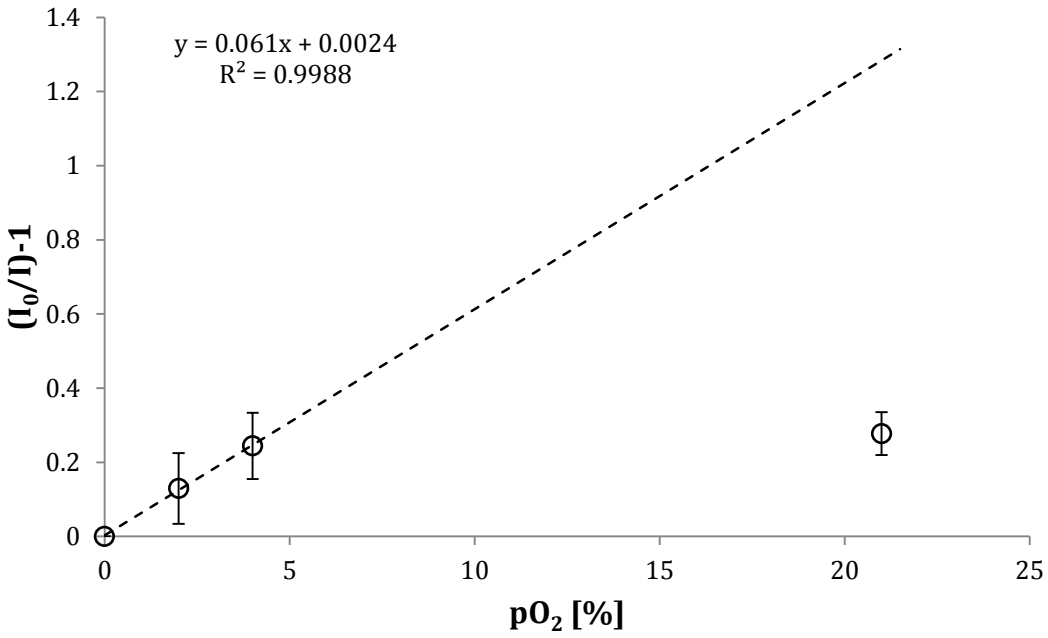

Figure 9: Stern-Volmer representation of the calibration data for the 1 mm diameter ruthenium/PDMS optode. Error bars represent the standard variation of the mean normalised intensity of 5 independent runs.

3.2.1.4 Testing in the microfabricated perfusion culture device

To test if the Ruthenium/PDMS sensor leached their dye in an aqueous environment under continuous perfusion, a TC-PS slide holding three sensor spots was integrated in the microfabricated perfusion culture device (figure 10).

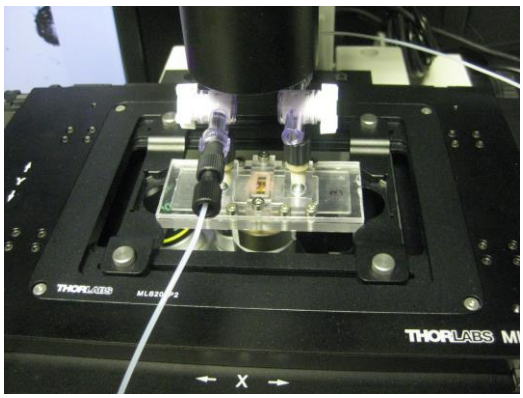

Figure 10: Measurement setup to test Ruthenium/PDMS sensor performance under continuous flow perfusion. The microfabricated culture device is fitted with a TC-PS slide integrating three 1 mm diameter sensors. The device is placed on an automated microscope stage controlled by a LabVIEW routine to acquire sequentially field of views of the sensors during perfusion.

The device was connected to a syringe pump to create a continuous perfusion in the chamber and placed on the top of the automated stage of an inverted fluorescence microscope to acquire sensor read-outs. The device was perfused at 300 µL/h (flow rate used in previous studies for the culture of human embryonic stem cells in the device) with an aqueous solution of sodium sulfite (10 g/L) in order to create an oxygen-free environment and maximize sensor intensity. Images were acquired sequentially every 6 seconds using stage automation to align the microscope objective with each sensor location. The recorded intensities are plotted over time in figure 11. As expected from the previous experiments, starting intensities varied from spot to spot. Intensities recorded decreased over time in all three sensors, although at different rates. Time-lapse images of the sensors (figure 12) showed that the integrity of the sensor matrix is degraded over time, with the dye leaching out in the perfusion medium as well as the PDMS matrix. It can be seen by observing the motion of the ruthenium particles over time and sudden losses of intensity in the central regions of the sensor. After examination of the slide post-experiment, it appeared that the sensor material was incompletely cured and dissolved when exposed to the perfusion of liquid.

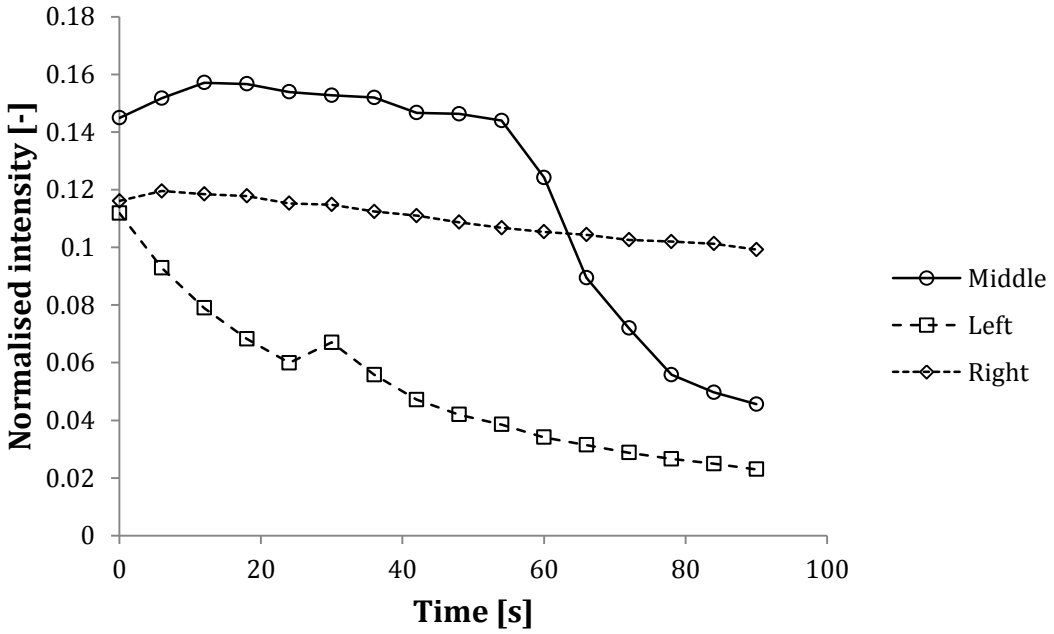

Figure 11: Timelapse intensity measurement of three optodes, integrated in the microfabricated culture device, under continuous perfusion of an anoxic solution of sodium sulfite at 300 µL/h.

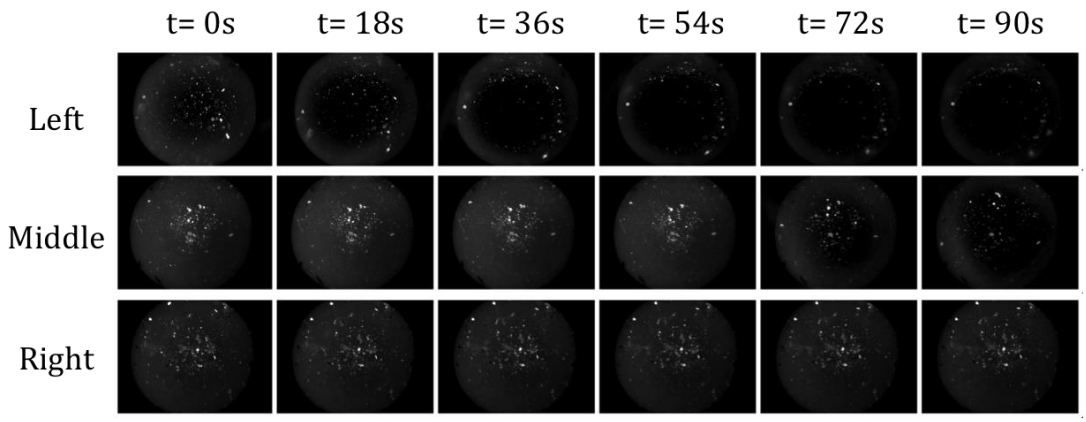

Figure 12: Timelapse fluorescent images of the three optodes (left, middle and right) integrated in the microfabricated culture device showing the dissolution of the ruthenium/PDMS matrix over time when exposed to water under continuous perfusion at 300 µL/h.

3.2.2 Integration of commercially-available optodes

Alongside the development of the ruthenium/PDMS optodes, integration of commercially available planar sensors (PreSens, Germany) was investigated. Commercial systems provide turnkey solutions for oxygen sensing that can be easily integrated with a wide range of standard culture systems and vessels such shaken flasks, multi-well plates or wave bags. These sensors have been previously successfully integrated in a microbiorector for microbial fermentation (Szita et al., 2005) and therefore constituted good candidates for integration in the stem cell culture device.

They required a two-point calibration (figure 13): at 0 and 100% water saturation. The 0% was established with a sodium sulfite solution (as per instructions of the manufacturer of the sensors) and the 100% with water that had been sparged with compressed air for 10 minutes to saturate the oxygen content. It was possible to obtain stable phase readings at 0% and 100% in under a minute. However it was noticed that when switching from the 0% calibration solution to water it was not possible to reach the same phase value than previously. Sodium sulfite is likely to be responsible for this behaviour. It is an oxygen scavenging specie and necessitates to be fully washed out of the system or it will continue to react and deplete the incoming oxygen in the perfusion. It is also important to consider that the solubility of oxygen in liquids is determined by the composition of the liquid, the temperature and the pressure. Therefore a 100% saturation point in water at room temperature is not equivalent to a 100% saturation point in culture media at 37˚C. It is therefore critical to establish the calibration of the sensors in exactly the same conditions than the culture they will monitor.

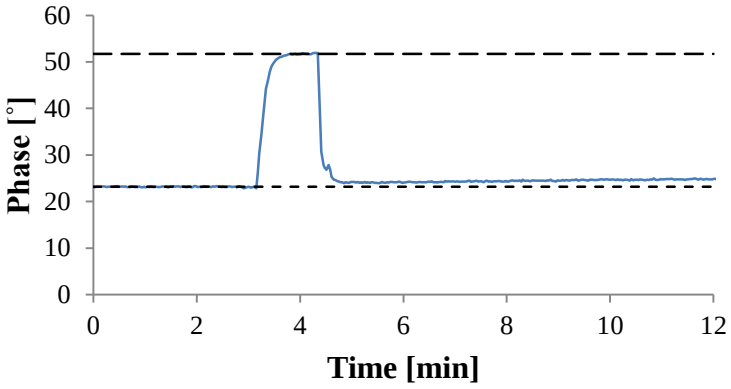

Figure 13: Calibration of a PreSens flow-through cell oxygen sensor. The blue line represents the phase reading of the sensor, the low dashed (short) black line the baseline for 100% water saturation, the high dashed (long) blackline the baseline for 0% water saturation.

Flow-through cell sensors were integrated at the inlet and outlet of the microfabricated device using standard Luer lock fittings to connect them between the tubing and the interconnects. Standard Luer-lock connectors provided adequate sealing for a use with continuous perfusion and the flow-cell sensors could be autoclaved and reused several times. The device with the flow-through cell sensors was perfused with water for over 20 hours at 300 µL/h in an incubator at 37˚C to test the stability of the measurements (figure 14). Over the period of time tested, a deviation inferior to 1% of the phase readings was measured, demonstrating that these sensors were suitable to measure oxygen in the inlet and outlet perfusion of the microfabricated culture device.

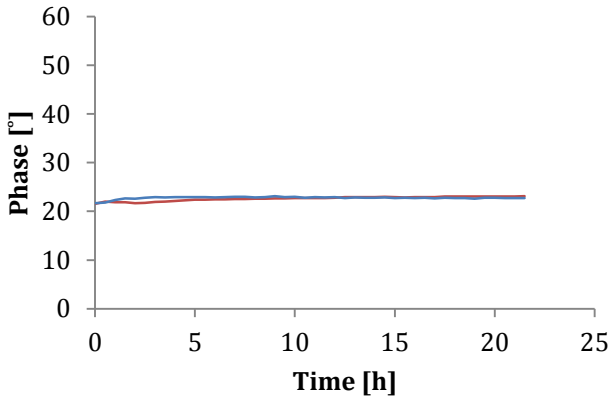

Figure 14: Phase reading of two flow-through cell oxygen sensors connected at the inlet (blue) and outlet (red) of the microfabricated culture device operated under perfusion with water at 300 µL/h in a cell culture incubator at 37˚C.

To integrate a planar sensor in the chamber for peri-cellular monitoring, a recess (125 µm depth, 2 mm diameter) was milled in the centre of a TC-PS microscope slide (figure 15). The sensor was placed in the recess and encapsulated in PDMS to ensure the sensor stays in place during perfusion. Because of the materials composing the slide and the sensor support layer, the resulting DO monitoring slide could not be autoclaved and the only sterilisation method available was incubation with ethanol. In addition, an autoclavable slide in glass was later designed (figure 16). It held a central recess (200 µm depth, 1 mm diameter) to be filled with oxygen-sensitive material and its fabrication was sub-contracted to the manufacturer of the sensor.

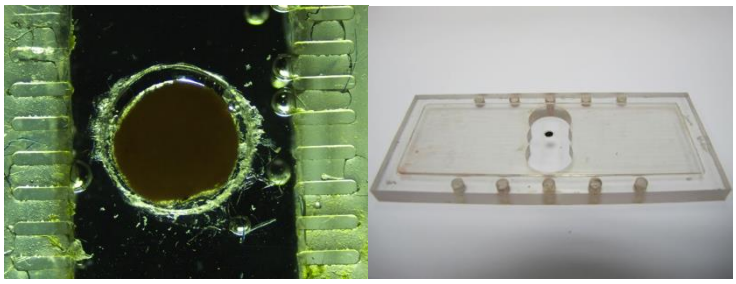

Figure 15: Integration of a PreSens 2 mm diameter sensor spots in a TC-PS slide in the microfabricated culture device.

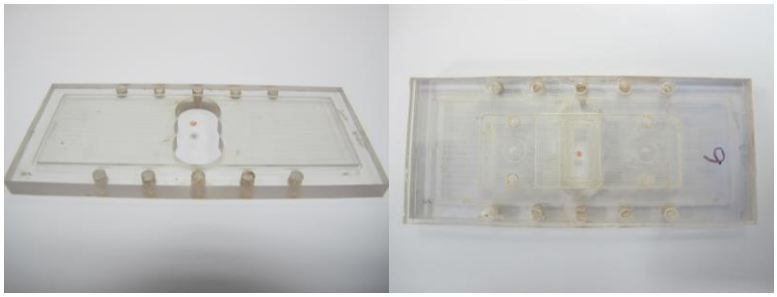

Figure 16: Glass slide with an integrated optode supported by a polycarbonate frame.

3.3 Summary of findings

Two approaches have been investigated for the integration of optodes in a microfabricated culture device previously developed.

An optode, consisting of a ruthenium fluorophore dispersed in a PDMS matrix, has been developed and tested. It can be simply fabricated by casting of a ruthenium/PDMS mixture in a mould. This fabrication process enables the rapid generation of optodes for testing and characterisation. These PDMS optodes present the advantage of being autoclavable and therefore are compatible with the asepsis requirement of cell culture. The fabrication process allows the simple creation of optodes for peri-cellular oxygen measurement onto the surface of the culture substrate.

The optode fabricated has a linear intensity response up to 1.66 mM of oxygen in the gas phase. However intensity measurements present a great variability due to their dependence to the fluorophore concentrations, illumination condition and sensitivity of the photodetector used. Additionally, the optodes were not physically stable in the aqueuous phase, and therefore this design had to be ultimately abandoned.

Commercial optodes were preferred as they constituted a robust and reliable approach to oxygen sensing.

4 Development of an instrumented microfluidic platform for stem cell bioprocessing

4.1 Stem cell bioprocessing requirements

To design an experimental setup and protocols for its operation, the requirements of the process studied were identified and categorized (figure 17). To expand or differentiate successfully pluripotent stem cells, the physical (temperature, hydrodynamic shear stress), the physicochemical (pH, osmotic pressure, dissolved oxygen tensions) and physiological (nutrients, metabolic waste, growth factors, extracellular matrix) parameters of the culture system must be controlled in a defined range. To assess the output of the process, it is also necessary to monitor the growth kinetics of the cells, as well as their health and phenotype. Understanding how these requirements are currently addressed in state-of-the-art techniques for two-dimensional culture of mESCs constitutes a first step to establish the foundations of a microfluidic culture platform to reproduce this process.

An overview of the requirements of lab-scale two-dimensional static culture and the strategies commonly used to address them is given below.

4.1.1 Asepsis

The maintenance of asepsis is fundamental to any cell culture process. In order to avoid the introduction of contaminants, the sterility of any piece of equipment, material or solution that will be in contact with the cells at any point of the process has to be assured. The requirement is typically satisfied by the use of gamma-irradiated disposable plasticware for the cell culture vessel and liquid-handling apparatus such as pipettes. Reusable equipment can be as well considered as long as it can be sterilised. Solutions have to be sterilised prior to use. Solutions such as growth media containing thermo-labile molecules are typically filtered while less sensitive solutions can be autoclaved. Finally, any steps requiring handling cells outside of their sterile vessels must be undertaken in a controlled environment such as a biosafety cabinet (BSC) by an operator trained to aseptic handling techniques. If any of these conditions cannot be satisfied, the growth medium can be supplemented with antibiotics to mitigate contamination risks. However, it should be taken in account that antibiotics may affect negatively the growth kinetics and the differentiation efficiency (Cohen et al., 2006). Therefore their use should be

discouraged if the focus of the experiments is to obtain biologically relevant data on the cell culture.

4.1.2 Temperature

The optimal temperature for a given cell line is generally defined by the body temperature of the organism from which it originated. Mouse and human stem cell lines are usually maintained at 37˚C in temperature-controlled incubators.

4.1.3 Osmotic pressure

The osmotic pressure is defined by the medium composition. However, during batch culture in an incubator at 37˚C, evaporation of medium in a non-sealed culture vessel, such as a multi-well plate or a T-flask, may lead to an increase of the osmotic pressure. To counteract this effect, a humidified atmosphere is created in culture incubator by evaporating water from a tray placed at the bottom of the incubator.

4.1.4 pH

As temperature, pH is critical to the maintenance of the biochemical reactions taking place in the cells. It has also an effect on the differentiation of stem cells in specific lineages (Wuertz et al., 2009). Optimal pH for stem cell culture is between 7.0 and 7.4 (Chaudhry et al., 2009). As osmotic pressure, pH is defined by the medium composition but will be affected by process conditions. As cells are growing, they will produce metabolic waste such as lactic acid that will decrease the pH of the solution. To balance the acidification of the medium by the cells, a bicarbonate buffering system is maintained in the culture by the addition of CO_2 in the gas phase (5-10%). However, buffering is unable to maintain the pH at optimal level over an extended period of time due to the continuous increase of biomass and resulting production of metabolic waste, and therefore it is necessary to perform media changes at regular intervals to maintain homeostasis. Media can be replaced manually in static culture vessels or in an automated fashion by integrating perfusion systems that will renew the medium at a defined rate (Koller et al., 1993; Zhao and Ma, 2005).

4.1.5 Dissolved oxygen tension

Dissolved oxygen tension is critical parameter for both proliferation and differentiation of pluripotent stem cells. In static culture vessels, oxygen is supplied passively from the headspace to the culture medium. Dissolved oxygen tensions achieved are directly proportional to the partial pressure of oxygen in the gas phase according to Henry's law:

$$pO_2 = k_H cO_2$$

Equation 4: Henry's law at constant temperature. pO_2 is the partial pressure of oxygen in the gas phase above the solution, k_H the Henry's constant for a given temperature and cO_2 the concentration of oxygen in the solution.

Therefore, in two-dimensional adherent stem cell culture, control of the oxygen supplied lies first in the control of oxygen partial pressure in the gas phase above the culture. The oxygen transfer rate from the gas phase to cells is defined by the interfacial area, the rate of diffusion of oxygen in the media and the concentration gradient:

$$OTR = \frac{dC}{dt} = k_L A\,(C^* - C) - OUR$$

Equation 5: Oxygen transfer rate (OTR) equation. C is the concentration of oxygen in the liquid phase, C* the solubility of oxygen in the system, $k_L A$ the volumetric mass-transfer coefficient of oxygen in the system, and OUR the oxygen uptake rate of the culture.

With no active mixing in static culture vessels, the interfacial area and diffusion path for oxygen transfer are only defined by the geometry of the culture vessel.

4.1.6 Hydrodynamic shear stress

Fluid movement in the culture vessel can cause physical damage to the cells by shear stress at the cell boundary. It is also known to promote the differentiation of pluripotent stem cells (Korin et al., 2009; Nsiah et al., 2014). In two-dimensional adherent culture, hydrodynamic shear stress is usually negligible due to the absence of liquid movement in static culture vessels. However hydrodynamic shear stress may occur during the passaging of the cells because of the pipetting and centrifuging steps required. Following well-defined and tested protocols in which

the boundaries for potentially damaging operations such as centrifugation have been clearly established can mitigate the effects of shear stress during manual handling of the cells (McCoy et al., 2009).

4.1.7 Nutrients and soluble factors

Nutrients such as glucose and glutamine are essential as energy source to sustain vital cell functions such as energy production and biosynthesis. Growth factors are required to modulate and control cell functions such as survival, self-renewal and differentiation. The right combination of these compounds defines the medium composition for a given application (expansion, differentiation). However during culture, they are subject to consumption to the cells or degradation due to the environmental conditions (such as temperature or pH) and need to be replaced at regular intervals by performing media changes. In addition, cell metabolism produces waste such as lactic acid (produced by glycolysis under oxygen-limited conditions) and ammonia (from glutamine utilisation) that needs to be removed to avoid cell growth inhibition.

4.1.7.1 Culture substrate

Anchorage-dependent cell lines require the correct substrate to ensure their survival and proliferation. The substrate is characterized by mechanical and physiological properties. Mechanical properties such as stiffness or roughness are defined by the choice of material used in the culture vessel. The physiological properties are provided by the addition of an extra-cellular matrix (ECM) and include binding sites for cellular adhesion molecules such as integrins and the retention of signaling factors. In static culture vessels such as T-flasks and multi-well plates, the culture substrate for adherent stem cells consists of a stiff polystyrene surface coated with an ECM such as gelatin, collagen, laminin or fibronectin.

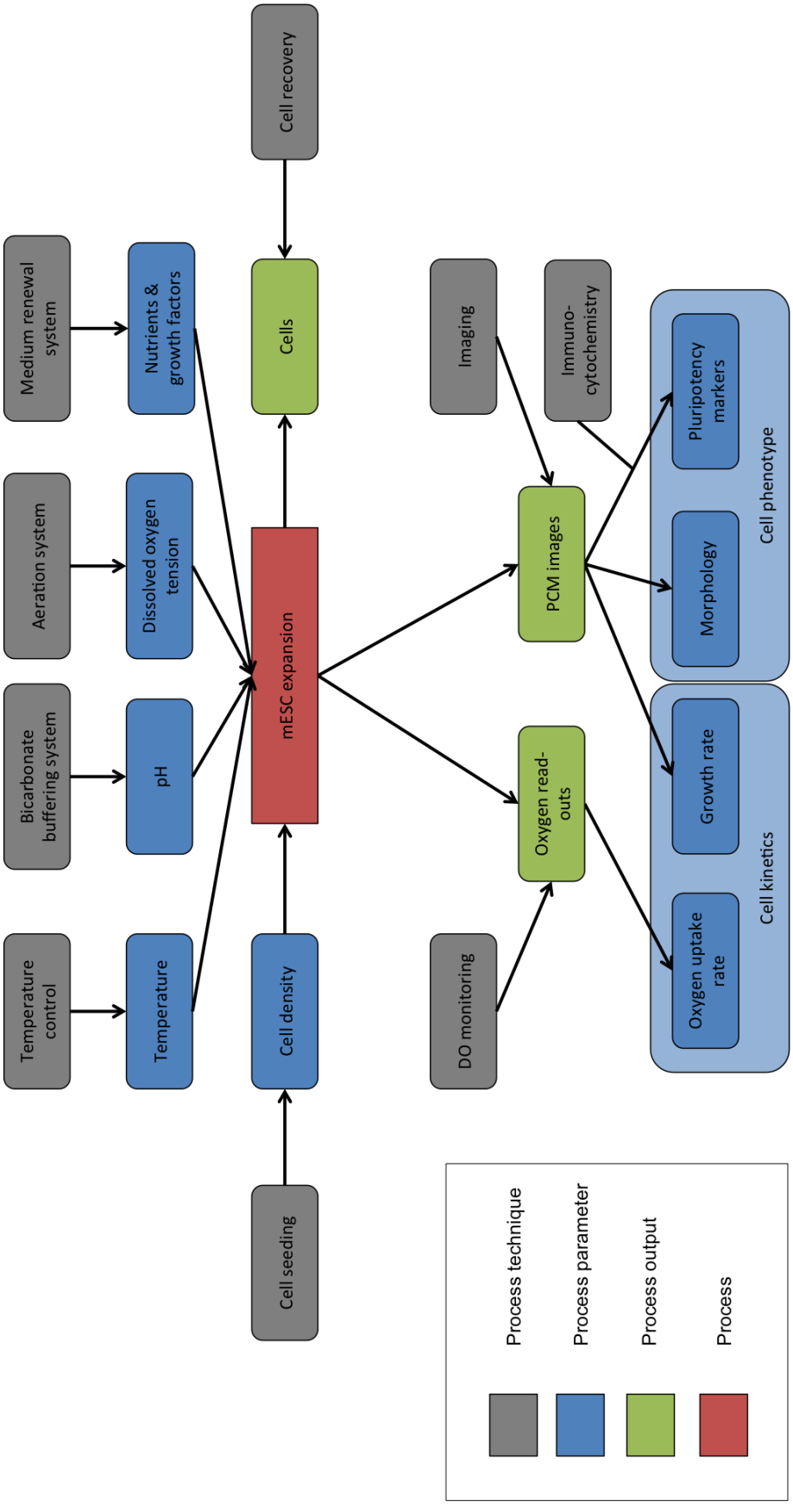

Figure 17: Schematic representation of process requirements for a mouse embryonic stem cell expansion.

4.2 Results & Discussion

The objectives of this study were (1) to establish an instrumented microfluidic platform integrating the oxygen monitoring system presented in Chapter 3 and (2) to design and test the operating procedures to sustain stem cell culture in this platform.

4.2.1 Microfluidic culture platform concept

A platform was designed to address the requirements for the expansion of mESCs: temperature control, media renewal, dissolved oxygen control and monitoring, pH maintenance and cell growth monitoring. It was established around the microfabricated modular device concept for adherent cell culture previously established (Reichen et al., 2012). A standard humidified cell culture incubator was used to maintain the device at optimal temperature during culture. A controllable pressure-driven perfusion system allowed for continuous renewal of the growth medium. The dissolved oxygen supplied to the cells was defined by the composition of the driving gas used for the perfusion. Dissolved oxygen tensions were monitored during the culture by optical sensors integrated in three locations of the system: inlet and outlet of the device, and *in situ* at the surface of the culture substrate. A bicarbonate buffering system was established by the presence of carbon dioxide in the driving gas of the perfusion system. The cell expansion was monitoring by phase-contrast microscopy (PCM), requiring the transfer of the system to an external microscope for the acquisition of images.

4.2.2 Experimental Setup

The microfabricated device and the fluidic system (including the medium reservoir) were placed on an incubator tray. The medium reservoir was connected to the pressure regulator and a cylinder of cell culture gas mix (21% O_2, 5% CO_2) as the driving gas, placed outside of the incubator. The 5% CO_2 in the culture gas mix was dissolved during perfusion in the medium to maintain the bicarbonate buffering system in the culture device. The voltage controlling the pressure regulator was

generated by a data acquisition interface (DAQ card) controlled by a software routine, while an external DC source powered the regulator. Flow-through cell (FTC) optical oxygen sensors were connected upstream and downstream of the device fluidic ports to provide inlet and outlet dissolved oxygen measurements. An optical fibre was aligned with the *in situ* oxygen sensor in the culture chamber, using a SMA flat adapter inserted at the bottom of the device. The optical fibres for the three sensors were connected to a multi-channel transmitter outside of the incubator to collect and process the read-outs.

This first-generation platform (figure 18) had the capacity to maintain cells at a constant temperature (using a standard cell culture incubator), while automatically renewing the medium with a controllable perfusion system, and performing automatically dissolved oxygen measurements in three locations of the system (inlet, outlet and *in situ*). However, visual assessment and imaging of the cells being cultivated required transfer of the system to an external microscope. To transfer the system outside of the incubator, it had to be reduced to a more portable setup. The perfusion system could be disconnected between the pressure regulator and the medium reservoir, as the air filter between the two components guaranteed the preservation of asepsis. In order to avoid uncontrolled flow movement caused by a pressure differential between the reservoir and the system outlet during transport, the three-way valves at the inlet and outlet of the device had to be closed, isolating the culture device from the rest of the fluidic system. The FTC fibres could be disconnected from the transmitter, while the flat adapter for the *in situ* sensor could be simply detached from the bottom of the device. Thus, the medium and waste reservoirs, the culture device and two optical fibres connected to the fluidic lines could be disconnected from the platform and transferred to a microscope for imaging without compromising the culture.

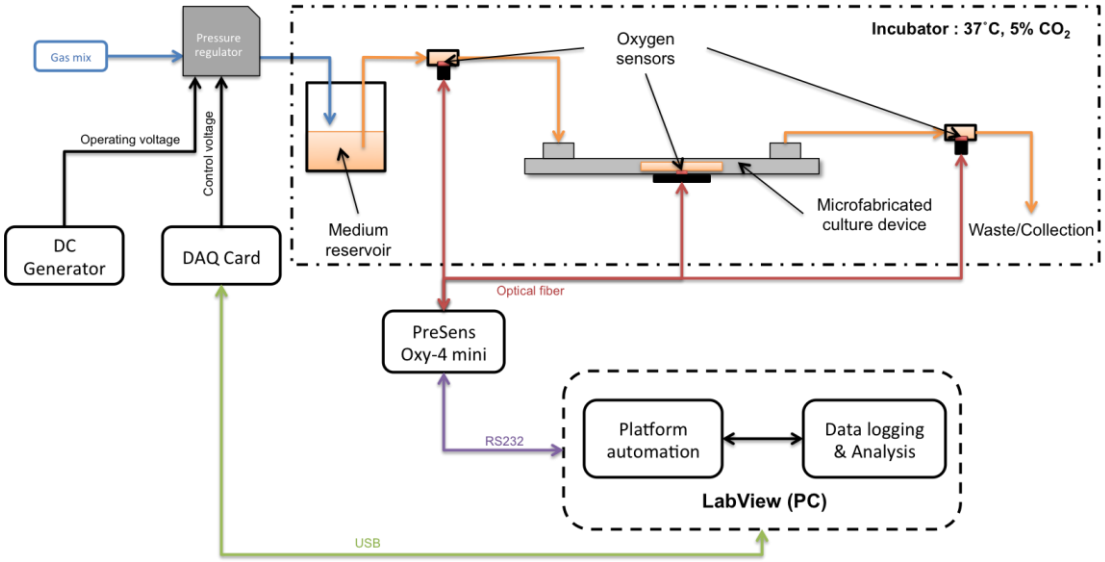

Figure 18: Schematic representation of the first generation platform for instrumented microfluidic cell culture.

4.2.3 Microfabricated culture device design

The device adopted the design established previously by Reichen et al. (2012). It consisted of a PDMS culture chip aligned with a rigid microscope format slide acting as culture substrate. The culture chip consisted of two PDMS layer. A top layer defined the fluidic channels connecting the inlet and outlet to the culture chamber. A 125-µm spin-coated PDMS layer was bound to the top layer to close the channels and elevated the flow level above the cells to reduce hydrodynamic shear stress during perfusion.

The chip/substrate assembly was packaged between a top polycarbonate frame in which an opening, aligned with the culture chamber, was created, and a bottom aluminum frame. An additional PDMS gasket was placed between the PDMS chip and the top frame to provide sealing for the re-insertable polycarbonate lid piece. Polycarbonate-interconnect blocks for threaded adapters were aligned with the through-hole of the top frame and the fluidic ports of the culture chip underneath. Compression and sealing of the device was achieved by ten M3 hex screws placed on the lateral sides of the packaging (five on each side). The interconnect blocks were attached to the top frame by two M3 screws each.

The culture chip consisted of two PDMS layer. A top layer defined the fluidic channels connecting the inlet and outlet to the culture chamber.

4.2.4 Pressure-driven perfusion system for long-term cultures

A pressure-driven system was designed to perfuse medium through the culture device. In pressure-driven systems, the liquid is displaced by the pressure exerted by the gas injected in the headspace of a sealed reservoir. The pressure drop, defined by the dimension, geometry and the surface roughness of the fluidic network, determines the resulting flow rate. Therefore a calibration was only valid for a specific network tested.

An autoclavable pressure-resistant glass bottle acted as a medium reservoir. It had an exhaust port to release pressure, a medium port connected to the inlet line of the device and a gas port connected to a pressure regulator controlling the driving gas headspace pressure and therefore the flow rate delivered. A particle filter is placed between the pressure regulator and the gas port to maintain asepsy in the reservoir. The voltage-controlled pressure regulator was interfaced with a control software routine via a data acquisition system to automate the control of flow rate.

Based on the previous work with the microfabricated device and human embryonic stem cell cultures (Reichen et al., 2013), the target flow rate was set at 300 µL/h. To assess that the perfusion system was able to operate in that range, flow rate was calibrated against control voltage of the pressure regulator. To characterize the flow rate, a pressurized reservoir containing water was connected to an upstream pressure regulator and the microfabricated device downstream. The control voltage of the pressure regulator was set by a software control routine and the flow rate was determined by collecting and weighing the fraction of water that had been perfused through the system for a given amount of time. This method was preferred to using an online flowmeter as it didn't introduce a bias due to the internal pressure drop of the flowmeter.

In the first setup tested, the lowest flow rate controllable was 15 mL/h (figure 19), 50 times higher than the target flow rate for cell culture. (300 µL/h) In order to decrease the flow rate range and increase the sensitivity of the pressure control over flow rate, a 40 cm piece of 100-µm internal diameter tubing was inserted at the outlet of the reactor. The increase of pressure drop of the system allowed achieving flow rates a thousand-fold lower in the system (figure 20).

As the integration of a resistance in the fluidic system will increase the pressure and affect the solubility of oxygen in the liquid phase, the pressure build-up of the system was measured (figure 21) using a pressure sensor connected via a T-junction at the exit of the reservoir. According to the established calibration a flow rate of 300 µL/h would generate a pressure increase of 0.111 millibar.

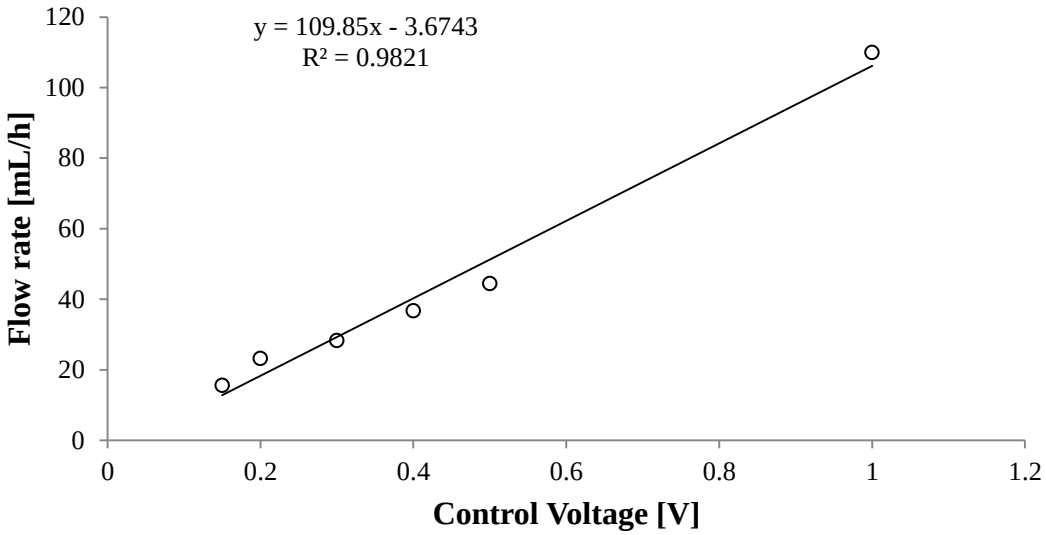

Figure 19: Calibration curve of the flowrate generated as function of the control voltage of the pressure regulator.

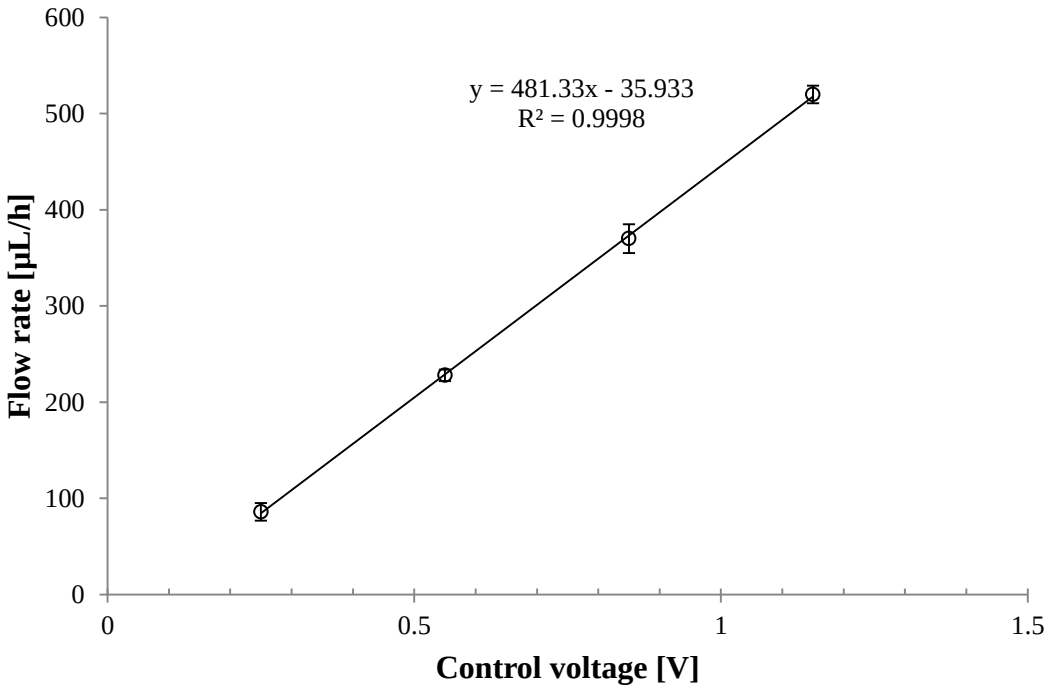

Figure 20: Calibration curve of the flow rate as function of the control voltage with a pressure resistance added to the system. Error bars represent the standard variation of the mean flow rate (n=3).

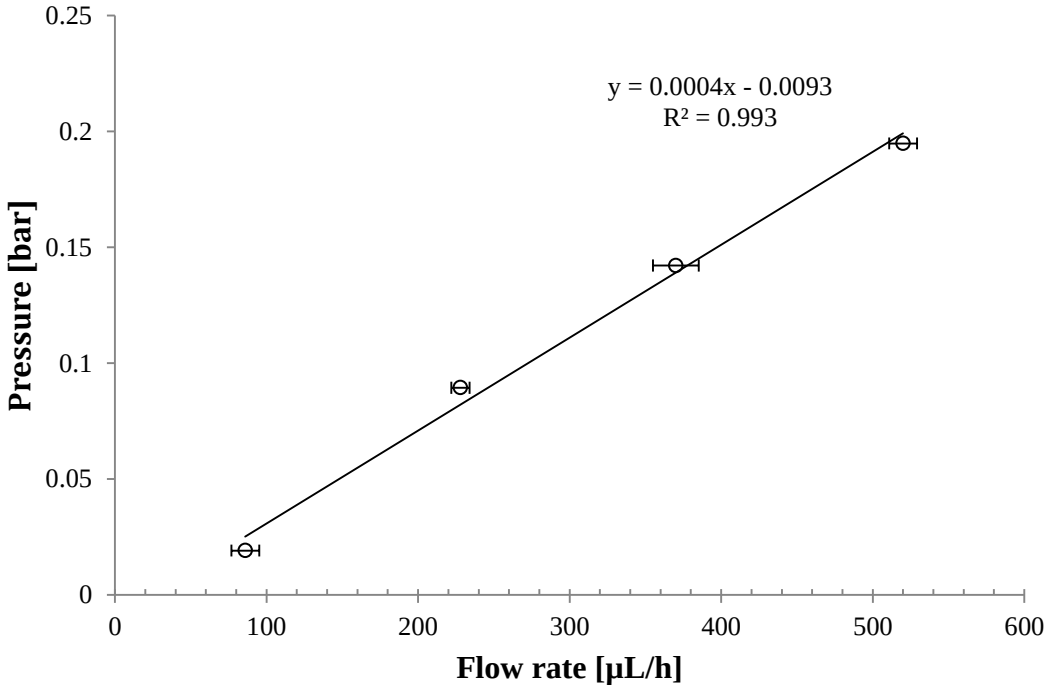

Figure 21: Pressure measured in the perfusion system as function of the flow rate. Error bars represent the standard variation of the mean flow rate (n=3).

4.2.5 Operating procedures for stem cell culture

A series of protocols for the operation of the microfabricated culture device and the monitoring systems had to be defined, tested and optimised to achieve optimal performance and robustness of the setup for the culture and monitoring of adherent stem cells over extended periods of time. These protocols encompassed all the aspects of a typical cell culture experiment in the microfabricated device from the sterilisation of the system components to the cell assays post-culture in order to create a seamless, robust and reproducible workflow for the operation of the culture platform. Initial protocols were adapted from standard protocols for adherent stem cell culture at bench scale and previous work done with the microfabricated cell culture device with human embryonic stem cells (Reichen et al., 2012) and tested in a top-down iterative approach with a benchmark process (two-dimensional expansion of mouse embryonic stem cells) in order to identify and address issues in the equipment or methods used.

The operation of the platform was divided in four major steps: preparation of the experimental setup, cell seeding, culture and monitoring, and end-point assays.

4.2.5.1 Preparation of a cell culture experiment

Preparation of the experimental setup included the sterilization of the platform components, the assembly of the device and perfusion system, priming of the fluidic network, alignment and calibration of the oxygen sensors, and coating of the culture substrate to sustain adherent cell culture.

The critical criterion for the preparation of the setup was the maintenance of asepsis to avoid the introduction of microbial contaminants. The modularity of the setup was an advantage to satisfy the requirement for asepsis. Each component of the device and the perfusion system could be sterilised separately with the adapted technique. With the exception of the oxygen-sensing TC-PS slide and the three-way valves containing a polyethylene (PE) stem, every other component was autoclavable. These parts were sterilised separately with a 70% ethanol solution.

The sterile components were assembled in two steps in a biosafety cabinet. The culture device was first assembled using sterile tweezers. The oxygen-sensing slide was first inserted, sensor facing upwards, on top of the bottom frame. The gasket

and the culture chip were inserted in the recess of the top frame. Then the two resulting assemblies were pressed against each other to align the culture chip with the culture slide. Screws were used to secure the stack of frames, chip and slide. The interconnect blocks were aligned with the inlet and outlet port on the top frame and also secured with screws. The surface of the culture chamber was coated with a gelatin solution through the open lid and incubated for at least 20 minutes at room temperature in the biosafety cabinet. Excess solution was then pipetted out. During the incubation time, cells were prepared for seeding (see section 4.2.5.3).

The perfusion system was assembled and connected to the device after the cell seeding and initial cell attachment period (detailed in section 4.2.5.3). This particular order was chosen to facilitate transfer of the device between the BSC and the incubator and ensure that the cells could settle on the culture substrate while minimizing the amount of disturbance caused by manual handling.

The liquid reservoir was first filled with 100 mL of sterile growth medium. The inlet tubing was connected to a FTC oxygen sensor, itself connected to the first three-way valve. Similarly the outlet tubing was connected to a second FTC oxygen sensor, itself connected to another three-way valve. The bypass tubing was used to connect the two valves together, creating a single-channel fluidic line from inlet to outlet. A sterile disposable syringe was connected to the inlet to wash the line with sterile water. The inlet was then connected to the outlet port of the liquid reservoir. Disposable syringes were connected to the free third port of the valves and used to draw medium from the reservoir to prime the perfusion line. The syringes were then disconnected and the valves were connected to the interconnect blocks of the culture device using threaded Luer-lock adapters. The fluidic channels of the device were primed following the procedure described in section 4.2.5.2.

The fully assembled system was transferred to the incubator. The pressure regulator was connected to a sterile air particle filter fitted on the inlet of the liquid reservoir. The optical fibre flat adapter was inserted under the bottom frame and aligned visually with the *in situ* oxygen sensor. The optical fibres for sensor read-out were connected to a transmitter linked to a computer to record the monitoring data.

The oxygen sensors were calibrated in two steps. Calibration of the 0% DO was performed prior to the assembly of the system for cell culture, by perfusion of an

anoxic sodium sulfite solution. The 100% DO was calibrated at the beginning of the culture to represent of the actual maximum oxygen saturation reachable under experimental conditions.

4.2.5.2 Priming and bubbles removal

Priming of the culture system fluidics was a critical step to obtain a bubble-free perfusion. In microfluidic devices, air bubbles are known to be very disruptive for the flow performance and the cell viability. We took advantage of the re-sealable lid feature of the device to create a temporary "bubble-trap" and perform bubble-free priming with minimum handling, while preserving the asepsis of the whole system.

A 10 cm segment of 1/16" OD tubing was used to create a bypass between the inlet and the outlet of the microfluidic reactor and two 3-way valves allowed to direct the flow in the desired direction through the bypass or the reactor (figure 22). At first, culture medium was pushed through the bypass, to prime the fluidics from the reservoir to the waste bottle (t_0). Then the inlet valve was opened to the reactor to prime the upstream area of the microfluidic chip. Excess medium and air bubbles accumulated in the open culture area and were manually removed by pipetting (t_1). The same operation was carried out in the downstream area of the chip, by opening the inlet valve to the bypass and setting the outlet valve to direct the flow from the bypass to the downstream channel (t_2). Once the totality of the fluidic network was primed, the lid was inserted on the culture chamber to seal the reactor (t_3).

The whole procedure could be performed using the same pressure-driven pump that was used for culture perfusion, decreasing the risk of external contamination during priming due to the connection of other pumping devices.

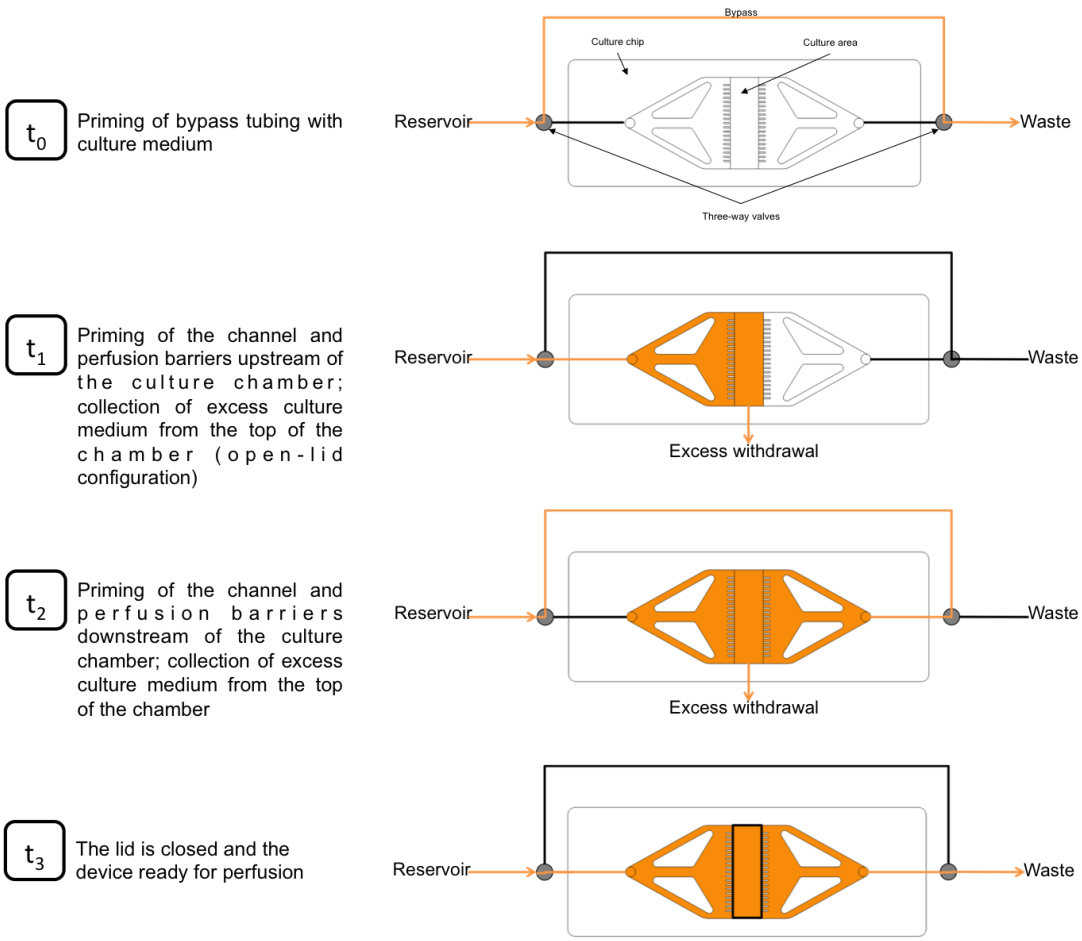

Figure 22: Bypass technique for device priming.

4.2.5.3 Cell seeding

Cell seeding consisted of the preparation of the inoculum to be seeded in the device culture chamber, the static seeding method and the incubation to ensure cell attachment to the culture substrate.

The inoculum was prepared with cells harvested from a T-25 culture in exponential phase following the typical passaging protocol. The recovered cells were manually counted with a haemocytometer to determine cell density and calculate the appropriate dilution required to reach the target cell seeding density of 10^5 cells/cm^2. The inoculum was seeded directly in the culture chamber through the open lid. A glass cover slip was then placed on the chamber opening to close it and the device was transferred in a Petri dish to an incubator. The culture device was incubated at 37˚C during at least 3 hours to let the cells adhere to the substrate. After incubation, the device was transferred back to the BSC to connect the perfusion system.

4.2.5.4 Culture and monitoring

The culture was performed in two phases: a static culture phase with a null flow rate for the first 18 hours, to ensure optimal cell adhesion in the device, followed by a continuous perfusion at 300 µL/h. During the static phase, the inlet and outlet valves were directed towards the bypass to isolate the culture device from the perfusion system. For the perfusion, the valves were directed towards the culture device, and the pressure regulator set a value corresponding to the desired flow rate according to calibration data. During the whole course of the culture, read-outs from the oxygen sensors were recorded every 5 minutes. To assess the growth and health of the cells, the system was transferred once per 24 hours to an external inverted microscope. The perfusion and DO monitoring were then stopped and the system disconnected as explained in section 4.2.2. Fields of view of the culture chamber were acquired by phase-contrast microscopy. An image analysis algorithm developed by (Jaccard et al., 2013) was used to process the images offline and determine cell confluence.

The culture was terminated in case of contamination, cell death and critical failure of the perfusion (including leaks and air bubbles) or monitoring system. If no significant faults occurred, the culture was maintained for up to 6 days (144 hours of culture), in order to achieve an experimental turnover not exceeding a week. 6 days of culture represented the duration of two passages in a T-flask, and constituted a middle ground between preserving experimental work time for repeats and optimisation, and demonstrating the robustness of the system for extended period of time.

4.2.5.5 End-point assays

At the end of the culture, immunocytochemistry assays were performed on-chip to assess the expression of pluripotency markers in the cells grown. Taking advantage of the resealable lid feature, the staining assays were conducted directly in the culture chamber, following the protocol typically used for multi-well plates. The lid was first removed to access the culture chamber. The cells were fixed, permeabilised and stained with primary and secondary antibodies directly on chip by manual pipetting of the solutions through the top frame opening. A glass cover slip was placed to seal the culture chamber and avoid the formation of a meniscus, and images of the stained cells were then acquired with an inverted fluorescence microscope.

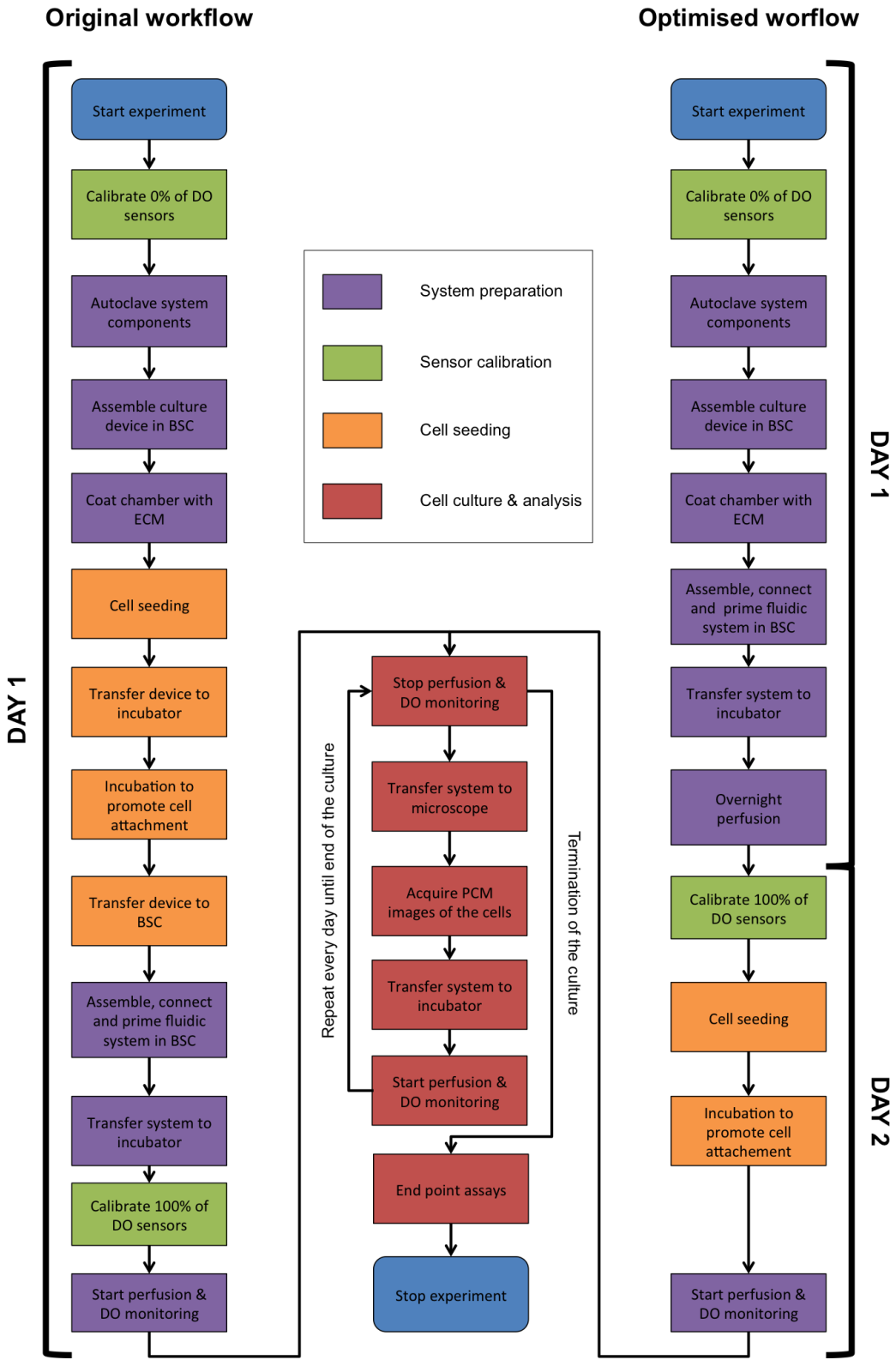

Figure 23: Diagram of the experimental procedures for the culture of mouse embryonic stem cells in the microfluidic platform. The original workflow on the left was the procedure tested in the culture experiments. The optimized workflow on the right was defined to address the issues encountered during the culture experiments. The common trunk in the middle represents the section of the workflow that wasn't altered.

4.2.6 Cell culture experiments

Nine culture experiments (Appendix Table 1) were performed following the procedure described in section 4.2.5. Five experiments were completed without any major failure occurring. Two experiments suffered microbial contaminations. One experiment was aborted due to an error of the operator during the transfer to the microscope. And lastly, in a single experiment, the cells failed to survive after seeding. The longest experiments achieved spanned over 6 days of culture and the shortest was terminated after 16 hours. The achievements and shortcomings of the approach tested are detailed and discussed in the following sections.

4.2.6.1 Maintenance of asepsis

Contaminations were a regular occurrence in first experiments attempted, despite the use of sterilised equipment and solutions, and the adherence to aseptic techniques for the preparation of the system in a biosafety cabinet. Two experiments were identified as infected by bacterial organisms. Infections were diagnosed by observing a rapid (under a day) change of colour of the phenol indicator of the medium, from orange to bright yellow, the apparition turbidity in the medium collected at the outlet of the system and a swarm of mobile small dark particles visible under phase-contrast microscopy (that translates as a very noisy background in the pictures shown in panel A and B of figure 24). These two experiments were aborted after two days of culture.

Retrospective analysis of the images of a third experiment showed the presence of groups of tiny dark particles around the cells (figure 24, panel C), indicating that it was likely to be also contaminated.

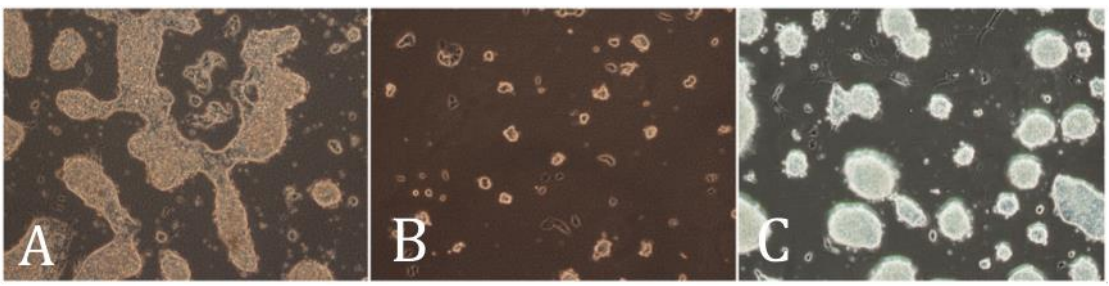

Figure 24: PCM images at 10x magnification of bacterial contaminations that occurred in three independent microfluidic culture experiments. A: Taken after 45 hours. B: Taken after 52 hours. C: Taken after 71 hours.

The equipment used and the steps of the procedure were reviewed after the first identified occurrence of contamination. Growth medium and ECM solutions were made anew. New parts were used for the device and the perfusion system. Handling of the sterile components and solutions in the biosafety cabinet was done with re-doubled attention to aseptic techniques. However, with the persistence of contamination events, it appeared that the most likely source of infections was the parts that could not be autoclaved: the oxygen-sensing TC-PS slide and the two three-way valves. It was decided to replace the TC-PS slide by an autoclavable slide with a similarly patterned oxygen-sensing coating and to use broad-spectrum antibiotics in the growth medium to prevent any reoccurrence of contamination. The four experiments performed with these modifications did not show any sign of contaminations.

4.2.6.2 Fluidics

Leaks in the perfusion system or culture device were not observed in any of the nine culture experiments performed in the incubator.

The priming method using the bypass proved to be effective at removing air bubbles from the system at the start of the culture. As shown in figure 25, after the priming was done, 6 hours after the seeding of the cells, very few bubbles were remaining the culture chamber. However, at the end of the static culture phase (21 hours after seeding), a larger number of bubbles were visible in the chamber. Under perfusion (46 and 71 hours after seeding), the bubbles gradually disappeared from the chamber.

We hypothesized that the apparition of new bubbles during the static culture phase might be caused by a combined effect of the temperature change when the device is transferred from a room temperature environment to a 37˚C incubator and liquid evaporation from the stagnant culture chamber. Increase of the temperature decreased the solubility of gases in the medium and gases in excess in the liquid phase coalesced in bubbles. That hypothesis would be consistent with the disappearance of bubbles during perfusion. At this point of the culture, the system was thermally balanced, eliminating the outgassing. The perfusion rate was sufficient to carry away the existing bubbles and compensate for evaporation. Thus, to eliminate the apparition of bubbles post-priming, it was decided to alter the

experimental protocol: assembling the device and perfusion system and letting it incubate overnight prior to cell seeding would ensure a thermally-balanced system. Additionally reducing the static culture phase would contribute to avoid the detrimental effect of evaporation.

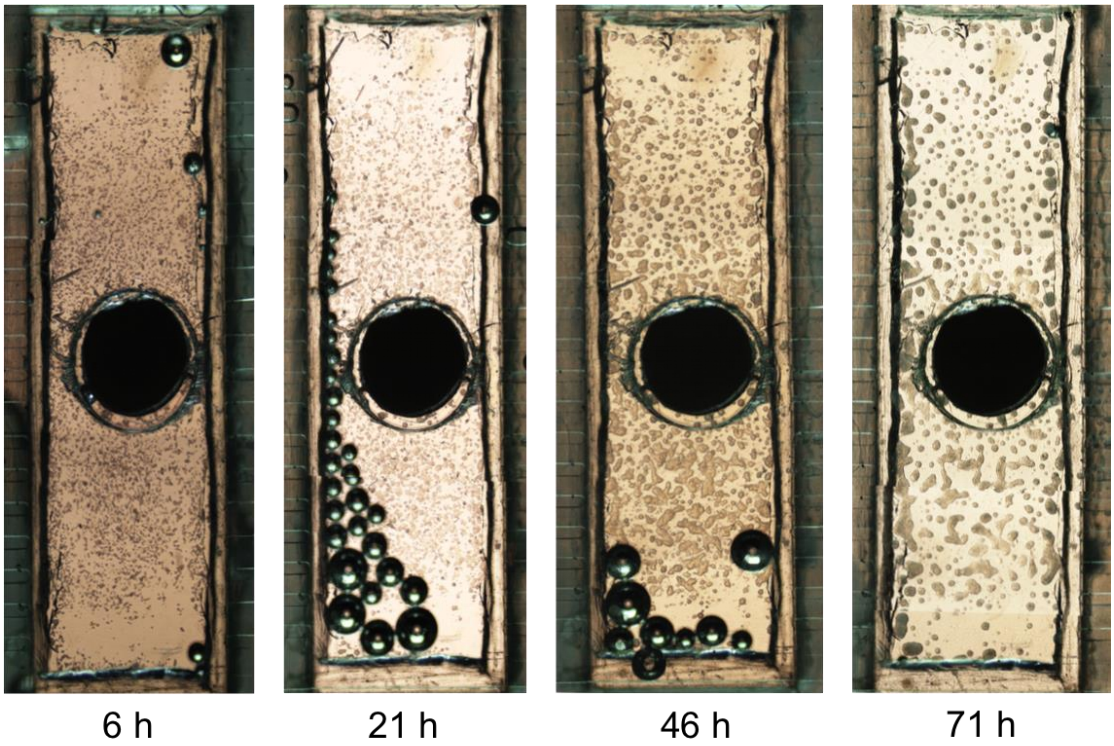

Figure 25: PCM images of the microfluidic cell culture chamber taken at different time of a culture experiment. Time is indicated relatively to the seeding time. Each image is constituted of four 2x magnification pictures stitched manually together.

4.2.6.3 Cell growth monitoring

Cell growth in the culture device was monitored offline, by transferring part of the culture system to an inverted microscope and acquiring manually PCM images of the culture chamber. The images were subsequently quantitatively analysed by a computational method based on local-contrast filtering and halo correction (Jaccard et al., 2013) to determine the confluency of the culture. The imaging routine was performed daily. As a control, part of the inoculum was seeded in a T-25 flask in parallel to the culture in the microfabricated device and imaged at the same time every day.

Results obtained showed similar growth trends in the control flask and in the microfluidic device (figure 26). Both vessels started at comparable confluencies

(approximately 3%). Growth was faster in the T-flask during the first 72 hours until the confluency reached a plateau between 50 and 55%. Growth in the microfluidic device progressed at an almost constant rate and a confluency of 75% was reached after 143 hours of culture.

In terms of morphology, the cells formed tighter clusters in the microfluidic device than in the T-flask. This phenotype was particularly obvious beyond 72 hours of culture (figure 27). Cells expanded in monolayer in the T-flask, while they formed multi-layered colonies in the device.

Although the aim of this study wasn't to compare growth performance and cell morphology in the microfluidic platform and in typical culture devices such as T-flasks, a few hypotheses could be formulated to explain the discrepancies observed.

The main difference between the two processes was the media renewal rate. The microfluidic reactor was constantly perfused at 300 µl/h. The culture chamber volume was approximately 25 µl; therefore a full chamber volume was renewed every 5 minutes. On the other hand, the T-flask was a static culture, with no media change performed. Therefore nutrients depletion and metabolic waste accumulation in the T-flask would have created an unfavorable environment for cell proliferation in the long run and affected negatively the growth rate. In the microfluidic device, the constant renewal of nutrients and removal of metabolic waste would have contributed to maintain a favorable environment for cell proliferation.

Hypotheses concerning the discrepancies in growth rates at the beginning of the culture and the colony phenotypes observed are more difficult to formulate without further studies. Differences in surface-to-volume ratio between the systems would have affected mass transfer of nutrients to the cells. Therefore comparative studies of growth kinetics should aim to maintain this parameter constant across the different systems tested. The effect of perfusion on the removal of cell-signaling factors has been shown to play a role on the proliferation and differentiation of stem cells (Blagovic et al., 2011), and might be responsible for the slower cell growth and the difference of phenotype observed in the microfluidic device. The formation of tight, multi-layered colonies might have favored the retention of essential autocrine and paracrine signaling molecules in the ECM that would have been washed-out by the perfusion otherwise.

The monitoring approach was successful at collecting qualitative (PCM images) and quantitative (confluency values) information on the state of the cells in culture. Overall, it integrated as intended in the experimental workflow. However, the transfer procedure was cumbersome and lengthy, and introduced a significant risk of failure of the system. It took on average an hour to stop the perfusion and DO monitoring, disconnect the system, transfer it to another lab, mount it on the microscope, acquire images of the chamber, transfer it back to incubator, reconnect the system and restart the perfusion and DO monitoring. Because PCM images were acquired manually, it was not possible to accurately to return to the same positions in the culture chamber day after day. Automating image acquisition using a programmable motorised microscope stage would allow to record time-lapse sequence of specific positions in the culture chamber, and could be used to study cell migration patterns and local growth rates. Performing the culture directly on a microscope stage would remove the need for stopping the perfusion and transferring the system and enable real-time online monitoring of the cell growth at a high sampling frequency.

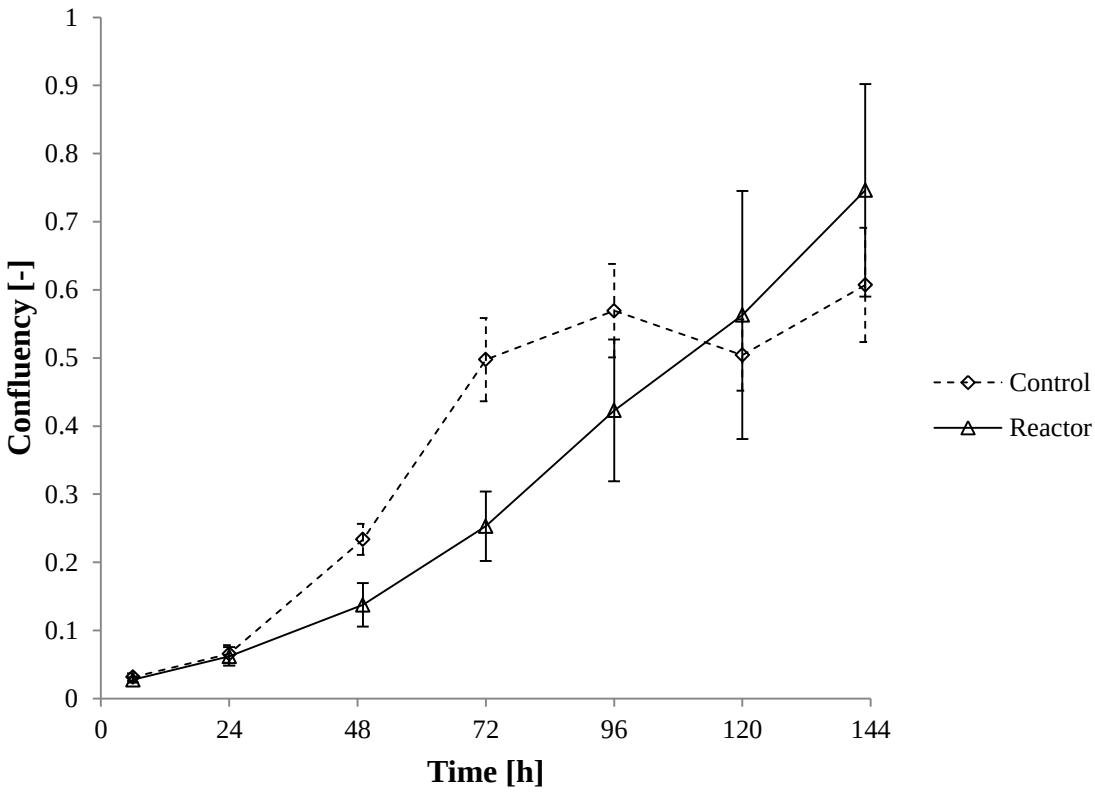

Figure 26: Confluency curves of mESCs grown in a T-25 flask (Control) and in the microfabricated culture device (Reactor). Each point represents the average computed confluency of ten 10x magnification PCM images. The error bars represent the standard variation of the average confluency.

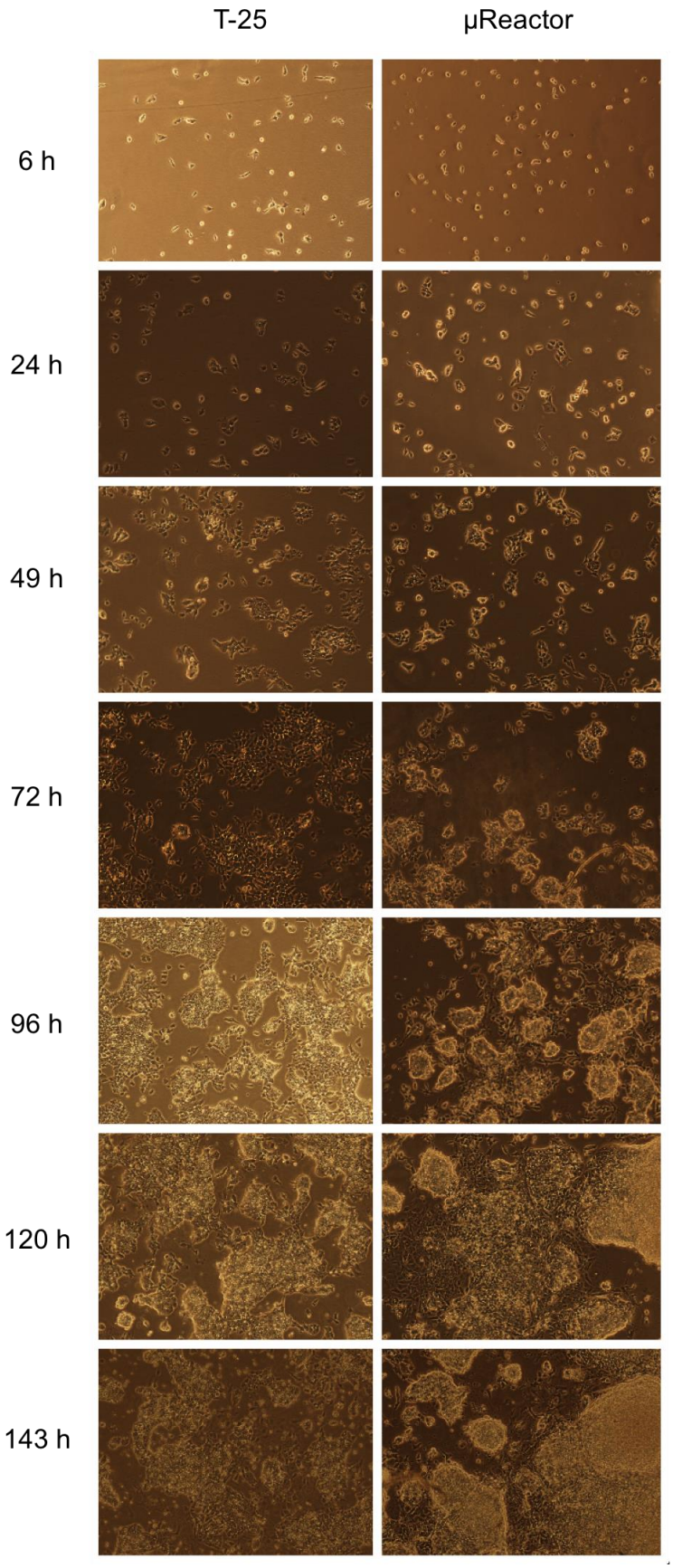

Figure 27: PCM images (10x magnification) of the expansion of mouse embryonic stem cells in a T-25 flask (left) and a microfluidic device (right).

4.2.6.4 Oxygen monitoring

Dissolved oxygen tensions were monitored online in the culture platform by optical sensor spots integrated in the perfusion system and in the culture chamber of the device (*in situ*). The sensors were read by optical fibers aligned with their locations. The optical fibres were connected to a transmitter outside of the incubator, which was interfaced with a computer to control the sampling frequency, analyse the read-outs, perform the calibrations and record the data generated. A two-point calibration at 37˚C was used, with the 0% established prior to the experiment and the 100% at the beginning of the culture. A new calibration was used for each experiment. The oxygen monitoring was stopped periodically to allow transfer of the system for cell imaging.

Excluding the experiments that failed because of contaminations, cell death and bubbles problems, complete oxygen profiles were obtained for five culture experiments (shown in Figure 28, 29 and 30): two experiments with monitoring at the inlet and *in situ* and three experiments with the complete three-locations (inlet, outlet, *in situ*) monitoring system.

4.2.6.4.1 Inlet measurements

Inlet measurements were intended to provide information of the level of dissolved oxygen supplied to the cells. At constant flow rate and temperature, it should have stayed constant according to Henry's law. However, the data collected indicated a great variation of inlet DO levels during the experiments and between independent experiments (Figure 28).

During the initial static culture phase, levels at the inlet immediately diverged from the established calibration. A common trend was observed in experiments (a), (b) and (c), where the initial DO level started higher than the calibrated 100% and decreased steadily before reaching a stable value. During the static phase, the inlet sensor was physically isolated from the culture chamber by a closed valve; therefore we could discard the hypothesis that the decrease observed at the inlet was linked with the cellular oxygen uptake in the device chamber. If the apparent decrease wasn't an effect of biological oxygen uptake, the validity of the calibration approach used had to be reconsidered. The 100% DO was calibrated at the

beginning of the culture, as it was assumed that it would be then representative of the actual maximum oxygen saturation reachable under the pressure and temperature conditions of the experiment. However this assumption was based on the hypothesis that temperature and pressure would be stable at the beginning of the experiment. As per the experimental procedure followed (see section 4.2.5), the perfusion system was connected to the already-seeded device in a biosafety cabinet at room temperature and then the complete system was transferred immediately to an incubator at 37˚C to start the culture phase. Thus, the sensors were actually calibrated at a temperature closer to room temperature than 37˚C. As the temperature of the system increased to reach equilibrium of the outer temperature, the solubility of oxygen in the medium decreased as well as the dissolved oxygen levels. Therefore, it was necessary to establish an approach to calibrate the sensors in thermally stable conditions.

In experiments (d) and (e), the 100% DO was calibrated at the beginning of the perfusion phase. The same trend of decreasing oxygen levels is observed, albeit less pronounced than in the previous experiments.

During the perfusion phase, in addition to the slight initial decrease caused by temperature changes, sudden variations of the oxygen levels at the inlet location could be observed after each imaging phase. These sudden variations in the oxygen baseline each time the monitoring system was disconnected and reconnected, seemed to indicate a problem in the reconnection and realignment of the fibres with the sensor, causing a shift in the apparent oxygen level measured.

These results indicated that the disconnection and reconnection of the monitoring system combined with transfers out of the incubator to acquire microscopy images was detrimental to the quality of the oxygen measurements collected.

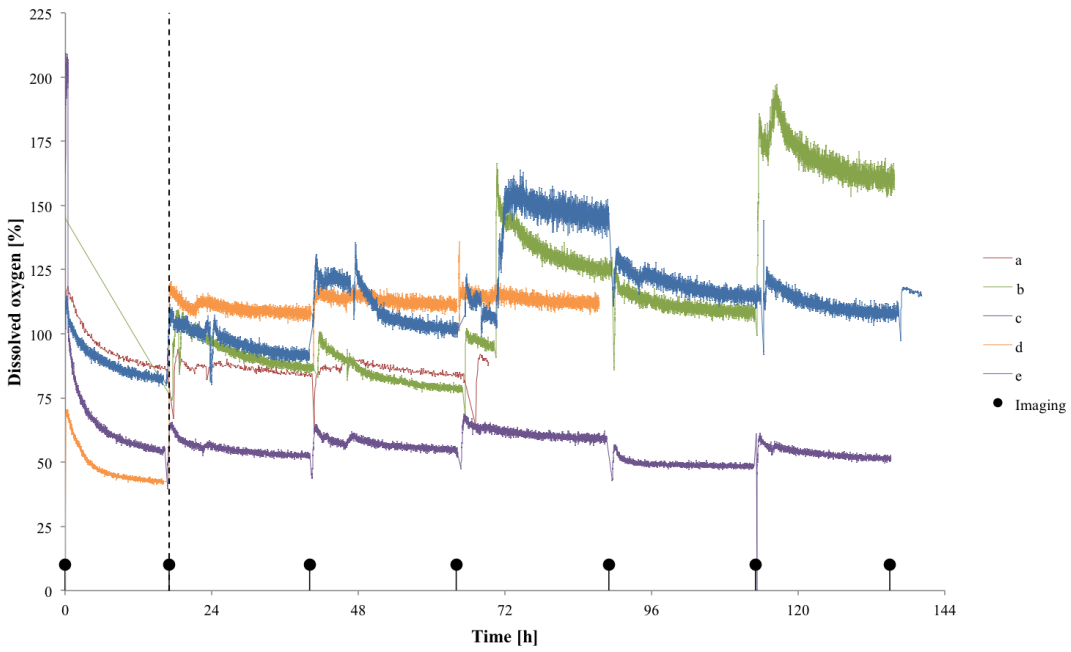

Figure 28: Dissolved oxygen profiles of five independent experiments (a to e) measured at the inlet of the microfabricated culture device. Black dots mark the interruption of the DO monitoring for the imaging. A vertical dashed line indicates the end of the static culture phase and the beginning of the perfusion phase.

4.2.6.4.2 Outlet measurements

Oxygen monitoring at the outlet of the culture device was intended to provide a measurement of the oxygen consumed by the cells in the device. By subtracting the outlet values from the inlet values, it would have been possible to calculate the oxygen uptake rate of the culture.

The data collected for the experiments (c), (d) and (e) is presented in the figure 29. The outlet measurements presented much less variations than those taken at the inlet. Over the course of each experiment, the trend of the outlet oxygen levels is slightly negative. Although, without usable reference measurements at the inlet, it was not possible to confirm that this trend was effectively due to measurable oxygen consumption in the device. The relative stability of the outlet measurements, compared to those at the inlet, seemed to indicate that the inlet sensor might have had a defect causing the variations in measured oxygen.

Negative DO spikes, coinciding with the imaging phases, were observed on the outlet measurements. Following the reconnection of the DO monitoring system, initial oxygen measurements were on average 25% lower than those previously

recorded. Oxygen levels then recovered to pre-imaging ranges in less than an hour. There is no strong indication that these spikes were caused by cellular respiration, as it would be expected that their magnitude and the recovery time would increase with the cell numbers (and therefore over time).

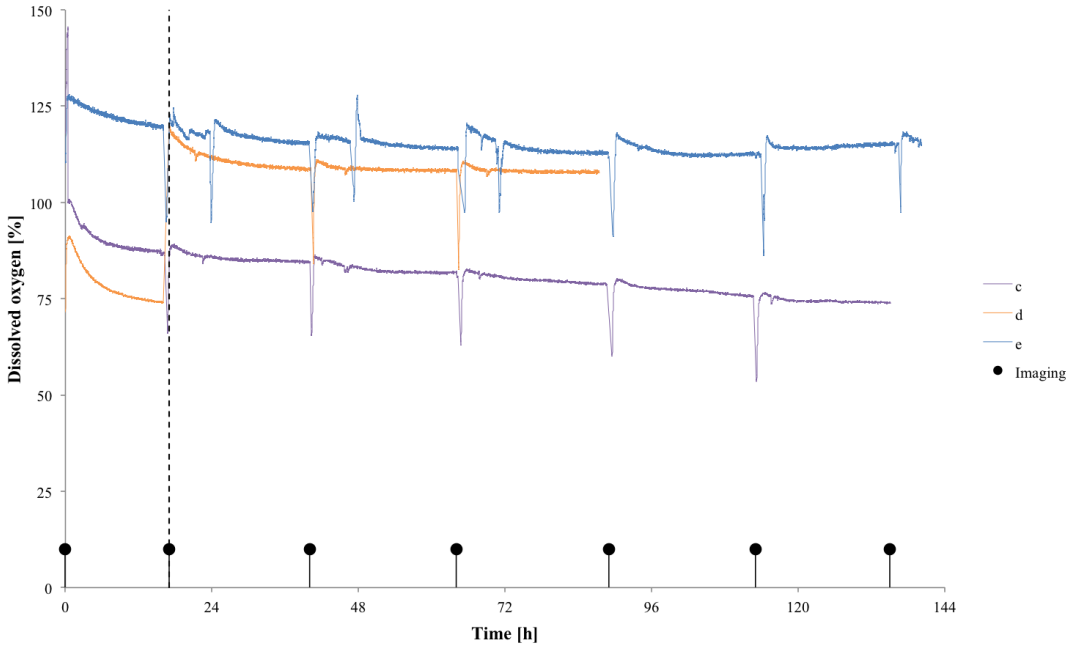

Figure 29: Dissolved oxygen profiles of three independent experiments (c to e) measured at the outlet of the microfabricated culture device. Black dots mark the interruption of the DO monitoring for the imaging. A vertical dashed line indicates the end of the static culture phase and the beginning of the perfusion phase.

4.2.6.4.3 In situ measurements

In situ measurements were provided by a planar sensor integrated in the culture slide of the device. Two types of slide designs were used in the experiments presented: a TC-PS slide and a glass slide. The TC-PS design was ultimately abandoned; as it didn't meet the requirements for asepsis (see section 4.2.6.1). Only the results from the experiment (a) were obtained with that design, the runs (b) to (e) were performed with the glass slide design (figure 30).

In situ measurements exhibited a rapid decrease of oxygen levels in four of the five completed experiments. In experiments (a), (c) and (d), *in situ* readings decreased to hypoxic levels (<5% DO) in less than three days. In experiment (e), the readings remained above 90% DO for the first three days and then rapidly decreased to

hypoxic levels during the fourth day of culture. In experiment (b), it took the whole duration of the experiment for the readings to steadily reach 25% DO.

The same measurement artefacts (initial DO decrease post-imaging and spikes) were observed in the *in situ* readings. However, there was a distinct decreasing trend in all experiments, though at different rates and timing. However, the fact that the cultures reached hypoxic peri-cellular levels in such a short period of time, under continuous perfusion of oxygenated medium, let us to hypothesise that the dramatic peri-cellular oxygen depletion might be as well another culture artifact. Cell overgrowth on the *in situ* sensor could limit oxygen transfer from the peri-cellular environment to the sensor matrix because of the oxygen diffusion and consumption in the cell clusters. Therefore apparent peri-cellular measurements could be effectively lower than the actual values.

To assess if cell overgrowth occurred on the *in situ* sensor, the cells were fixed and stained post-culture with DAPI (a nuclear marker). The device was then imaged upside-down to visualise any positively stained cells present on the top of the *in situ* sensor. The images obtained (figure 31) confirmed the presence of cell clusters overgrowing the sensor. Further studies would be required to understand how cell overgrowth quantitatively affects *in situ* measurements: for example, if a correlation exists between the percentage of the sensor area covered by the cells and the oxygen measurement. If there was one, the *in situ* sensor would act indirectly as a confluency measurement method). It is also necessary to study strategies to prevent cell overgrowth in order to obtain accurate peri-cellular oxygen reading (see future work section).

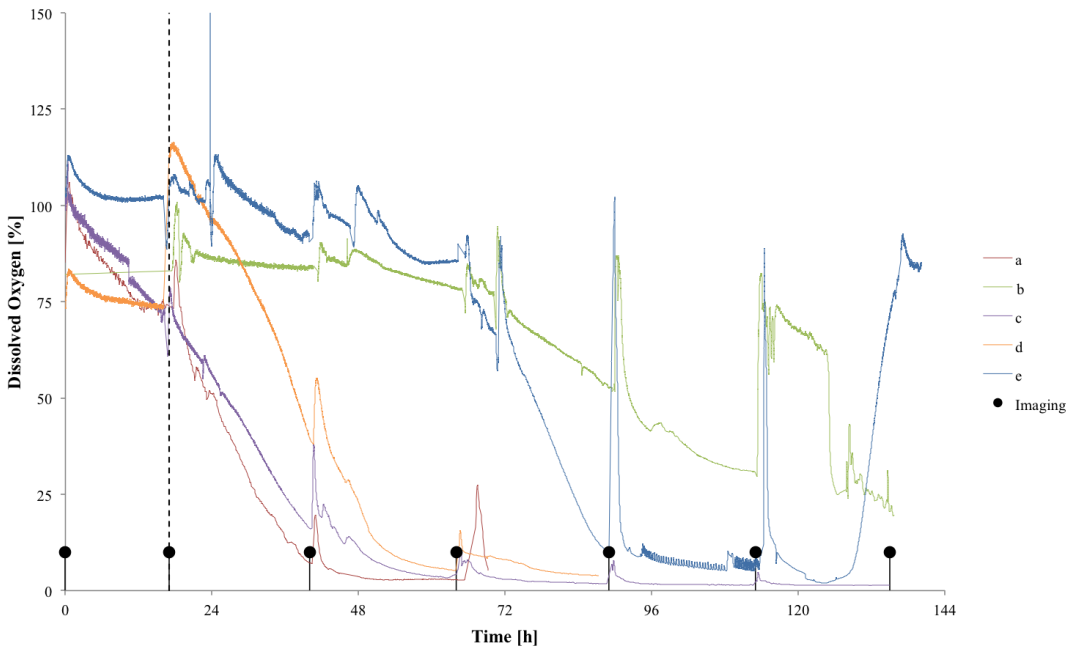

Figure 30: Dissolved oxygen profiles of five independent experiments (a to e) measured in the chamber of the microfabricated culture device. Black dots mark the interruption of the DO monitoring for the imaging. A vertical dashed line indicates the end of the static culture phase and the beginning of the perfusion phase.

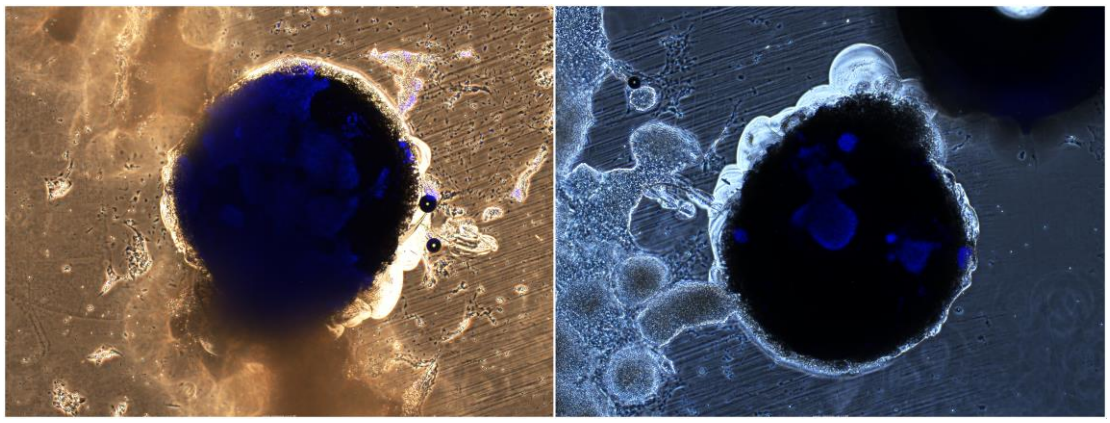

Figure 31: Composite microscopy images (phase contrast/epifluorescence, 4x magnification) of the *in situ* sensor after two independent culture experiments. Cells overgrowing the sensor appear in blue as they stain positively for DAPI.

4.2.6.5 End-point assays

Cells were stained on chip for pluripotency markers at the end of the culture. Initial staining experiments were performed with a single primary antibody targeting Nanog, a pluripotency marker for mouse embryonic stem cells, in order to assess the feasibility of the procedure. Taking advantage of the resealable lid of the device,

the staining was done directly in the culture chamber. The device was disconnected from the perfusion system and brought to a biosafety cabinet. The lid was opened and all the steps of the staining protocol described in section 2.4.1 were performed in the open chamber. Once the staining was completed, the device brought to an inverted microscope to image the cells. The first results obtained (figure 32) showed very few cell colonies present in the culture chamber after the staining procedure. Approximately 10 small clusters of cells were found in total by visual inspection of the chamber. All of them were positive for Nanog expression. That constituted a first indication that the pluripotency of mouse embryonic stem cells was maintained during culture in the microfluidic device. However, the staining procedure needed to be improved to reduce cell loss. The losses occurred most likely during the opening of the lid and the manual pipetting of solutions in and out of the chamber. Both these operations induce hydrodynamic shear stress on the cells. By pulling the lid out of the sealing gasket, the liquid below is as well pulled upwards and released downwards when the lid is entirely removed. In order to minimise the stress induced by the lid opening, it was decided to start the staining procedure by gently perfusing phosphate buffered saline (PBS) through the device with a syringe connected to the inlet. The perfusion induced a slight pressure in the device and avoided the aspiration and release of the liquid in the chamber when the lid was removed. Pipetting of the solutions (fixing agent, permeabilising agent, antibodies and nuclear stain) was then performed in a designated corner of the chamber to restrict damages to this area. The device was gently tilted to spread the solutions over the whole chamber area. The solutions were washed and removed from the device by perfusing and withdrawing PBS in the chamber through the channels of the chip with a syringe connected to the inlet. The subsequent culture staining following this modified procedure exhibited lesser cell loss post-staining (Figure 33). Theoretically, it would be possible to perform all the staining protocol by sequential perfusion of the reagents through the device using the perfusion system. The accurate control of flow rate would allow reducing further the shear stress inflicted to the cells during the procedure. However, it would as well require the integration of an automated valve system to switch seamlessly between the reagent solutions. The perfusion system would also have to be able to inject small sample volume to avoid the waste of expensive reagents such as antibodies.

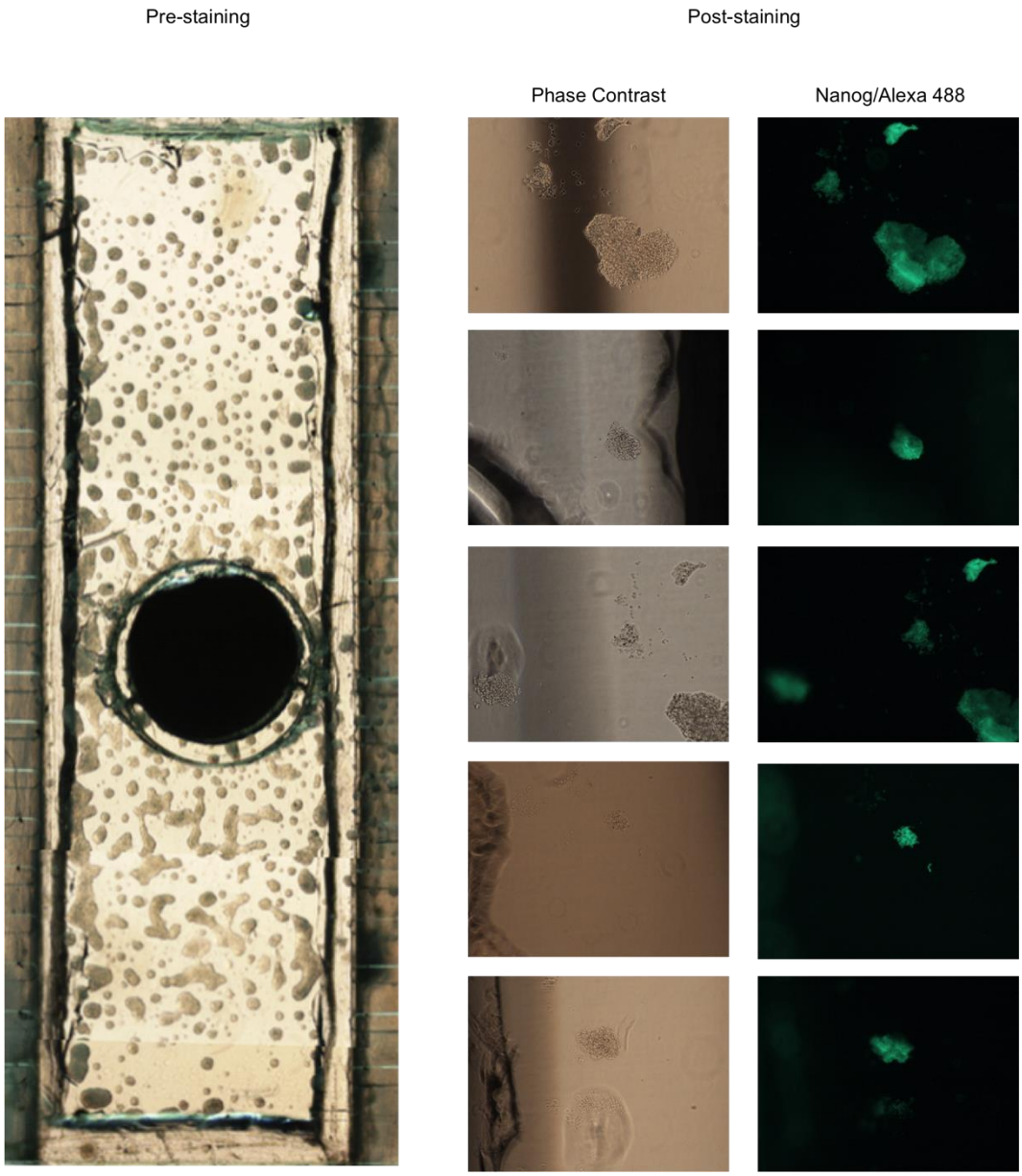

Figure 32: Microscopy images of mouse embryonic stem cells in the microfabricated culture device before and after staining procedure. Pre-staining: whole chamber view constituted of four 2x magnification PCM images taken after 71 hours of culture. Post-staining: Microscopy images of the colonies remaining in the chamber after the staining procedure: in the left column 10x magnification PCM images, in the right column fluorescent images at 470 nm emission wavelength to detect Anti-nanog Alexa 488 conjugates.

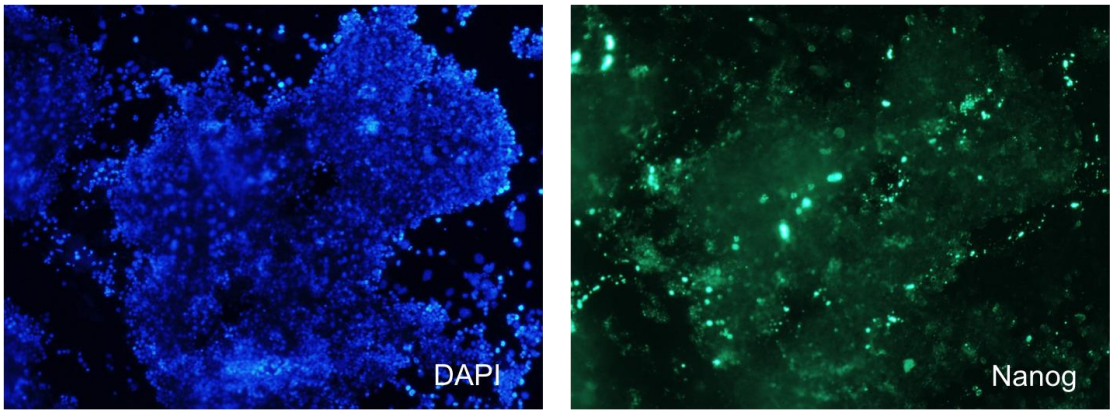

Figure 33: Epifluorescence microscopy images of mESCs cultivated in the microfabricated device: DAPI (left) and Nanog/Alexa 488 stains (right) of the same cell cluster. The staining procedure was performed following the improved protocol designed to minimise cell loss during the washing steps.

4.3 Summary of findings

A microfluidic platform with online oxygen monitoring has been developed for adherent stem cell culture. The platform used a standard cell culture incubator to house the culture device and maintain the cells at optimal temperature. A pressure-driven perfusion system was connected to the device to control the medium renewal rate, supply dissolved oxygen and maintain the pH. Oxygen concentration levels were monitored in three locations of the system with the optodes presented in section 3.2.2. To quantify cell growth, the device was transferred to an external microscope to image the cells growing in the culture chamber. An image analysis algorithm was used to determine cell confluency from PCM images.

An ensemble of procedures was defined to ensure the robust operation of the platform. Cell culture experiments with mouse embryonic stem cells were performed to assess the performance of the platform and the suitability of the procedures. Modifications to the protocols were brought to address contaminations and improve the efficiency of the end-point immunostaining assays. The platform was able to sustain the expansion of mouse embryonic stem cells for up to 6 days. However the oxygen profiles gathered were not usable due to variations caused by temperature changes and optical fibre re-alignements after each imaging phase outside of the incubator. This led to the development of the automated platform for seamless monitoring presented in Chapter 5.

5 An automated microfluidic platform for the seamless monitoring of oxygen and confluency in mouse embryonic stem cell cultures

5.1 Seamless monitoring strategies

The first-generation microfluidic platform, presented in Chapter 4, was able to sustain stem cell culture for up to 6 days. However the need to transfer the device out of the incubator for imaging impacted negatively the performance of the oxygen monitoring setup. Frequent realignments of the optical fibres for the sensor read-outs after the imaging phase rendered unusable the calibrations established at the beginning of the experiment. The temperature difference between the incubator and the microscope created outgassing cycles.

In order to overcome these issues, it was necessary to design a platform that would be able to monitor dissolved oxygen tensions and perform image acquisition of the culture chamber without the need of removing the culture device from a temperature-controlled environment or interrupting the perfusion. Both monitoring systems (dissolved oxygen levels and culture chamber imaging) would have to be able to operate in parallel without negatively affecting the performance of the other.

5.1.1 Microscopy in a temperature-controlled environment

Two approaches exist to enable image acquisition of cells in a temperature-controlled environment: bringing the microscope inside the incubator or creating a temperature-controlled environment on the sample holder of the microscope. The first approach requires the development or the purchase of specific microscopy equipment. The second can be achieved in two-ways: using a cage incubator around the microscope stage or using smaller temperature-controlled chamber that would fit around the cell sample and maintain it at defined temperature, and partial gas and vapour pressure. The second approach is more suited to standard format culture ware such multi-well plates or petri dishes. The cage incubator will accommodate any device fitting on the stage of the microscope but will limit environmental control to temperature. Contrary to a traditional cell culture incubator, a cage incubator isn't usually sealed. The most accessible approach is to use a cage-incubator, as specialised microscopes for incubators are expensive and on-chip temperature control will involve consequent development and testing time.

5.1.2 Monitoring of confluency and oxygen in the culture chamber

Potential conflict between the oxygen and the confluency monitoring system arise in the culture chamber. Both systems require physical alignment on this location of the system in order to acquire images for the confluency monitoring and collect the *in situ* sensor read-out for the oxygen monitoring. Two approaches exist to solve this issue: parallel monitoring and alternated monitoring. Parallel monitoring consists in performing both measurements at the same time. In order to achieve parallel monitoring, both the camera optics and the optical fibre have to be able to align simultaneously with their sample. As the in situ sensor is integrated on the cell substrate, the ideal alignment angle for both optics and fibre is from the bottom of the reactor. However it is not physically possible to align them at the same time from the bottom because of the diameter of the optics and optical fibre compared to the footprint of the culture chamber. With significant redesign of the culture device, it would be possible to create waveguides allowing performing oxygen sensor read-outs using a diverted path. However, given the time scale of stem cell cultures, there are no requirements for absolutely simultaneous oxygen and confluency measurements and therefore alternated monitoring constitutes a more convenient approach to the situation. To achieve alternated monitoring, the optics and fibre must be aligned sequentially with the measurement positions. It requires the ability to return accurately to a given position. For this task, motorised stages are particularly well suited. The culture device would be placed on a stage programmed to cycle between the optics and fibre position at a given rate. When aligned with the oxygen sensor, the fibre will collect the read-outs; when aligned with the optics, images of the culture chamber will be acquired. This approach requires subsequent automation of the monitoring systems in order to synchronize the read-outs with the positioning of the device. The use of an automated stage would also enable the interrogation of fixed recorded locations providing high-resolution images that could be used to track cell migration patterns or determine local confluency growth rates.

5.2 Results & Discussion

The objectives of this study were (1) to test and optimize the automated monitoring platform and to (2) gather quantitative data on mouse embryonic stem cell growth kinetics in the microfabricated device.

5.2.1 Automated culture platform concept

A platform (figure 34) was designed to enable seamless monitoring of dissolved oxygen tensions and cell confluency in a microfabricated culture device operated in perfusion. The device was placed on the stage of a motorized inverted microscope fitted with a cage incubator to enable online monitoring of cell confluency during the culture. The motorized stage of the microscope was used to create the seamless alternated monitoring of confluency and oxygen in the culture chamber. The optical fibre for the *in situ* DO sensor was mounted to the side of the microscope objective using a specially designed collar adapter. The three-dimensional stage positions for imaging of the whole culture area and read-out of the *in situ* DO sensor were recorded and recalled sequentially by a software control routine. This approach enabled to generate high-resolution images of the whole culture area without compromising *in situ* DO monitoring capabilities. The perfusion system remained identical to the first-generation platform presented in Chapter 4.

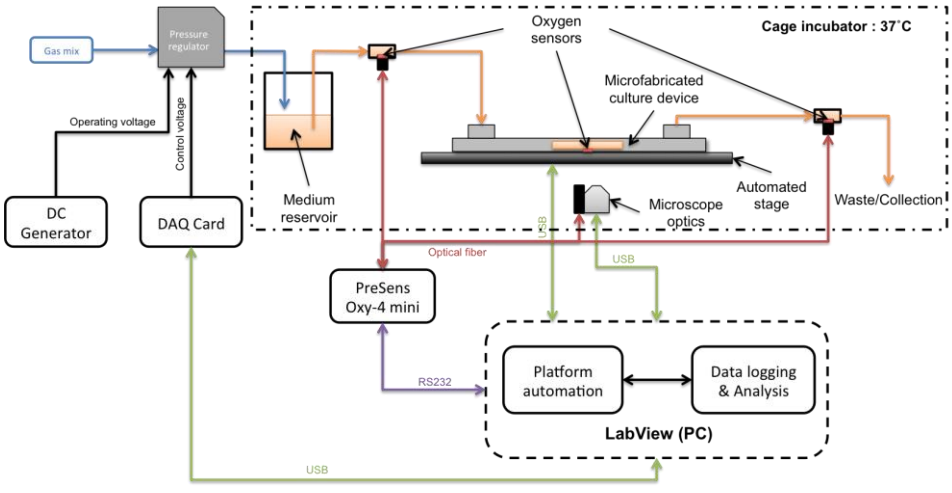

Figure 34: Schematic representation of the automated platform for instrumented microfluidic cell culture.

5.2.2 Automation

Seamless monitoring was designed as a loop (figure 35), where the stage cycled through different positions at a defined rate before resetting to a default position. The automation of the monitoring loop was realized using LabVIEW virtual instruments controlling the functions of the microscope (stage, objective turret, illumination intensity) and the digital camera (image acquisition, resolution, exposure, gain). The LabVIEW virtual instruments were designed and built in collaboration with Nicolas Jaccard and Rhys Macown. This work contributed specifically to the integration of the *in situ* DO measurement scheduling in the stage control routine. A graphical user interface (GUI) was integrated enabling the user to control manually the function of the microscope, visualize a continuous live-stream from the digital camera to assist in the tuning of the imaging settings and more importantly define time-lapse sequences for imaging and *in situ* DO monitoring. The sequences were created by the user, by recording the three-dimensional positions of the stage for each field of view to be imaged, and setting the repeating interval of the whole sequence. Specific settings for the illumination intensity and the objective type could be associated with each imaging steps. The user could as well define a position aligning the optical fibre mounted on the objective with the *in situ* DO sensor. This particular position would be interpreted as a default position for the stage between each imaging cycle. Between each imaging step, the control routine would also shut down the illumination to avoid phototoxic effects on the cells and photobleaching of the DO sensor.

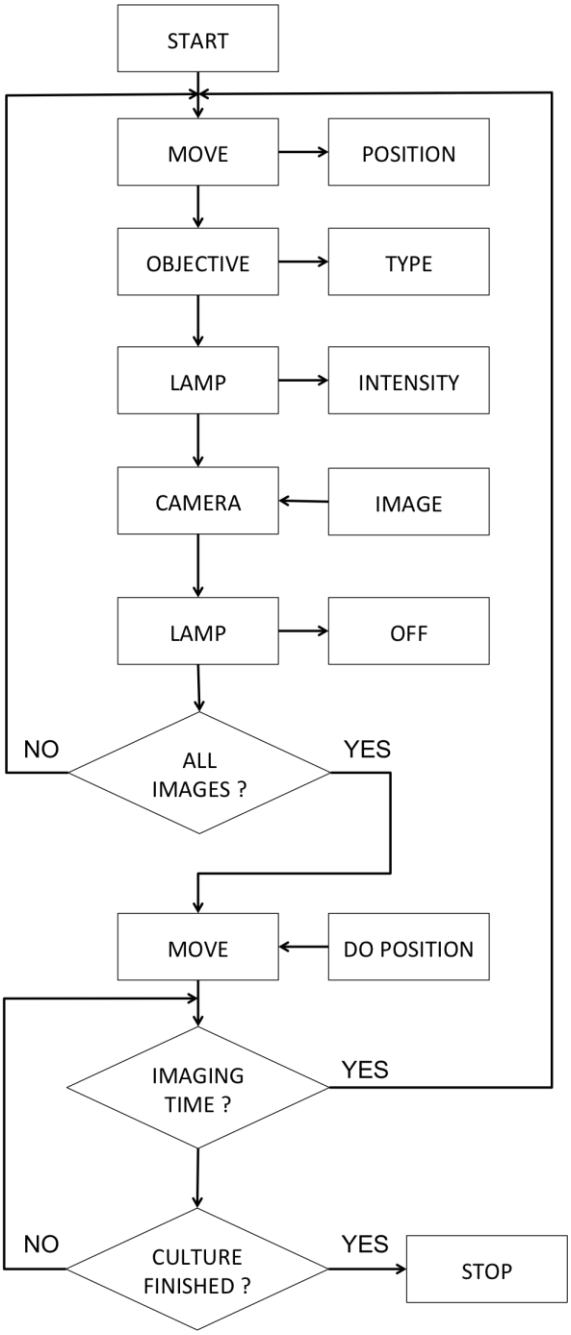

Figure 35: Schematic of the monitoring loop for the automation system**.**

5.2.3 Operating procedure

The automated platform was operated following a procedure derived from the one of the first-generation platform (figure 36). The device was sterilised and assembled in exactly the same fashion. After ECM coating, the perfusion system was assembled and connected to the device. The fluidic network was then primed using the bypass technique to remove air bubbles. Once primed and closed, the device and perfusion system were transferred onto the stage of the microscope.

The flow-through cell sensors were connected to the transmitter with optical fibres. A third optical fibre was mounted on the side of the 10x objective of the microscope using the collar adapter. The optical fibre was aligned with the *in situ* sensor using the motorised stage. To assist with finding the optimal position, the control software for the transmitter was used to read-out the intensity of the sensor. The stage position was recorded in the monitoring automation software when the intensity was at the highest value measured. This would ensure an optimal signal-to-noise ratio for the sensor read-outs. The perfusion was then started alongside with the oxygen monitoring. After an overnight incubation and controlling that phase values measured were stable, the sensors were calibrated for 100% DO. After the calibration, the perfusion and oxygen monitoring were stopped.

A cell inoculum was prepared according to the standard procedure and seeded in the open chamber of the device on the stage of the microscope. The lid was then closed and the cells let to adhere in the culture chamber for three hours. After that incubation period, cell adhesion was checked visually on the microscope. Once the cells had properly adhered to the substrate, 60 imaging positions were manually recorded in the monitoring automation software to cover the whole culture area of the chamber. The imaging sequence was set to repeat every 30 minutes and the DO monitoring to perform measurements in the three locations every 15 minutes.

Once the monitoring routine was set up, the perfusion was started. The system was checked at least twice a day during the course of the culture (up to 6 days) to detect any faults or issues. At the end of the culture, the cells were stained on chip following the optimised protocol previously described (section 4.2.6.5).

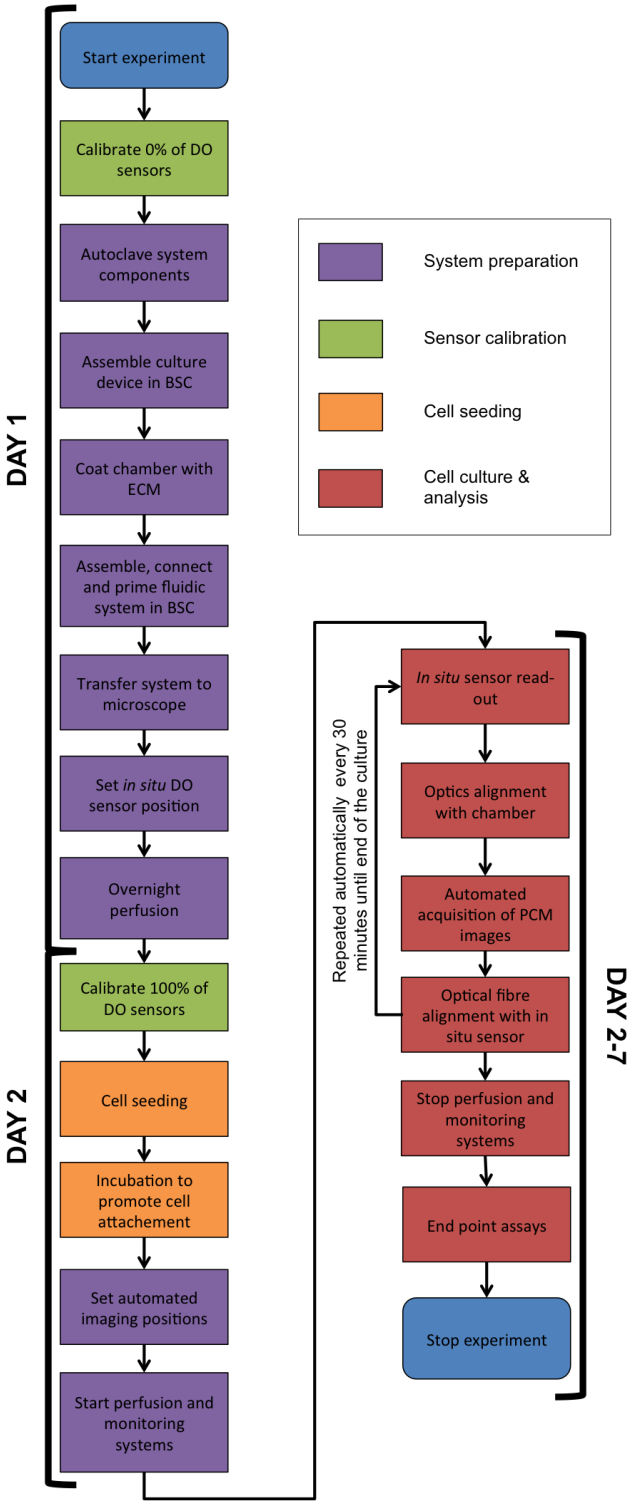

Figure 36: Diagram of the experimental procedure for the culture of mouse embryonic stem cells in the microfluidic automated platform.

5.2.4 Cell culture experiments

A total of 14 cell culture experiments (Appendix Table 2) were performed on the automated platform. Five of them didn't suffer from any failure and were carried

beyond 5 days of culture. Three experiments were aborted because of leaks in the device, two because of air bubbles in the culture chamber, and one because of clogging of the outlet tubing. Software-related issues prevented the monitoring systems to function in two experiments. And lastly, a single case of contamination was observed.

5.2.4.1 Maintenance of asepsis

A single event of contamination was observed in the culture experiments performed on the automated platform. Contrary to previous occurrence in the first-generation platform, the contamination was not limited to the culture device but extended to the medium reservoir. It also occurred despite the presence of antibiotics in the culture medium. A new stock of the antibiotics was then used for the following experiments. As contaminations did not reoccurred after the introduction of the new stock, it indicated that the antibiotic solution aliquot previously used might have been improperly stored or handled.

5.2.4.2 Fluidics

Three issues affected the fluidic system during the culture experiments: air bubbles, clogging of the tubing and leaks in the culture device.

Air bubbles were spotted on the first day of culture in two experiments. Unlike the experiments in the first-generation platform, they continued to increase in size over the next days despite the continuous perfusion. In one case, the culture chamber was finally totally dried out after 48 hours of culture. These results indicated that the rate of evaporation out of the device exceeded the medium renewal rate. It was a consequence of the lack of humidity in the microscope cage incubator. To remediate the evaporation problem, a water pan was added at the bottom of the cage incubator. Its content was renewed daily to maintain a humidified atmosphere in the cage during the whole course of the culture experiments.

Clogging at the end of the outlet capillary occurred in one of experiment. It stopped the perfusion and an arrest of the cell growth was observed after 24 hours of culture. This incident stressed the fact that small-diameter capillaries are particularly sensitive to fouling by medium components. Over an extended period of use and

despite the systematic cleaning of all the system parts after each experiment, the fouling will lead to the clogging of the tubing.

The last and most serious issue with the fluidic system was the repeated leaking of the culture device. Leaks will alter the performance of the pressure-driven system as they induce a pressure decrease in the whole system. They result from a lack of sealing at the interface of the device components. This lack of sealing promotes also contaminations from the external environment. Finally, the medium leaking from the device may seriously damage the microscope components underneath the stage (objective turret and filter blocks) and cause long-term interruption of the experiments. Therefore leaks cannot be tolerated at any level in the automated platform.

The occurrence of leaking in the new platform was linked to the introduction of a new bottom frame design to accommodate the *in situ* optical fibre. This new design was 2-mm thinner than the previous design used in the experiment in the first generation platform. To improve sealing at the interface of the culture chip and the packaging frames, a system of aluminium brackets was introduced (figure 37). The brackets (designed by Rhys Macown) fitted around the interconnect blocks and were screwed together with the top and bottom frame to increase the rigidity of the packaging and minimise the lateral bending of the frames. Experiments where these brackets were used did not experience any leakages.

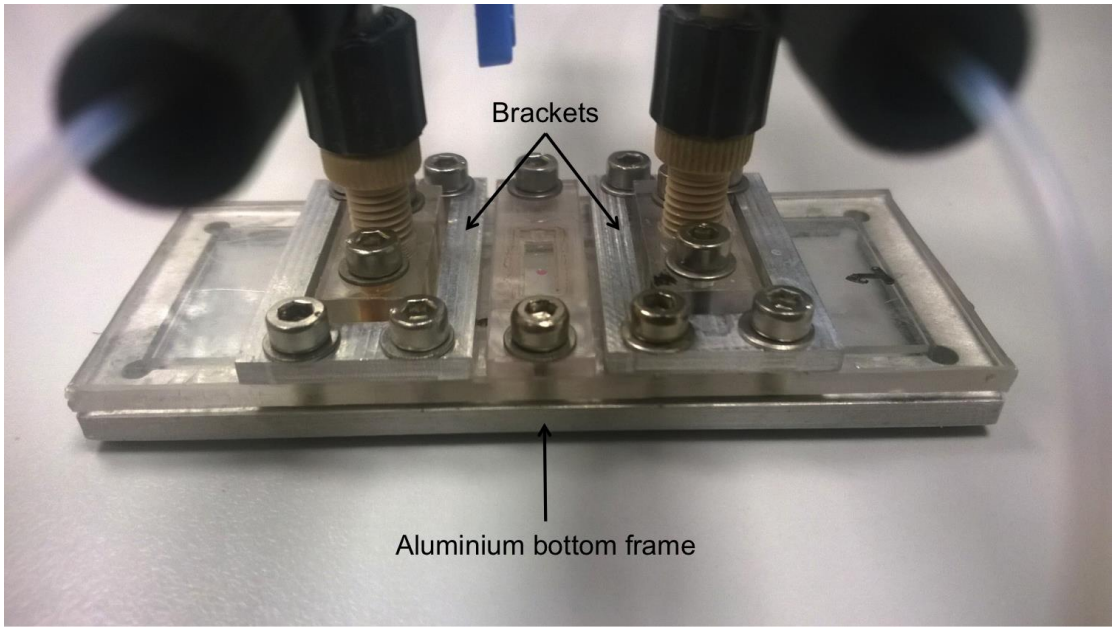

Figure 37: Microfabricated device with new aluminium bottom frame design and brackets to improve the rigidity of the packaging.

5.2.4.3 Confluency monitoring

Images of the culture chamber were acquired and saved automatically following the sequence defined at the end of the cell-seeding phase. The imaging sequence was manually defined by the user. Each imaging step was recorded in the monitoring automation software with its associated stage coordinates, light intensity settings and objective magnification. The monitoring loop was repeated every 30 minutes throughout the experiment. The saved images were processed after the end of experiment to determine confluency. This approach enabled to generate high-resolution confluency curves (figure 38).

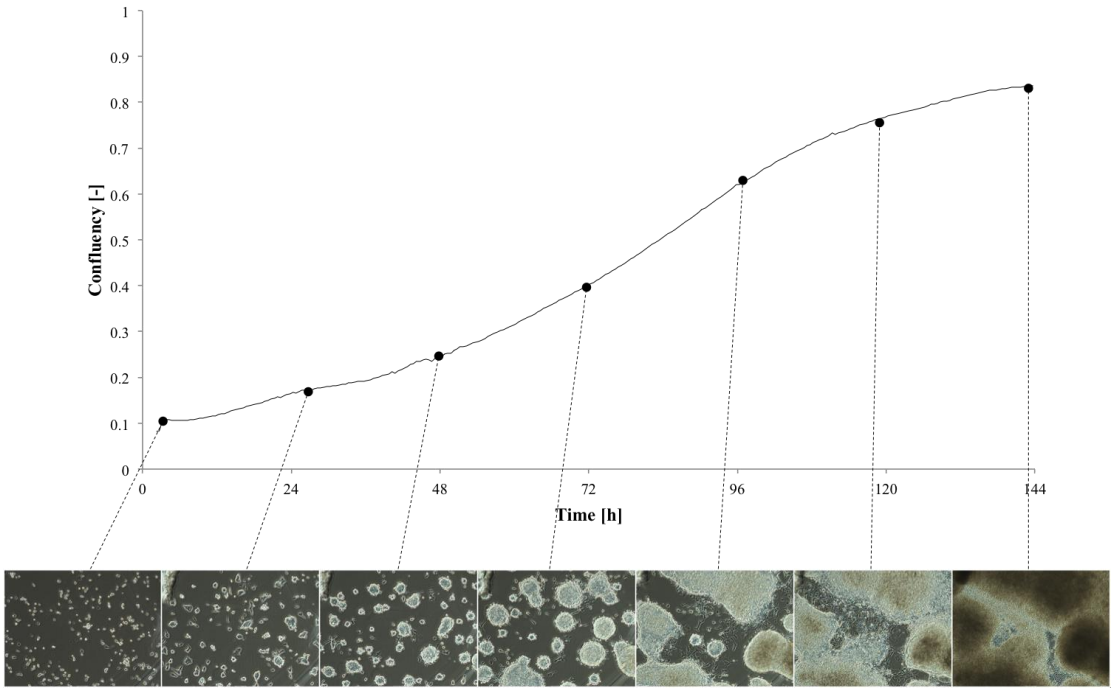

Figure 38: Confluency curve of mESC grown in the automated microfluidic platform for 144 hours. The culture chamber was imaged in 60 locations every 30 minutes to generate high-resolution growth curve. The timelapse PCM sequence underneath the curve illustrate the progression of the confluency in the same location of the culture chamber day after day.

5.2.4.4 Pluripotent markers expression

Cells were stained at the end of the culture, for two pluripotency markers: Nanog, shown previously, and SSEA-1, a membrane marker. The co-staining was carried out with success (figure 39) using the improved staining protocol developed for the microfabricated device in chapter 4.

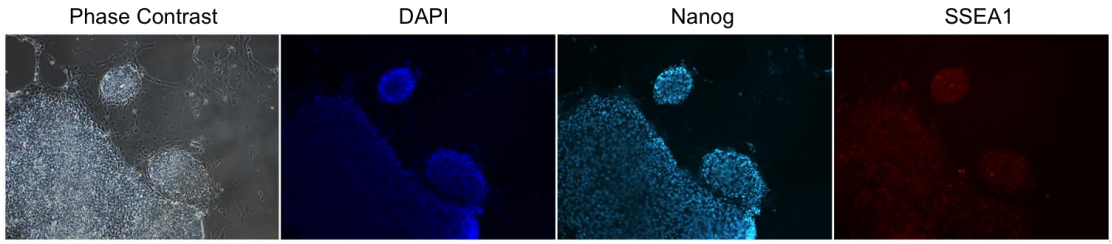

Figure 39: Endpoint on-chip immunostaining of mESCs for pluripotency markers (Nanog/SSEA1).

5.2.4.5 Oxygen monitoring

The automation loop controlling the microscope stage (see section 5.2.2) enabled the operation of the oxygen monitoring system without interruption. As it can be seen in the results presented in the figure 40, the oxygen curves did not display the sudden shifts previously associated with the interruption of the monitoring system.

The issue of unstable readings and inaccurate calibration due to temperature shifts was solved by the addition of an overnight incubation period, prior to calibration of the sensors and seeding of the cells. Oxygen values recorded at all the locations were stable (around 200 µM) at the beginning of the experiments A, B and C. Inlet readings remained stable in all experiments, indicating that the medium was perfused at constant flow rate and pressure through the system. Outlet readings showed a steady decrease of oxygen levels during the course of the experiments, down to 140 µM after 144 hours in A, and 170 µM after 144 and 120 hours in experiment B and C. *In situ* measurements followed the same trend previously displayed by the experiments in the first-generation platform, reaching null values after 72 hours in experiments A and B, and at the end of experiment C (120 hours).

By overlaying the average confluency curves, obtained by image analysis, with the oxygen curves, the relation between the biomass (approximated here by the confluency) and the oxygen consumption rate of the system became apparent. Experiment A, which displayed the lowest oxygen levels at the outlet at the end of the culture (140 µM), displayed the highest confluency (83%). Experiments B and C displayed higher oxygen levels (170 µM) and lower end confluency (79% and 56% respectively).

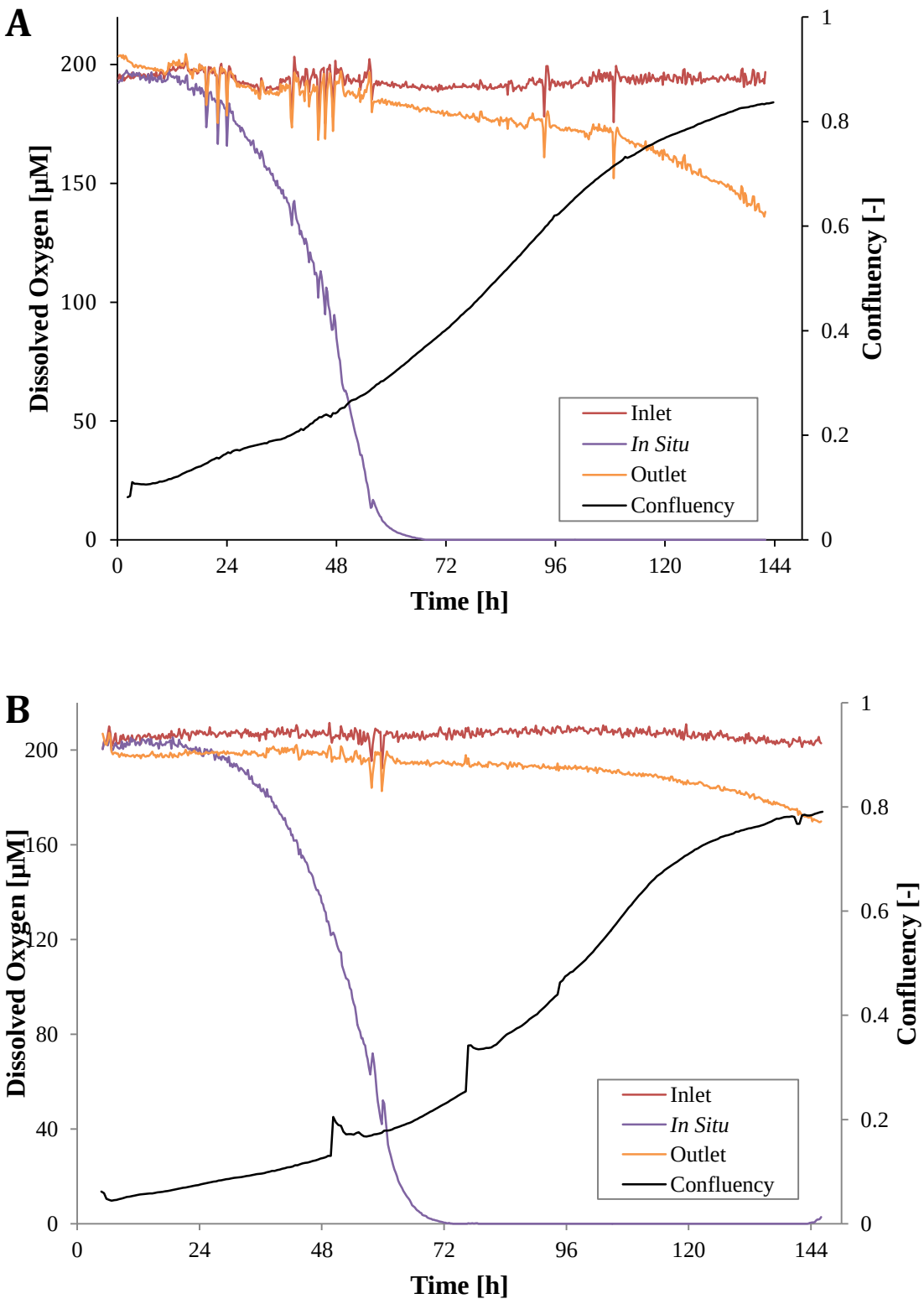
A
Dissolved Oxygen [µM]
Confluency [-]
Time [h]
Inlet
In Situ
Outlet
Confluency
B
Dissolved Oxygen [µM]
Confluency [-]
Time [h]
Inlet
In Situ
Outlet
Confluency

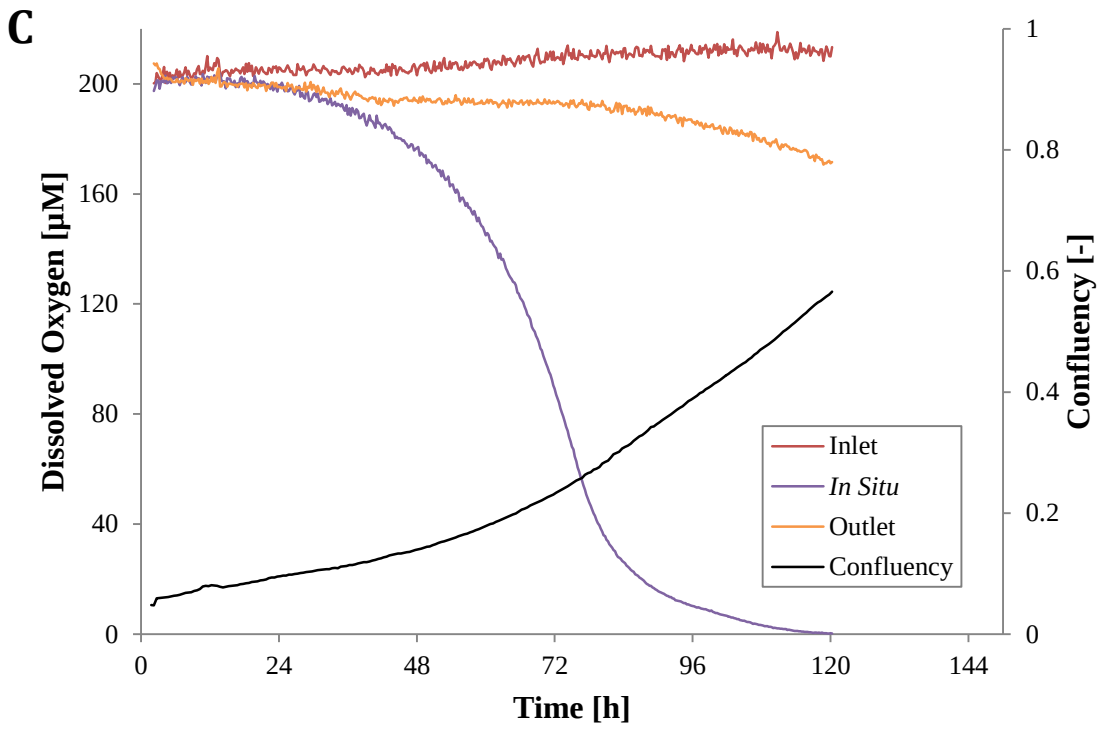

Figure 40: Real-time oxygen and confluency monitoring of three independent mESC cultures (A, B and C) in the automated microfluidic culture platform.

The bulk oxygen consumption rate (OCR) of each of the three experiments was calculated by subtracting the outlet readings from the inlet readings for each time point recorded. The bulk OCR, as a function of cell density, is a driving force in the formation of oxygen concentration gradients. Therefore at equal perfusion rate and chamber height, the relation between bulk OCR and peri-cellular oxygen concentrations should be reproducible across experiments. However, as shown in figure 41, the correlation curves between the three experiments did not match. This indicated that *in situ* DO readings did not provide an accurate measurement of peri-cellular oxygen levels.

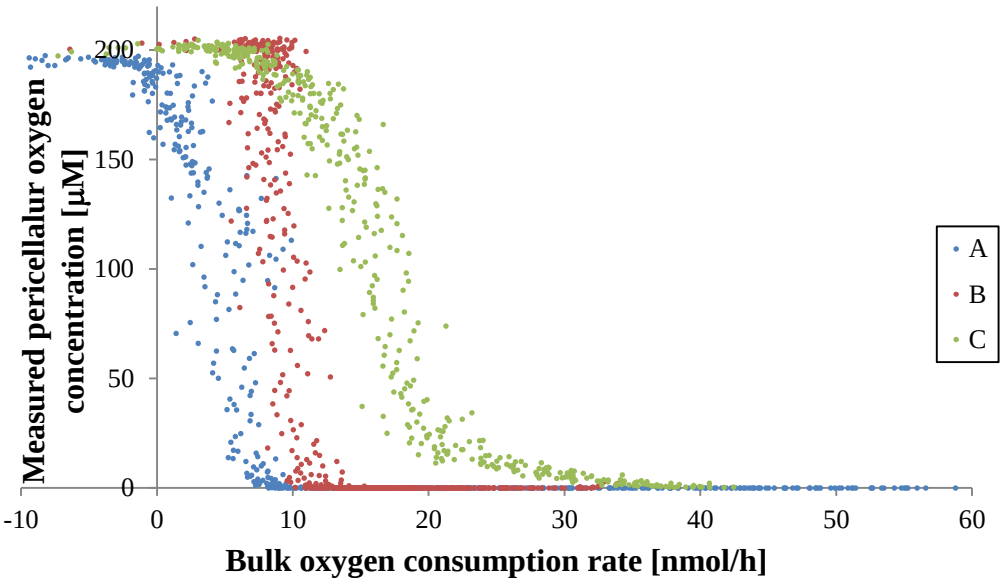

Figure 41: Correlation between calculated bulk oxygen consumption rate and measured peri-cellular oxygen concentrations for three independent cultures of mESC in the automated microfluidic platform.

To investigate the hypothesis, made in chapter 4, that *in situ* measurements were affected by cell overgrowth, confluency values were plotted against *in situ* readings for the three cultures (figure 42). Curves for experiment A and C showed a good overlap, while experiment B showed lower *in situ* readings at equivalent confluency values. Nevertheless, the apparent stronger correlation between *in situ* readings and confluency than between *in situ* readings and bulk OCR tends to confirm the hypothesis previously made that, with cell overgrowth, the *in situ* sensor provides measurement of cell coverage rather than peri-cellular oxygen levels. The difference observed between A/C and B in figure 42 could be explained by differences in cell distribution at the surface of the sensor.

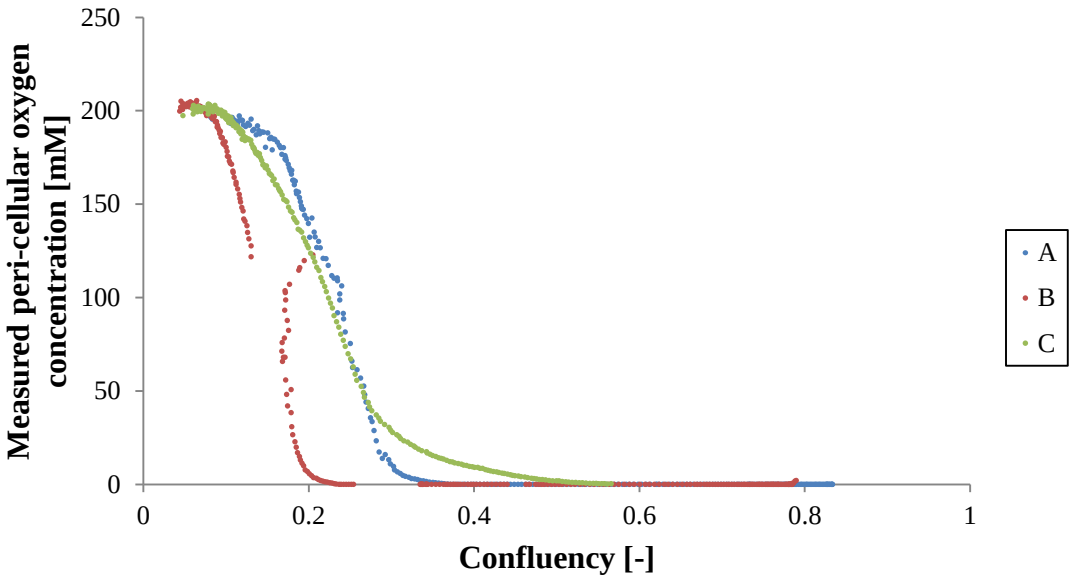

Figure 42: Correlation between confluency and measured peri-cellular oxygen concentrations for three independent cultures of mESC in the automated microfluidic platform.

5.2.4.6 Cell densities estimation

To characterise further the relation between cell growth and dissolved oxygen consumption, it was attempted to calculate cell densities from packing-corrected confluency (PCC) values, as demonstrated by Jaccard *et al.* (2013) with mESC cultures in 6-well plates. A correlation model (figure 43) between confluency and PCC was established using PHANTAST (Jaccard et al., 2013) and applied to the data set of each experiment to obtain corrected confluency values. The correction factor to derive cell densities from PCCs was obtained from the cell counts made prior to seeding to prepare the inoculum. The adjusted growth curves (figure 44) showed final cell densities of 1.00×10^6 (experiment A), 8.33×10^5 (experiment B) and 3.39×10^5 cells/cm^2 (experiment C) that are consistent with the values reported in the literature for confluent mouse embryonic stem cell cultures (Oh et al., 2005). The estimation of cell densities was used to calculate growth rates and doubling times of the cultures by fitting an exponential model to the curves: for A, a growth rate of 0.0245 h^{-1} (doubling time 28.3 h), for B, a growth rate of 0.0252 h^{-1} (doubling time 27.5 h) and for C, a growth rate of 0.0168 h^{-1} (doubling time 41.3 h). The doubling times were longer than those reported in the literature (Tamm et al., 2013). It must be noted that these values are only approximations and were not cross-validated with cell counts at different confluency values, due to the impracticality of performing sacrificial trials or live staining with the current

platform design. The main limitation of the method is the assumption that cells are growing strictly in a monolayer configuration. PCM images taken during the cultures (figure 38) showed that cells grew in multi-layers in the later stages of the culture. Therefore it is likely that the cell densities reported by the PCC method are underestimated and that doubling times are actually faster than those reported here.

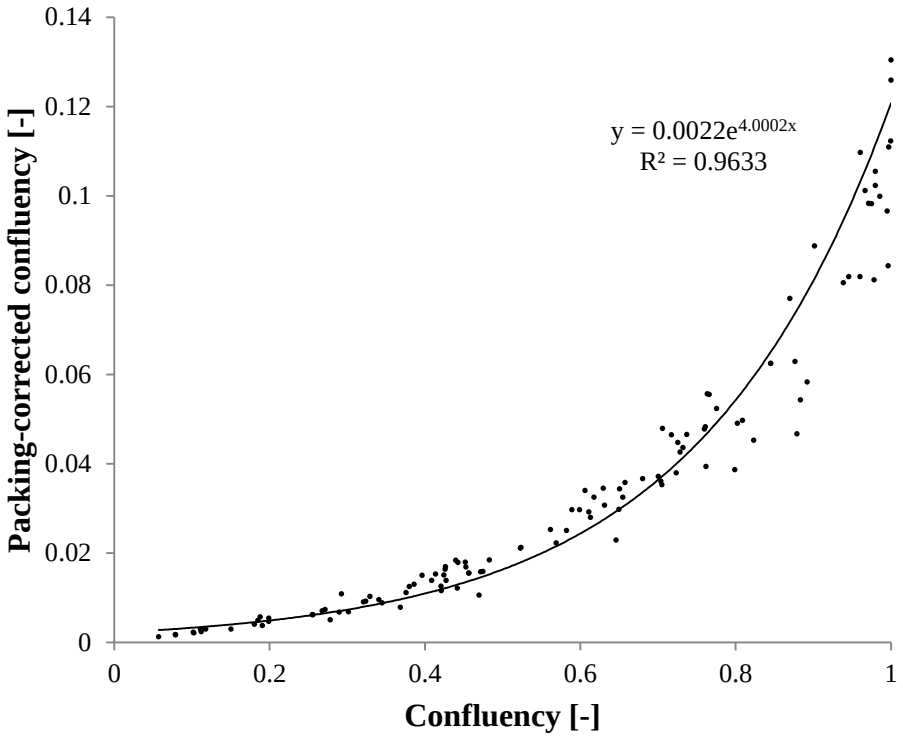

Figure 43: Correlation between confluency and packing-corrected confluency PCC values obtained from 120 PCM images randomly selected from the experiments A, B and C (40 images per experiments).

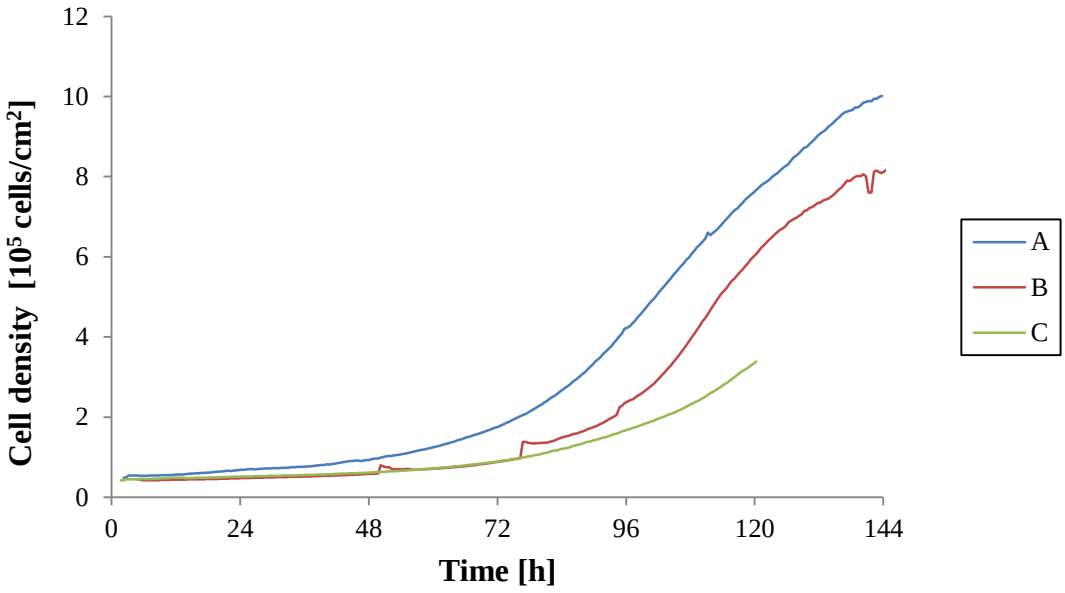

Figure 44: Cell densities estimated by packing-corrected confluency for the three mESC cultures (A, B and C) in the automated microfluidic platform.

5.2.4.7 Specific oxygen uptake rate

To calculate the specific oxygen uptake rates (sOURs), the difference between inlet and outlet readings was plotted against the corresponding cell densities estimated for each of the three culture experiments. The resulting sOURs were plotted as function of the cell density (figure 45) as a metric of culture progression, to allow comparison between the three experiments independently of their growth rate. The plots indicated that sOURs increased with cell density up to 10^5 cells/cm^2 and then stabilised around 7 amol/cell.s for experiments A and B and 20 amol/cell.s for experiment C. These values are in the same order of magnitude than the maximal sOUR (29 amol/cell.s) for embryonic stem cell lines grown in normoxic conditions (20% O_2) reported by Powers et al.(2008).

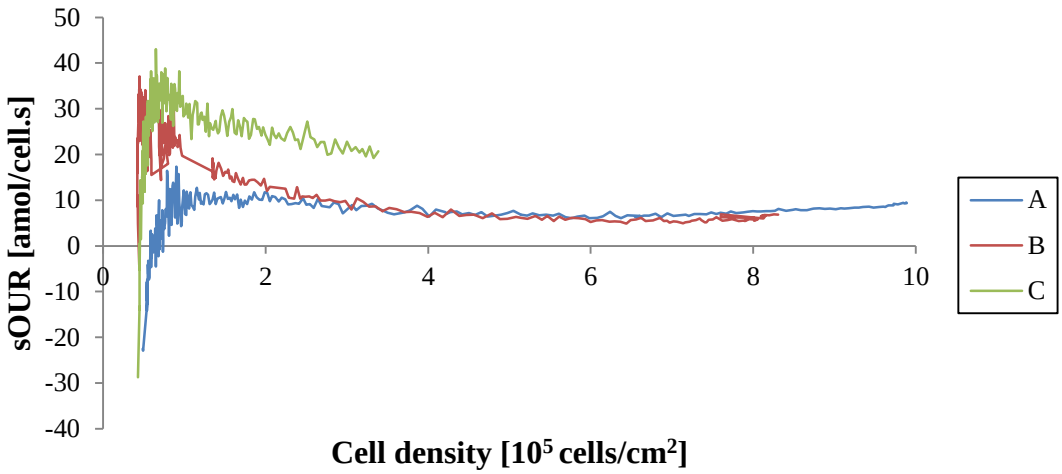

Figure 45: Specific oxygen consumption rate (sOUR) as function of the estimated cell density for the three mESC cultures (A, B and C) in the automated microfluidic platform.

A correlation was established between mean sOURs for cell densities superior to 10^5 cells/cm^2 and growth rates (figure 46). It was found that the more cells consumed dissolved oxygen, the slower they grew. This result could be attributed to two factors. First, the cells in culture C experienced a lower peri-cellular oxygen level and therefore their uptake was limited by the availability of oxygen in their microenvironment. Secondly, other factors of their microenvironment (such cell signaling factors) could have pushed the cells towards a more anaerobic metabolism. Unfortunately, because of cell overgrowth on the *in situ* sensor, it was not possible to conclude on the effect of peri-cellular oxygen levels. In addition the correlation was established on a very limited set of experiments (three) and therefore more investigation is needed to, first, confirm the trend observed and, second, examine the hypotheses proposed.

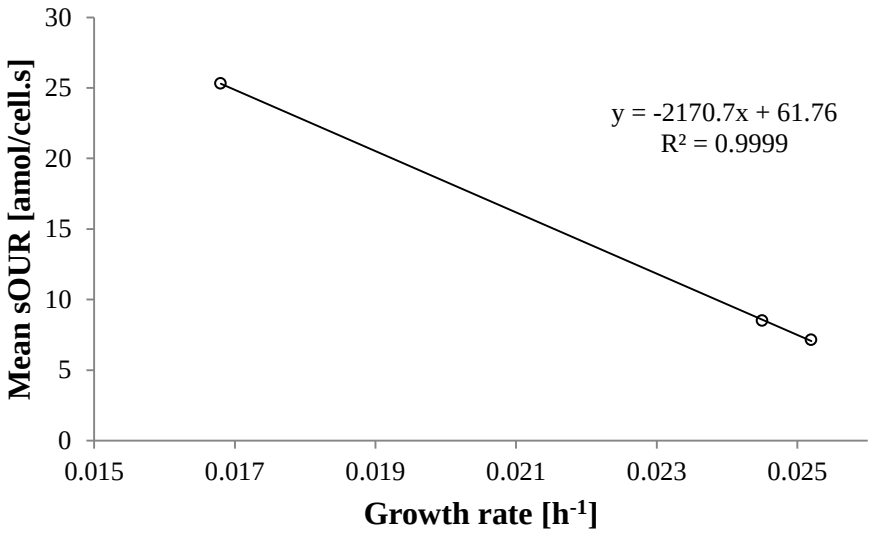

Figure 46: Correlation of mean sOURs and growth rates for the three mESC cultures in the automated microfluidic platform.

The measurements of sOURs at low cell densities (< 10^5 cells/cm^2) (figure 45) presented a lot of variations, due to the noise of the oxygen measurements from which oxygen uptake rates were derived. The overlapping noise of the inlet and outlet sensors created apparent negative oxygen uptake rates at the beginning of the plot. It is therefore difficult to conclude if the increase of sOUR is correlated with the cellular lag phase after seeding or if it is a measurement artifact due to the lower sensitivity of the optodes at higher oxygen concentrations. This uncertainty reduces the applicability of the current platform to address low-density cell cultures in normoxic conditions.

5.3 Summary of findings

An automated microfluidic culture platform has been developed to tackle the shortcomings of the previous-generation platform based around the use of standard cell culture incubators and offline cell imaging. The new platform relied on a motorised microscope with temperature control to carry out parallel oxygen and cell growth monitoring without interruption and interference. A software routine enables the automated cycling of oxygen and confluency measurement schedules.

The ability to operate the device directly on the microscope stage allowed simplifying the operating procedure and improving the robustness and repeatability of the oxygen sensor readings.

The seamless integration of oxygen and cell growth monitoring enabled the automated collection of high-resolution growth and oxygen consumption profiles. It was possible to estimate cell densities from confluency using a computational approach. From the cell densities, the growth rate, doubling time and specific oxygen uptake rates were calculated for each of the culture experiments. The values obtained were in good agreement with the literature available, despite the necessary approximations consented. The results obtained with the instrumented microfluidic platform constitute a first proof-of-concept of non-invasive characterisation of cell growth kinetics in adherent cell culture.

6 Conclusions

Pluripotent stem cells are a promising renewable source of tissue for regenerative medicine therapies and drug discovery. However, many challenges remain before these applications can become widespread. Embryonic stem cells naturally develop in an environment different from the traditional culture systems used for animal cell culture. Therefore, in order to achieve controlled expansion and differentiation of ESC, new culture systems capable of reproducing and modulating the stem cell niche are needed. Microfluidic culture systems have emerged as particularly capable tools to precisely control and interrogate the cellular microenvironment. A modular microfabricated device for the culture of adherent pluripotent stem cells has been previously developed by the Szita group (Reichen et al., 2012).

The aim of this thesis was to develop and demonstrate oxygen monitoring of pluripotent stem cell cultures in the microfabricated device.

First, the integration of optical oxygen sensors was investigated. A Ruthenium/PDMS optode design was explored as a way to generate easily multiple sensor configurations in the culture chamber for peri-cellular oxygen monitoring using rapid prototyping fabrication techniques. This type of sensor could be interrogated using an epifluorescence microscope. However the dye/PDMS matrix proved to be unstable in aqueous phase, and this design was ultimately abandoned in favor of existing commercial solutions. Commercially-available optodes were adapted to the device to enable oxygen monitoring in three locations of the culture system: at the inlet and outlet of the device, using flow-through cell sensors, and at the bottom of the culture chamber, with a bespoke sensor slide adapted to the culture device format.

Then, a microfluidic platform, combining the culture device, the oxygen monitoring system, a pressure-driven perfusion system and a standard cell culture incubator, was established to demonstrate long-term monitoring of pluripotent stem cell cultures. Standard operating procedures were defined and tested to meet the requirements for stem cell culture. Cell growth was monitored offline using image analysis techniques (Jaccard et al., 2013) to determine non-invasively cell

confluency. The pressure-driven system enabled long-term perfusion of growth medium without the need to refill the reservoir, decreasing the risk of contaminations or introduction of air bubbles in the fluidic system. The priming of the device was improved by the addition of an external tubing junction between the inlet and outlet ports. It acted as a bypass, allowing redirecting the flow upstream and downstream of the culture chamber and using the open chamber as a temporary bubble trap. Expansion of mouse embryonic stem cells for up to 6 days was demonstrated with that platform. However, the reliability of the oxygen monitoring system was negatively impacted by the offline-imaging schedule.

The conflict between cell imaging and oxygen monitoring led to the development of an automated platform designed around a motorised microscope stage with a cage incubator. The temperature control provided by the incubator allowed performing cultures on the stage of the microscope. It removed the need to transfer the device out of the incubator for imaging. A software routine was developed to automate the imaging schedule. *In situ* oxygen read-outs were achieved by bringing an optical fibre in close proximity of the slide, using a bespoke collar adapter mounted on the microscope objective. The position of the fibre tip could be recorded and recalled by the software routine. This approach enabled seamless cycling between imaging and oxygen read-out position and the generation of high-resolution timelapse data on cell growth and oxygen levels in the culture system. Specific oxygen uptake rates of adherent stem cell cultures were determined non-invasively by combining the oxygen and confluency data gathered.

This work represents a first step towards the integration of feedback-based control strategies for stem cell bioprocessing. Due to the dynamic nature of stem cells' interactions with their microenvironment, the ability to base decision-making processes on actual culture data is paramount to the development of robust bioprocesses for stem cell-based products. The microfluidic system presented in this work enabled the culture of embryonic stem cells over extended period of times. It performed consistently for up to 6 days of continuous culture and there was no indication that it would break down beyond that period (providing that there is enough growth medium in the perfusion reservoir). In addition, the seamless integration of oxygen monitoring with cell imaging enabled to determine non-invasively specific oxygen uptake rates in adherent stem cell cultures. The level of

automation of the platform reduces operator-induced variability (for medium renewal schedule or cell counting) and makes the process less labor-intensive than conventional static vessels for adherent cell culture. Contrary to many microfluidic systems for stem cell culture, the system presented here does not aim at exploiting specific features of the microscale to investigate specific aspects of cell culture such as shear forces or soluble gradients, but is rather intended as a scale-down instrumented platform to investigate stem bioprocessing as a whole, akin to existing systems for suspension cultures.

This work also highlights the challenges associated with the development of robust microfluidic culture platforms. These challenges relate to the specific requirements of the sub-components of the platform: microfluidic systems (e.g. sealing, priming), cell culture (e.g. asepsis, homeostasis), monitoring systems (e.g. calibration, integration). These requirements are addressed not only by the design and development of suitable systems, but as well by the establishment of robust operating procedures. Ultimately the operation of microfluidic culture platforms has to be organised in a coherent workflow to ensure the optimal performance of each of its sub-components and obtain repeatable results.

7 Future Work

Many challenges associated with the operation of the instrumented microfluidic platform have been tackled. However, some additional engineering challenges emerged during the development of the platform and the oxygen monitoring system. The capacity of the platform for bioprocessing could be extended by the addition of new monitoring and control systems. The instrumented platform in its current state offers also a series of engaging new research opportunities in the field of stem cell bioprocessing development.

The current oxygen monitoring system allowed measuring oxygen consumption between the inlet and outlet of the culture device, however the peri-cellular monitoring requires improvements to perform as intended. The issue of cell overgrowth on the sensor needs to be tackled in order to obtain accurate peri-cellular measurements. Several approaches could be investigated:

- Polymer coatings such as PEG could be used to prevent cell adhesion and growth on the sensor top. Strategies to restrict (e.g. stencil, microprinting) the coating to the sensor top need to be developed and tested.
- Optodes from different manufacturers could be tested, to assess if some them may be less prone to cell overgrowth
- The *in situ* sensor could be slightly elevated above the substrate plane. This would require a robust fabrication process to ensure that the elevation is repeatable.

There is also a need to understand how oxygen levels are distributed spatially in the chamber. The ruthenium/PDMS optodes presented in chapter 3 were originally designed to enable the mapping of oxygen concentrations across the culture chamber. If the problem of structural stability of these optodes in aqueous phase can be solved (by altering the fabrication protocols), they could assist to verify experimentally physical model predictions.

The integration of oxygen monitoring constitutes only a first step towards the establishment of a novel tool for bioprocessing development. The monitoring data

could be used to set up feedback-loop control strategies. In order to modulate oxygen levels in the culture devices, several options could be investigated:

- The pressure-driven system could be developed further to include a gas mixing stage. It would allow dynamically modulating the oxygen level in the medium reservoir of the perfusion system.
- The current lid designed could be altered to include a gas-permeable membrane, allowing passive or active oxygenation directly in the culture chamber.

The integration of optodes for oxygen monitoring could be translated to the detection of other analytes based on similar physical principles, such as pH or CO_2.

While these recommendations would greatly increase the potential of the current platform, a series of studies on stem cell bioprocessing could already take place in the current system:

- Culture at low oxygen tensions could be performed, by using a hypoxic gas mixture as driving gas for perfusion. The current monitoring systems would allow studying the effect of low oxygen concentrations on growth kinetics and oxygen uptake rates. End point assays such as immunocytochemistry or qPCR to detect the expression of specific genetic markers would complement the results.
- These hypoxic studies could be combined with studies on the effect of flow rate (in respect to hydrodynamic shear stress and medium replenishment)

Appendix

Table 1: Summary of the mESCs culture experiments performed in the microfluidic culture platform

Main results	Duration post-seeding	Experiment outcome	Actions
Cell death after seeding	16 hours	No adherent cells observed at first imaging point.	Use new device parts.
Air bubble introduced during transfer	24 hours	Air introduced in the chamber during transfer to the microscope.	Close the valves during transfer
Completed experiment. Unsuccessful staining	71 hours	Confluence reached a plateau and decreased after 46 hours. Most of the cells were lost during post-culture staining	Possible contamination. Optimisation of on-chip staining protocol required
Seeding error Contamination	45 hours	Calculation error for seeding density. Bacterial contamination.	Use new device parts Use new solutions
Contamination	52 hours	Bacterial contamination.	Switch to autoclavable DO slide. Use antibiotics in medium
Completed experiment	137 hours		
Completed experiment	133 hours		Calibrate 100% DO At the beginning of perfusion
Completed experiment	138 hours		
Completed experiment	85 hours		

Table 2:Summary of the mESCs culture experiments performed in the automated microfluidic culture platform

Main results	Duration post-seeding	Experiment outcome	Actions
Evaporation (*in situ* DO n/a)	48 hours	Bubbles caused by evaporation Culture totally dried-out after 48 hours.	Addition of a water pan in the cage incubator
Contamination (*in situ* DO n/a)	93 hours	Contamination in the reservoir	Use new antibiotic stock solution
Bubbles in the chamber Bottom frame to thick for *in situ* fibre	119 hours	Persistent bubbles in the chamber	Use new aluminium frame
Experiment completed (*in situ* DO n/a)	117 hours		
Leaking	0 hours	Leaking through the lid	Check integrity of lid gasket
Leaking	0 hours	Leaking between the frames	Use new top plate
Leaking	0 hours	Leaking between the frames	Addition of aluminium brackets to prevent leaking
Software crash	48 hours	Image acquisition and stage control crash	Deactivate network connections, software update and reinstall/update drivers
Software crash	70 hours	Image acquisition and stage control crash	Optimise automation software to reduce RAM requirements
Perfusion failure	61 hours	Clogging of the outlet capillary by dried medium. Cell growth arrest	Change outlet capillary

		after 24 hours
Experiment completed	137 hours	DO decreasing at the inlet Cells recovered from the inlet FTC sensor
Experiment completed	144 hours	
Experiment completed	144 hours	
Experiment completed	120 hours	

References

Alberts, B., Johnson, A., Lewis, J., Walter, P., Raff, M., Roberts, K., 2002. Molecular Biology of the Cell 4th Edition. *Garland Science*.

Ateghang, B., Wartenberg, M., Gassmann, M., Sauer, H., 2006. Regulation of cardiotrophin-1 expression in mouse embryonic stem cells by HIF-1alpha and intracellular reactive oxygen species. *Journal of Cell Science*, 119, 1043–1052.

Barnbot, S.B., Lakowicz, J.R., Rao, G., 1995. Potential Applications of Lifetime-Based, Phase-Modulation Fluorometry in Bioprocess and Clinical Monitoring. *Trends in Biotechnology*, 13, 106–115.

Becerra, J., Santos-Ruiz, L., Andrades, J.A., Mari-Beffa, M., 2011. The Stem Cell Niche Should be a Key Issue for Cell Therapy in Regenerative Medicine. *Stem Cell Reviews and Reports*, 7, 248–255.

Berthier, E., Young, E.W.K., Beebe, D., 2012. Engineers are from PDMS-land, Biologists are from Polystyrenia. *Lab on Chip*, 12, 1224–1237.

Blagovic, K., Kim, L.Y., Voldman, J., 2011. Microfluidic perfusion for regulating diffusible signaling in stem cells. *PLoS ONE*, 6, e22892.

Chaudhry, M.A., Bowen, B.D., Piret, J.M., 2009. Culture pH and osmolality influence proliferation and embryoid body yields of murine embryonic stem cells. *Biochemical Engineering Journal*, 45, 126–135.

Chen, S.S., Fitzgerald, W., Zimmerberg, J., Kleinman, H.K., Margolis, L., 2007. Cell-Cell and Cell-Extracellular Matrix Interactions Regulate Embryonic Stem Cell Differentiation. *Stem Cells*, 25, 553–561.

Chung, B.G., Flanagan, L.A., Rhee, S.W., Schwartz, P.H., Lee, A.P., Monuki, E.S., Jeon, N.L., 2005. Human neural stem cell growth and differentiation in a gradient-generating microfluidic device. *Lab on Chip*, 5, 401–406.

Clark, L.C., Wolf, R., Granger, D., Taylor, Z., 1953. Continuous recording of blood oxygen tensions by polarography. *Journal of applied physiology*, 6, 189–193.

Cohen, S., Samadikuchaksaraei, A., Polak, J.M., Bishop, A.E., 2006. Antibiotics reduce the growth rate and differentiation of embryonic stem cell cultures. *Tissue Engineering*, 12, 2025–2030.

Dertinger, S., Chiu, D., Jeon, N., Whitesides, G., 2001. Generation of gradients having complex shapes using microfluidic networks. *Analytical Chemistry*, 73, 1240–1246.

Dias, J., Gumenyuk, M., Kang, H., Vodyanik, M., Yu, J., Thomson, J.A., Slukvin, I.I., 2011. Generation of Red Blood Cells from Human Induced Pluripotent Stem Cells. *Stem Cells and Development*, 20, 1639–1647.

Duffy, D., McDonald, J., Schueller, O., Whitesides, G., 1998. Rapid prototyping of microfluidic systems in poly (dimethylsiloxane). *Analytical Chemistry*, 70, 4974–4984.

Forsyth, N.R., Kay, A., Hampson, K., Downing, A., Talbot, R., McWhir, J., 2008. Transcriptome alterations due to physiological normoxic (2% O_2) culture of human embryonic stem cells. *Regenerative medicine*, 3, 817–833.

Fung, W.-T., Beyzavi, A., Abgrall, P., Nguyen, N.-T., Li, H.-Y., 2009. Microfluidic platform for controlling the differentiation of embryoid bodies. *Lab on Chip*, 9, 2591–2595.

Gibbons, J., Hewitt, E., Gardner, D.K., 2006. Effects of oxygen tension on the establishment and lactate dehydrogenase activity of murine embryonic stem cells. *Cloning and Stem Cells*, 8, 117–122.

Gilmore, A.P., Owens, T.W., Foster, F.M., Lindsay, J., 2009. How adhesion signals reach a mitochondrial conclusion - ECM regulation of apoptosis. *Current Opinion in Cell Biology*, 21, 654–661.

Gomez-Sjoberg, R., Leyrat, A.A., Pirone, D.M., Chen, C.S., Quake, S.R., 2007. Versatile, Fully Automated, Microfluidic Cell Culture System. *Analytical Chemistry*, 79, 8557–8563.

Gustafsson, M.V., Zheng, X.W., Pereira, T., Gradin, K., Jin, S.B., Lundkvist, J., Ruas, J.L., Poellinger, L., Lendahl, U., Bondesson, M., 2005. Hypoxia requires Notch signaling to maintain the undifferentiated cell state. *Developmental Cell*, 9, 617–628.

Hazeltine, L.B., Selekman, J.A., Palecek, S.P., 2013. Engineering the human pluripotent stem cell microenvironment to direct cell fate. *Biotechnology Advances*, 31, 1002–1019.

Heng, B.C., Vinoth, K.J., Liu, H., Hande, M.P., Cao, T., 2006. Low temperature tolerance of human embryonic stem cells. *International Journal of Medical Sciences*, 3, 124–129.

Jaccard, N., Griffin, L.D., Keser, A., Macown, R.J., Super, A., Veraitch, F.S., Szita, N., 2013. Automated method for the rapid and precise estimation of adherent cell culture characteristics from phase contrast microscopy images. *Biotechnology and Bioengineering*, 3, 504-517.

Jaccard, N., Macown, R.J., Super, A., Griffin, L.D., Veraitch, F.S., Szita, N., 2014. Automated and Online Characterization of Adherent Cell Culture Growth in a Microfabricated Bioreactor. *Journal of Laboratory Automation*, 5, 437-443.

Jauniaux, E., Gulbis, B., Burton, G.J., 2003. The human first trimester gestational sac limits rather than facilitates oxygen transfer to the foetus--a review. *Placenta*, 24 Suppl A, S86–93.

Jeong, C.-H., Lee, H.-J., Cha, J.-H., Kim, J.H., Kim, K.R., Kim, J.-H., Yoon, D.-K., Kim, K.-W., 2007. Hypoxia-inducible factor-1 alpha inhibits self-renewal of mouse embryonic stem cells in Vitro via negative regulation of the leukemia inhibitory factor-STAT3 pathway. *Journal of Biological Chemistry*, 282, 13672–13679.

Jiang, X., Xu, Q., Dertinger, S.K.W., Stroock, A.D., Fu, T.-M., Whitesides, G.M., 2005. A general method for patterning gradients of biomolecules on surfaces using microfluidic networks. *Analytical Chemistry*, 77, 2338–2347.

Jung, D.R., Kapur, R., Adams, T., Giuliano, K.A., Mrksich, M., Craighead, H.G., Taylor, D.L., 2001. Topographical and physicochemical modification of material surface to enable patterning of living cells. *Critical Reviews in Biotechnology*, 21, 111–154.

Karp, J.M., Yeh, J., Eng, G., Fukuda, J., Blumling, J., Suh, K.-Y., Cheng, J., Mahdavi, A., Borenstein, J., Langer, R., Khademhosseini, A., 2007. Controlling size, shape and homogeneity of embryoid bodies using poly(ethylene glycol) microwells. *Lab on Chip*, 7, 786–794.

Khoury, M., Bransky, A., Korin, N., Konak, L.C., Enikolopov, G., Tzchori, I., Levenberg, S., 2010. A microfluidic traps system supporting prolonged culture of human embryonic stem cells aggregates. *Biomedical Microdevices*, 12, 1001–1008.

Kim, L., Toh, Y.-C., Voldman, J., Yu, H., 2007. A practical guide to microfluidic perfusion culture of adherent mammalian cells. *Lab on Chip*, 7, 681–694.

Kim, L., Vahey, M.D., Lee, H.-Y., Voldman, J., 2006. Microfluidic arrays for logarithmically perfused embryonic stem cell culture. *Lab on Chip*, 6, 394–406.

Kim, T.-S., Misumi, S., Jung, C.-G., Masuda, T., Isobe, Y., Furuyama, F., Nishino, H., Hida, H., 2008. Increase in dopaminergic neurons from mouse embryonic stem cell-derived neural progenitor/stem cells is mediated by hypoxia inducible factor-1α. *Journal of Neuroscience Research*, 86, 2353–2362.

Koller, M.R., Bender, J.G., Miller, W.M., Papoutsakis, E.T., 1993. Expansion of Primitive Human Hematopoietic Progenitors in a Perfusion Bioreactor System with IL-3, IL-6, and Stem Cell Factor. *Nature Biotechnology*, 11, 358–363.

Korin, N., Bransky, A., Dinnar, U., Levenberg, S., 2007. A parametric study of human fibroblasts culture in a microchannel bioreactor. *Lab on Chip*, 7, 611–617.

Korin, N., Bransky, A., Dinnar, U., Levenberg, S., 2009. Periodic "flow-stop" perfusion microchannel bioreactors for mammalian and human embryonic stem cell long-term culture. *Biomedical Microdevices*, 11, 87–94.

Lanfer, B., Seib, F.P., Freudenberg, U., Stamov, D., Bley, T., Bornhäuser, M., Werner, C., 2009. The growth and differentiation of mesenchymal stem and progenitor cells cultured on aligned collagen matrices. *Biomaterials*, 30, 5950–5958.

Leclerc, E., Sakai, Y., Fujii, T., 2004. Microfluidic PDMS (polydimethylsiloxane) bioreactor for large-scale culture of hepatocytes. *Biotechnology Progress*, 20, 750–755.

Lee, Y.H., Tsao, G.T., 1979. Dissolved oxygen electrodes. *Advances in Biochemical Engineering*, 13, 35-86.

Lee, Y.M., Jeong, C.H., Koo, S.Y., Son, M.J., Song, H.S., Bae, S.K., Raleigh, J.A., Chung, H.Y., Yoo, M.A., Kim, K.W., 2001. Determination of hypoxia region by hypoxia marker in developing mouse embryos in vivo: A possible signal for vessel development. *Developmental Dynamics*, 220, 175–186.

Li, J., Zhang, Y.-P., Kirsner, R.S., 2003. Angiogenesis in wound repair: Angiogenic growth factors and the extracellular matrix. *Microscopy Research and Technique*, 60, 107–114.

Lin, Z., Cherng-Wen, T., Roy, P., Trau, D., 2008. In-situ measurement of cellular microenvironments in a microfluidic device. *Lab on Chip*, 9, 257–262.

Liu, W., Deng, Y., Liu, Y., Gong, W., Deng, W., 2013. Stem Cell Models for Drug Discovery and Toxicology Studies. *Journal of Biochemical and Molecular Toxicology*, 27, 17–27.

Lübbers, D.W., Opitz, N., 1976. Quantitative Fluorescence Photometry with Biological Fluids and Gases. In: Oxygen Transport to Tissue—II, *Advances in Experimental Medicine and Biology*, 65–68.

Matsuo, I., Kimura-Yoshida, C., 2013. Extracellular modulation of Fibroblast Growth Factor signaling through heparan sulfate proteoglycans in mammalian development. *Current Opinion in Genetics & Development*, 23, 399–407.

McCoy, R., Hoare, M., Ward, S., 2009. Ultra scale-down studies of the effect of shear on cell quality; Processing of a human cell line for cancer vaccine therapy. *Biotechnology Progress*, 25, 1448–1458.

McLimans, W.F., Crouse, E.J., Tunnah, K.V., Moore, G.E., 1968. Kinetics of Gas Diffusion in Mammalian Cell Culture Systems .I. Experimental. *Biotechnology and Bioengineering*, 10, 725–740.

Mehta, G., Lee, J., Cha, W., Tung, Y.-C., Linderman, J.J., Takayama, S., 2009. Hard Top Soft Bottom Microfluidic Devices for Cell Culture and Chemical Analysis. *Analytical Chemistry*, 81, 3714–3722.

Mehta, G., Mehta, K., Sud, D., Song, J.W., Bersano-Begey, T., Futai, N., Heo, Y.S., Mycek, M.-A., Linderman, J.J., Takayama, S., 2007. Quantitative measurement and control of oxygen levels in microfluidic poly(dimethylsiloxane) bioreactors during cell culture. *Biomedical Microdevices*, 9, 123–134.

Merkel, T., Bondar, V., Nagai, K., Freeman, B., Pinnau, I., 2000. Gas sorption, diffusion, and permeation in poly(dimethylsiloxane). *Journal of Polymer Science: Polymer Physics*, 38, 415–434.

Metallo, C.M., Mohr, J.C., Detzel, C.J., dePablo, J.J., VanWie, B.J., Palecek, S.P., 2007. Engineering the Stem Cell Microenvironment. *Biotechnology Progress*, 23, 18–23.

Metzen, E., Wolff, M., Fandrey, J., Jelkmann, W., 1995. Pericellular pO_2 and O_2 consumption in monolayer cell cultures. *Respiration Physiology*, 100, 101–106.

Mittal, N., Rosenthal, A., Voldman, J., 2007. nDEP microwells for single-cell patterning in physiological media. *Lab on Chip*, 7, 1146–1153.

Mohyeldin, A., Garzón-Muvdi, T., Quiñones-Hinojosa, A., 2010. Oxygen in stem cell biology: a critical component of the stem cell niche. *Cell Stem Cell*, 7, 150–161.

Mondragon-Teran, P., Lye, G.J., Veraitch, F.S., 2009. Lowering oxygen tension enhances the differentiation of mouse embryonic stem cells into neuronal cells. *Biotechnology Progress*, 25, 1480–1488.

Nakanishi, J., Takarada, T., Yamaguchi, K., Maeda, M., 2008. Recent advances in cell micropatterning techniques for bioanalytical and biomedical sciences. *Analytical Sciences*, 24, 67–72.

Nock, V., 2009. Control and measurement of oxygen in microfluidic bioreactors. *University of Canterbury*.

Nock, V., Blaikie, R., David, T., 2008. Patterning, integration and characterisation of polymer optical oxygen sensors for microfluidic devices. *Lab on Chip*, 8, 1300–1307.

Nsiah, B.A., Ahsan, T., Griffiths, S., Cooke, M., Nerem, R.M., Mcdevitt, T.C., 2014. Fluid Shear Stress Pre-Conditioning Promotes Endothelial Morphogenesis of Embryonic Stem Cells Within Embryoid Bodies. *Tissue Engineering Part A*, 20, 954-965.

Oh, S.K.W., Fong, W.J., Teo, Y., Tan, H.L., Padmanabhan, J., Chin, A.C.P., Choo, A.B.H., 2005. High density cultures of embryonic stem cells. *Biotechnology and Bioengineering*, 91, 523–533.

Park, J.Y., Kim, S.-K., Woo, D.-H., Lee, E.-J., Kim, J.-H., Lee, S.-H., 2009. Differentiation of neural progenitor cells in a microfluidic chip-generated cytokine gradient. *Stem Cells*, 27, 2646–2654.

Park, T.H., Shuler, M.L., 2003. Integration of cell culture and microfabrication technology. *Biotechnology Progress*, 19, 243–253.

Powers, D.E., Millman, J.R., Bonner-Weir, S., Rappel, M.J., Colton, C.K., 2010. Accurate Control of Oxygen Level in Cells During Culture on Silicone Rubber Membranes with Application to Stem Cell Differentiation. *Biotechnology Progress*, 26, 805–818.

Powers, D.E., Millman, J.R., Huang, R.B., Colton, C.K., 2008. Effects of oxygen on mouse embryonic stem cell growth, phenotype retention, and cellular energetics. *Biotechnology and Bioengineering*, 101, 241–254.

Prasad, S.M., Czepiel, M., Cetinkaya, C., Smigielska, K., Weli, S.C., Lysdahl, H., Gabrielsen, A., Petersen, K., Ehlers, N., Fink, T., Minger, S.L., Zachar, V., 2009. Continuous hypoxic culturing maintains activation of Notch and allows long-term propagation of human embryonic stem cells without spontaneous differentiation. *Cell Proliferation*, 42, 63–74.

Purpura, K.A., George, S.H., Dang, S.M., Choi, K., Nagy, A., Zandstra, P.W., 2008. Soluble Flt-1 Regulates Flk-1 Activation to Control Hematopoietic and Endothelial Development in an Oxygen-Responsive Manner. *Stem Cells*, 26, 2832–2842.

Randers Eichhorn, L., Bartlett, R.A., Frey, D.D., Rao, G., 1996. Noninvasive oxygen measurements and mass transfer considerations in tissue culture flasks. *Biotechnology and Bioengineering*, 51, 466–478.

Regehr, K.J., Domenech, M., Koepsel, J.T., Carver, K.C., Ellison-Zelski, S.J., Murphy, W.L., Schuler, L.A., Alarid, E.T., Beebe, D.J., 2009. Biological implications of polydimethylsiloxane-based microfluidic cell culture. *Lab on Chip*, 9, 2132.

Reichen, M., Macown, R.J., Jaccard, N., Super, A., Ruban, L., Griffin, L.D., Veraitch, F.S., Szita, N., 2012a. Microfabricated Modular Scale-Down Device for Regenerative Medicine Process Development. *PLoS ONE*, 7, e52246.

Reichen, M., Veraitch, F.S., Szita, N., 2013. Development of a Multiplexed Microfluidic Platform for the Automated Cultivation of Embryonic Stem Cells. *Journal of Laboratory Automation*, 18, 519–529.

Schmidt, S., Friedl, P., 2009. Interstitial cell migration: integrin-dependent and alternative adhesion mechanisms. *Cell and Tissue Research*, 339, 83–92.

Sud, D., Mehta, G., Mehta, K., Linderman, J., Takayama, S., Mycek, M.-A., 2006. Optical imaging in microfluidic bioreactors enables oxygen monitoring for continuous cell culture. *Journal of Biomedical Optics*, 11, 050504.

Suzuki, M., Yasukawa, T., Shiku, H., Matsue, T., 2008. Negative dielectrophoretic patterning with different cell types. *Biosensors and Bioelectronics*, 24, 1049–1053.

Szita, N., Boccazzi, P., Zhang, Z., Boyle, P., Sinskey, A.J., Jensen, K.F., 2005. Development of a multiplexed microbioreactor system for high-throughput bioprocessing. *Lab on Chip*, 5, 819–826.

Takahashi, K., Tanabe, K., Ohnuki, M., Narita, M., Ichisaka, T., Tomoda, K., Yamanaka, S., 2007. Induction of Pluripotent Stem Cells from Adult Human Fibroblasts by Defined Factors. *Cell*, 131, 861–872.

Takebe, T., Sekine, K., Enomura, M., Koike, H., Kimura, M., Ogaeri, T., Zhang, R.-R., Ueno, Y., Zheng, Y.-W., Koike, N., Aoyama, S., Adachi, Y., Taniguchi, H., 2014. Vascularized and functional human liver from an iPSC-derived organ bud transplant. *Nature*, 499, 481–484.

Tamm, C., Pijuan Galitó, S., Annerén, C., 2013. A comparative study of protocols for mouse embryonic stem cell culturing. *PLoS ONE*, 8, e81156.

Thomas, P.C., Halter, M., Tona, A., Raghavan, S.R., Plant, A.L., Forry, S.P., 2009. A noninvasive thin film sensor for monitoring oxygen tension during in vitro cell culture. *Analytical Chemistry*, 81, 9239–9246.

Unger, M.A., 2000. Monolithic Microfabricated Valves and Pumps by Multilayer Soft Lithography. *Science*, 288, 113–116.

Veraitch, F.S., Scott, R., Wong, J.-W., Lye, G.J., Mason, C., 2008. The impact of manual processing on the expansion and directed differentiation of embryonic stem cells. *Biotechnology and Bioengineering*, 99, 1216–1229.

Villa-Diaz, L.G., Torisawa, Y.-S., Uchida, T., Ding, J., Nogueira-de-Souza, N.C., O'Shea, K.S., Takayama, S., Smith, G.D., 2009. Microfluidic culture of single human embryonic stem cell colonies. *Lab on Chip*, 9, 1749–1755.

Vollmer, A.P., Probstein, R.F., Gilbert, R., Thorsen, T., 2005. Development of an integrated microfluidic platform for dynamic oxygen sensing and delivery in a flowing medium. *Lab on Chip*, 5, 1059–1066.

Westfall, S.D., Sachdev, S., Das, P., Hearne, L.B., Hannink, M., Roberts, R.M., Ezashi, T., 2008. Identification of Oxygen-Sensitive Transcriptional Programs in Human Embryonic Stem Cells. *Stem Cells and Development*, 17, 869–882.

Whitesides, G.M., 2006. The origins and the future of microfluidics. *Nature*, 442, 368–373.

Wuertz, K., Godburn, K., Iatridis, J.C., 2009. MSC response to pH levels found in degenerating intervertebral discs. *Biochemical and Biophysical Research Communications*, 379, 824–829.

Xia, Y., Whitesides, G.M., 1998. Soft Lithography. *Annual Review of Material Sciences*, 28, 153–184.

Young, E.W.K., Beebe, D.J., 2010. Fundamentals of microfluidic cell culture in controlled microenvironments. *Chemical Society Reviews*, 39, 1036–1048.

Zhao, F., Ma, T., 2005. Perfusion bioreactor system for human mesenchymal stem cell tissue engineering: Dynamic cell seeding and construct development. *Biotechnology and Bioengineering*, 91, 482–493.